



NTNU – Trondheim
Norwegian University of
Science and Technology

3-D Printed Paper as Structural Material

Improving the Mechanical Properties of
Paper Laminate with Epoxy

Daniel Ihlen Ekelund

Master of Science in Mechanical Engineering

Submission date: July 2015

Supervisor: Martin Steinert, IPM

Norwegian University of Science and Technology
Department of Engineering Design and Materials

Abstract

This project has in two stages explored the possibilities and potential for improving the mechanical properties of the laminated paper material created with Mcor Technologies' 3D printer IRIS. The first stage explored the effects of coating, soaking or vacuum infusing five hardening agents—wood glue, diluted wood glue, urethane wood lacquer, epoxy wood finish, and lamination epoxy—on specimens of the material, whose strong and weak axis were afterwards tested with three-point bending tests. Except for the lamination epoxy, none of the agents responded well to the infusion or improved the material's properties particularly with any of the treatments. The lamination epoxy however, did, and was therefore investigated further with a second series of eight 2 by 2 cm specimens that were longer than the first, to provide more reliable results from the bending test. The measurements were compared to theoretical specimens of pure epoxy and aluminium, whose corresponding bending stiffness and strength was calculated using classic beam theory. Infused and heat treated, the composite paper laminate was stiffer than the theoretical aluminium in both orientations, twice so if accounting for the difference in density, and over two thirds as strong compared to its weight.

Key-words: 3D printing, paper composite, vacuum infusion, epoxy, three-point bending

Norwegian:

Sammendrag

Dette prosjektet har utforsket mulighetene og potensialet for å bedre de mekaniske egenskapene til papirmaterialet som modeller printet med Mcor Technologies' 3D-printer IRIS er laget av. I førsteomgang ble virkningene av å belegge, bløtlegge eller vakuumentreke prøver av materialet med fem forskjellige herdere undersøkt: tre-lim, fortynnet tre-lim, uretanbasert tre-lakk, epoksy tre-finish, og laminerings epoksy. Prøvenes sterke og svake akse ble deretter testet med trepunkts bøytester, som gav verdier for stivheten og styrken. Med unntak av lamineringsepoksyen trakk ingen av herderne godt inn i materialet og forbedret ikke dets egenskaper spesielt med noen av behandlingene. Det gjorde derimot lamineringsepoksyen, som deretter ble undersøkt videre ved å trekkes inn i åtte lengre prøvestykker, for å gi mer pålitelige resultater fra bøytesten. Målingene ble sammenlignet med teoretiske prøver av ren epoksy og aluminium. Deres teoretiske stivhet og styrke ble beregnet ved bruk av klassisk bjelketeori. Fylt med epoksy og varmebehandlet ble papirlaminatet stivere enn det teoretiske aluminiumet, om både det sterke og svake aksene. Tar man forskjellen i tetthet med i betraktningen var papermaterialet to ganger så stivt som aluminiumslegeringen og to-tredjedeler så sterkt.

Stikkord: 3D printing, papirkompositt, vakuumentrekking, epoksy, trepunkts bøyetest

**MASTER THESIS SPRING 2015
FOR
STUD.TECHN. Daniel Ihlen Ekelund**

3D printed paper as structural material

Mcor Iris prints 3-dimensional models by cutting and gluing together sheet by sheet of A4 standard office paper. Regular colour images can be printed onto the sheets beforehand to create coloured models. The process is inexpensive and yields high quality models, although with inferior mechanical properties compared to printed aluminum and plastic.

The candidate shall therefore investigate supplementary processes and other possibilities for improving the mechanical properties of the paper models printed by Mcor Iris, without severely compromising their beneficial price, weight and environmental effects.

In points, the candidate shall:

- Define at least two standardized types of specimens and the procedures to be used for testing their mechanical properties.
 - Investigate the effects of various types of resin infusion and drying methods on the models' properties.
 - Investigate the printing method's performance with hollow, truss-based model designs.
 - Investigate other possible strengthening processes.
 - If possible, test similar specimens of printed aluminum for comparison.
- Specimens shall be tested using the defined procedures and compared.

Formal requirements:

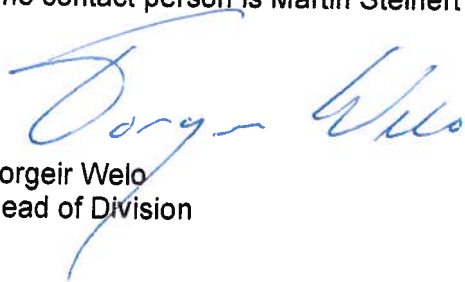
Three weeks after start of the thesis work, an A3 sheet illustrating the work is to be handed in. A template for this presentation is available on the IPM's web site under the menu "Masteroppgave" (<http://www.ntnu.no/ipm/masteroppgave>). This sheet should be updated one week before the master's thesis is submitted.

Risk assessment of experimental activities shall always be performed. Experimental work defined in the problem description shall be planned and risk assessed up-front and within 3 weeks after receiving the problem text. Any specific experimental activities which are not properly covered by the general risk assessment shall be particularly assessed before performing the experimental work. Risk assessments should be signed by the supervisor and copies shall be included in the appendix of the thesis.

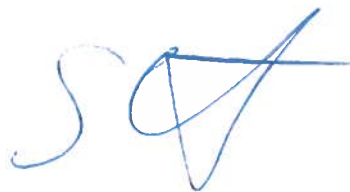
The thesis should include the signed problem text, and be written as a research report with summary both in English and Norwegian, conclusion, literature references, table of contents, etc. During preparation of the text, the candidate should make efforts to create a well arranged and well written report. To ease the evaluation of the thesis, it is important to cross-reference text, tables and figures. For evaluation of the work a thorough discussion of results is appreciated.

The thesis shall be submitted electronically via DAIM, NTNU's system for Digital Archiving and Submission of Master's theses.

The contact person is Martin Steinert



Torgeir Welo
Head of Division



Martin Steinert
Professor/Supervisor



Preface and Acknowledgements

3D Printed Paper as Structural Material is the name of my Master thesis, written and delivered in July 2015 as the concluding work to my Master of Science degree in Mechanical Engineering at the Norwegian University of Science and Technology (NTNU) in Trondheim.

I would like to acknowledge the welcoming and motivating environment at Troll Labs—the rapid prototyping lab at which I have spent many of my days this spring—started and managed by Professor Martin Steinert, to whom I owe many thanks for spiking and adding to my interest in prototyping, 3D printing and front end developing, and for being my advisor on this Master thesis. Thanks to you and to the rest of those working at Troll Labs or in PLM Lab, my office space, for a good environment and friendly conversations, for showing interest and being interesting.

Most of all, thanks to those closest to me, for never ceasing to believe that this day would come.

Table of Contents

List of Figures	xiii
List of Tables.....	xiv
Abbreviations.....	xv
1 Introduction and Motivation	1
2 Printing in Three Dimensions	2
2.1 Material Deposition Methods.....	2
2.2 Selective Hardening Methods	3
2.3 Laminated Object Manufacturing	4
3 3D Printing with Paper.....	7
3.1 Mcor IRIS.....	7
3.1.1 Selective Deposition Lamination.....	9
3.1.2 Printing Speed.....	10
3.2 Characteristics of Paper.....	12
3.3 Characteristics of the 3D Printed Paper Material.....	13
3.3.1 Mechanical Properties.....	14
3.3.2 Creep.....	15
3.3.3 Truss-based Structures	15
4 Strengthening the Thick Paper Laminate.....	17
4.1 Three-point Bending Tests	18
4.1.1 Test Setup.....	18
4.1.2 Equations.....	19
4.1.3 Stiffness, Shear and the Issue with Elastic Moduli.....	20
5 Quantitative Tests.....	22
5.1 Test Specimens.....	22
5.1.1 Initial Weight.....	23
5.2 Hardening Agents.....	24

5.3	Vacuum Infusion	26
5.3.1	Equipment.....	26
5.3.2	Infusion Process.....	26
5.4	Supplementary Treatments.....	27
5.5	Amount of Agent Absorbed.....	29
5.6	Results of the Quantitative Bending Tests	30
5.6.1	Observations during Testing	33
6	Qualitative Testing	36
6.1	Qualitative Specimens.....	36
6.2	Treating the Specimens	36
6.3	Testing	38
6.4	Results for the Qualitative Specimens	38
6.4.1	Comparing with Aluminium and Pure Epoxy.....	40
7	Conclusion	42
7.1	Further Work	43
8	References.....	45
	Appendix.....	49

List of Figures

Figure 1-1 Ultimaker 2, a popular FDM printer [1].....	3
Figure 1-2 Blueprinter, prints by sintering nylon powder [2].....	4
Figure 1-3 Mcor IRIS 3D printer [3]	6
Figure 2-1 Colour models created with IRIS [4]	7
Figure 2-2 Inside Mcor IRIS.....	8
Figure 2-3 De-cubing a part after print	10
Figure 2-4 Lacquered bat and ball printed with IRIS	13
Figure 2-5 Manually deforming the paper material.....	15
Figure 2-6 Beams with truss-based structures	16
Figure 3-1 Measurements of a three-point bending test	18
Figure 3-2 Three-point bending test equipment and setup	19
Figure 4-1 The five specimen types used for the quantitative tests.....	23
Figure 4-2 Hardening agents explored during the quantitative testing.....	25
Figure 4-3 Vacuum infusion equipment for quantitative specimens	26
Figure 4-4 Vacuum infusing specimens with RIMR135 epoxy.	27
Figure 4-5 Soaking specimens in Classic Uretan Lakk and wood glue.....	28
Figure 4-6 Specimens wetted by the diluted wood glue	29
Figure 4-7 Stiffness measurements of the infused specimens	32
Figure 4-8 Deformation and buckling of the untreated paper laminate.....	33
Figure 4-9 Specimens treated with urethane wood lacquer.	34
Figure 4-10 Failure along the mid plane of epoxy infused specimen “20–”	34
Figure 4-11 Brittle breaks of epoxy infused specimens with vertical layers	35
Figure 4-12 Vertically and horizontally layered specimen infusion profiles.....	35
Figure 5-1 Specimens ready for infusion.....	37
Figure 5-2 Specimens soaking up the epoxy after degassing	37

Figure 5-3 Curing the specimens	37
Figure 5-4 Fracture surfaces of qualitative specimens 5–8	39
Figure 5-5 Failure of qualitative specimen with flat layers	39
Figure 5-6 Cyclic loading of specimen 4..	40

List of Tables

Table 2-1 Comparing printing speeds	12
Table 2-2 Characteristic values for MultiCopy Original	13
Table 3-1 Bending test equations	20
Table 4-1 Specimen types for quantitative testing	23
Table 4-2 Typical properties of RIMR 135 lamination epoxy	24
Table 4-3 Specimens' average and variance in weight increase.	29
Table 4-4 Stiffness and strength of the aluminium and untreated paper specimens	30
Table 4-5 Weight increase, stiffness and maximum strength for the treated specimens.....	31
Table 5-1 Results from the bending tests of the qualitative specimens	38
Table 5-2 Comparing infused paper laminate, epoxy and aluminium	41

Abbreviations

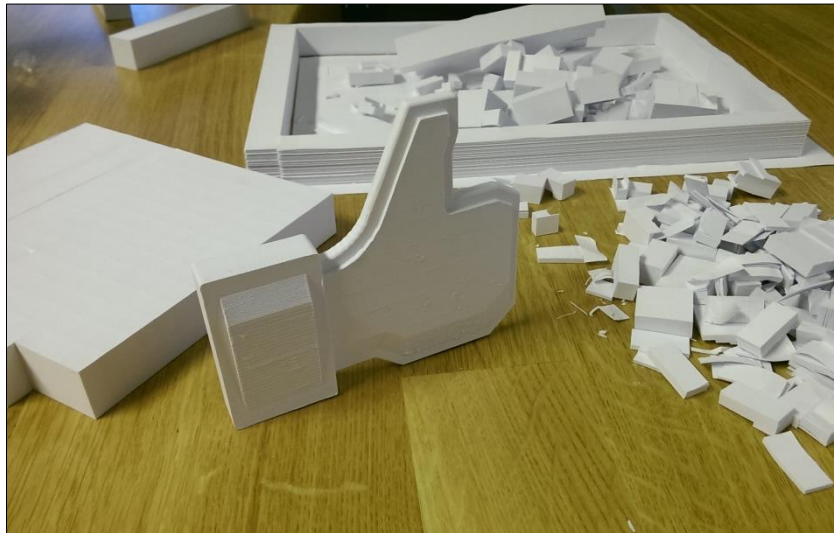
- ABS** Acrylonitrile Butadiene Styrene
- FDM** Fused Deposition Modelling
- FFF** Fused Filament Fabrication
- IPM** Department of Engineering Design and Materials, NTNU
(Institutt for Produktutvikling & Materialer)
- LOM** Laminated (or Layered) Object Manufacturing
- PC** Polycarbonate
- SDL** Selective Deposition Lamination
- SL** Stereolithography
- SLM** Selective Laser Melting
- SLS** Selective Laser Sintering

1 Introduction and Motivation

Mcor IRIS enables the versatile capabilities of 3D printing for an inexpensive and readily available material—paper. The material it creates can be described as a paper laminate, which is sturdy enough for hobby models and some prototyping purposes, but far away from aluminium and the more resilient plastics that can also be 3D printed. It is however, porous, and can therefore absorb hardening agents that solidifies, making it stiffer and stronger.

This project has explored the possibilities and potential for improving the mechanical properties of the paper laminate created with IRIS, primarily by using vacuum infusion to saturate specimens with epoxy. Other agents and application methods were also explored. The specimens were tested in three-point bending to see how stiff and strong the “paper composite” could become.

Aluminium is one of the metals that can be 3D printed, but the cost of doing so is sky high. The paper models however costs less to make than any other 3D printing method and material on the market. If this material could be treated with a hardening agent to become as sturdy as aluminium, that would it make a very compelling option for 3D printing robust parts.



2 Printing in Three Dimensions

The popularity of and attention around additive manufacturing—*3-D printing*—have grown exponentially the last decade. Simply put, it is the process of creating three-dimensional physical objects from virtual models, by gradually and accurately “adding” material to form the object. Contrary to the specialized qualities of *subtractive* manufacturing (machining), moulding or other manufacturing methods, additive manufacturing has the unique capability to produce object of virtually any shape at reasonable speed, low cost and with negligible changeover time. This makes it a potent tool for producing prototypes, complex parts and unique objects—ranging from car parts to mobile covers to prosthetics, even to biological organs[5]. Many 3D printing methods have been developed, all generally utilizing one of three principles: Material deposition, selective hardening, or lamination. Each principle has its own benefits, limitations and applications.

2.1 Material Deposition Methods

Material deposition—often referred to as *Fused Filament Fabrication* (FFF)[6] or by Stratasys’ trademarked term *Fused Deposition Modelling* (FDM)[7]—is most widely used, likely due to the printers’ simplicity in use and the many lower-budget desktop solutions that have arisen[8]. Typically, FDM printers build models by heating a thermoplastic close to the melting point and accurately depositing it layer by layer. The plastic is extruded through a nozzle onto the build, where it cools and solidifies, bonding to the surrounding material. Most thermoplastics found in traditional manufacturing can be used; desktop printers often use ABS or PC. Voluminous solids are created with a hollow internal grid structure to save material and time, but are still time-consuming to print. Temporary support structures are created where necessary, for example under overhangs, and are removed after print (some FDM printers utilize a dedicated support material, which can be dissolved in a water solution or solvent). Because of this, FDM is most efficient for small and thin models, whereas spacious geometries with overhangs are tedious. Build quality and accuracy varies from poor to good over the wide price range of existing machines. Due to the high user-friendliness, low price and mediocre quality of the models, FDM printers have become a popular choice for any application where thermoplastics can be used and where shape is the most important factor—from hobbyists to prototyping.



Figure 2-1 Ultimaker 2, a popular FDM printer

2.2 Selective Hardening Methods

Selective hardening methods, such as Selective Laser Sintering (SLS) and Stereolithography (SL), typically use more complex and expensive printers but are more versatile and precise than other methods. These processes also enable creation of larger models and utilization of a wide range of materials, from plastics to metals to ceramics[9,10]. This makes it an industry favourite. The concepts behind SLS and SL are very similar: A thin layer of material is deposited on top of the build and a laser traces the shape of the model, solidifying the material. The model is lowered to accommodate a new layer and the process repeats. The difference is in which material is used and in which form. SLS printers use finely powdered plastics, metal or ceramic components, which is spread over the build and selectively *sintered* (heated to just below melting temperature, bonding the particles together by diffusion) by a laser. The surrounding powder acts as scaffolding for the model and can in many cases be reused. A closely related group of methods termed SLM (“M” for melting) or DMLS/M (Direct Metal Laser Sintering/Melting) can be used to create finished metal components, for example in aluminium[11], with properties comparable to or even better than similar alloys[12,13]. SLAs (Stereolithography Apparatuses) on the other hand create models from a bath of liquid photopolymer, which solidifies when exposed to light of a certain wavelength. Temporary support structures are required. Both methods require some after-processing to remove excess powder or polymer (limiting the possibilities for hollow structures) as well as a strengthening post-print heat treatment (not for DMLS). Selective hardening methods create highly accurate models with good material properties, but at a matching cost.



Figure 2-2 Blueprinter, prints by sintering nylon powder.

2.3 Laminated Object Manufacturing

Laminated (or Layered) Object Manufacturing (LOM) is arguably the crudest and least versatile principle. Like most additive manufacturing methods it is a layer-by-layer approach to building physical models from virtual ones. Many variations of LOM has been developed and utilized over the years, but typically the process repeats four steps: A thin sheet of material is positioned onto the build area and then bonded to the previous layer using a combination of adhesive, heat and pressure. The outline of the model corresponding to that particular layer is cut into the sheet, and a new coat of adhesive is applied. A new sheet of material is positioned on top and so on. Usually the surrounding (waste) material is left on the build plate to act as scaffolding, and is cut into smaller sections to simplify removal when the print is finished.

LOM has not gained the same popularity as the other methods, but does nevertheless feature some unique qualities. Most significantly, each layer of the model is created from an already solid sheet of material that covers the whole build-area. The printed models are therefore solid by default—it is not necessary (nor realistically possible) to create the internal grid structure typical for material deposition methods. It follows that closed hollow structures cannot be created as a single piece, but must be printed in two or more parts and combined afterwards (similar to moulded parts). Furthermore, and contrary to the other principles, LOM thus creates wide and voluminous models very efficiently, whereas tall and thin shapes require wasteful amounts of time and material.

The precision of LOM-based solutions is comparable to lower-budget FDM printers. The area in which LOM excels however is its low operational cost, due to the material being added as solid, pre-fabricated sheets. This speaks for LOM as a hobbyist or prototyping

solution. On the other hand, the laminated structure of the models is transversely isotropic, with the strength in the vertical direction being governed by the quality of adhesion between the layers. This may discourage use of LOM for certain common applications, for example for mechanical parts or functional every-day objects, where FDM for example excels. Furthermore, the fixed layer thickness results in prominent stair-stepping on curved surfaces.

There are companies today using variations of LOM on industrial scale[14], and a few attempts has made at crating commercially available solutions. Helisys Inc. were the first to release a LOM-based desktop 3D printer. Perhaps being ahead of its time, the technology did not catch on the way we have seen with FDM for example, partly due to reliability issues[15]. Helisys ceased operation in 2000 and was bought by Cubic Technologies, who still services and supplies parts for their products[16]. Israeli Solido 3D and Japanese Kira attempted the same road but both met a similar faiths after few years[17,18]. Solido's SD300 Pro, which makes plastic models, is still distributed by Solid Model USA[19]. Kira's Rapid Mockup printer introduced using a knife to cut paper (although a special type of paper) and is the one most similar to the printers currently supplied by Irish Mcor Technologies—their newest addition to the market, Mcor IRIS, being the basis for this thesis. Mcor Technologies has received a lot of support and attention for their printers and continue to grow rapidly[20,21]. It can be said that they have successfully added LOM to the list of commercial 3D printing methods.



Figure 2-3 Mcor IRIS 3D printer

3 3D Printing with Paper

3.1 Mcor IRIS

IRIS was unveiled in 2012 and is the second 3D printer from Mcor Technologies—Matrix 300+ the first, in 2009. Both utilize a LOM-based printing method developed by Mcor termed Selective Deposition Lamination (SDL) and ordinary office paper as building material. Conflicting with the typical strategy in the 2D and 3D printer industry, both machines are relatively expensive (\$45,455 for IRIS versus \$2,950 for Ultimaker 2 and \$28,500 for Blueprinter [22–24])—instead they advertise very low operational cost due to the low material expense: printing with IRIS costs less than 1/5 of competing 3D printers, according to Mcor[25]. Like the paper, the water-based glue is biodegradable, making IRIS an “eco-friendly” printer.

Using paper also enables IRIS to create realistic full colour models, which is unique for 3D printers. In addition to the 3D printer, similar to the one in Matrix 300+, IRIS incorporates a 2D printer to print the colours of the models as images on the pages before they are used with the 3D printer. A specialized ink is used that permeates the paper completely to achieve solid colour. This feature has resulted in Mcor becoming a favourite among designers, architects and educators—in any application where colour is as important as shape.

Figure 2-3 Mcor IRIS 3D printer shows the exterior of the Mcor IRIS. The part on top is the 3D printer, while the 2D printer and consumables are located in the cabinet below. The 3D printer by itself weighs around 160 kg—quite far from the desktop-friendly Ultimaker 2’s 11



Figure 3-1 Colour models created with IRIS

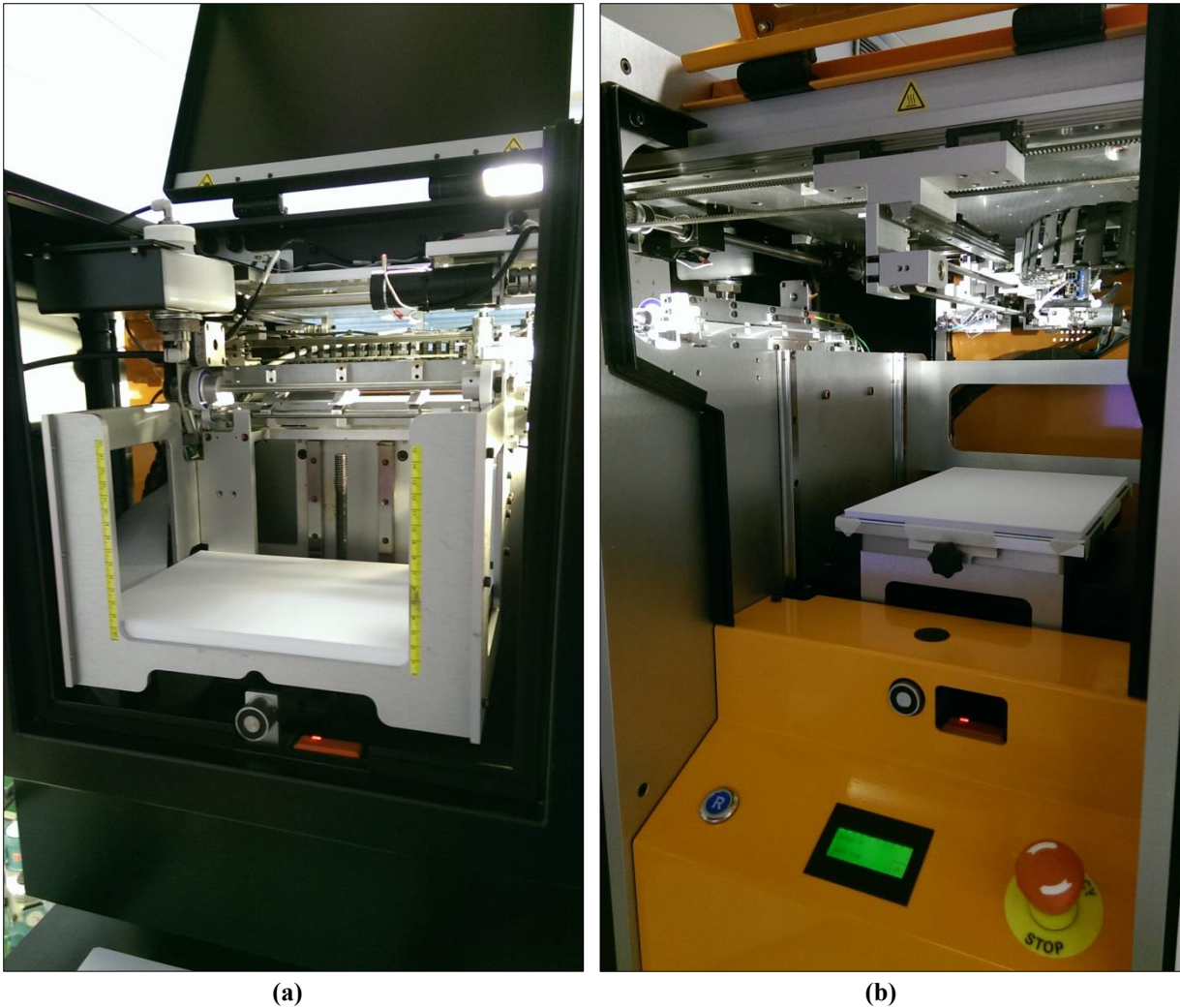


Figure 3-2 Inside Mcor IRIS: (a) Paper depot and glue container; (b) build area and user interface.

kg. There are a lot more components and moving parts in a LOM-based printer than an FDM printer, so creating a desktop model is difficult. Two doors on the 3D printer gives access to the paper depot and glue container on the left side (also seen in Figure 3-2: a), and to the build area in the middle orange part (Figure 3-2: b). The centre interface includes an emergency stop button, a reset button and a touch display to start, stop, open and prepare the machine for print.

Both printers (3D and 2D) are controlled via SliceIT—Mcor’s own “prepare-and-print” program. 3D models are loaded into SliceIT in STL, OBJ or VRML format, and positioned as wished within the build volume. SliceIT then generates the layers that will be cut of out the paper sheets and the build can be started. SliceIT controls and oversees the print through the whole process and must therefore be up and running from start to finish.

To create coloured models the paper is first loaded into the 2D printer, which, using the layers generated by SliceIT, prints an image of each layer's exterior colour onto its page. The paper is then loaded into the 3D printer and the build is started as usual. Using a barcode and markings also printed onto each page, IRIS checks the order and orientation of them and can make small corrections to the alignment to assure that the pages are loaded correctly onto the build.

Instead of using a laser to cut the layers, like in most other LOM-based 3D printers, IRIS uses a knife. Even though it is made from tungsten-carbide, the knife dulls from cutting the paper and should be changed every 7,000 meter of cut-length to maintain the accuracy and quality of the print. A 4–5 cm tall model like the bat in Figure 3-4 may require 1,000–1,500 meter cutting distance. To apply the adhesive, IRIS uses a small wheel which feeds glue off a dispenser and applies it as stripes or dots onto the paper. This is the feature that primarily enables the SDL method.

The knife holder and glue applicator is part of a multi-tool assembly, which also includes a page grabber and sensors for scanning the markings for colour models. The assembly is controlled like the printer head of an FDM printer—two pulleys on rails moves it over the build corresponding to a Cartesian coordinate system's x and y axes, while the build plate itself is raised and lowered by a separate motor, covering the z axis. The multi-tool assembly performs all actions of the printing process, except preparing the next paper sheet from the paper depot—that is done by four rollers, one page at the time.

3.1.1 Selective Deposition Lamination

In addition to using a knife instead of a laser, the main difference between SDL and the typical LOM process described earlier is how the glue is applied. Instead of a solid even layer of adhesive over the whole build, SDL only applies a low amount of glue within the sections of the waste material. The actual models are glued solidly, whereas the waste material can easily be broken due to the scarce glue holding it together.

Like most 3D printing methods, SDL is a layer-by-layer process that repeats a set series of steps.

The very first sheet of paper is manually attached to the build plate with masking tape, forming a stable foundation upon which the model is built. From there, the process repeats the following:

1. Selectively apply a thin layer of glue on the top layer.



Figure 3-3 De-cubing a part after print

2. Grab, pull in and place a new sheet of paper on top of the build.
3. Raise and press the build against the heat plate to bond the sheets.
4. Cut the model's outline and the waste sections' grid pattern in the new top sheet.
5. Check if the build is finished and if not, return to step 1.

When the build *is* finished, the resulting block of paper is detached from the build plate and the models are “dug out” from it manually. The *de-cubing* process (or *weeding* as Mcor calls it) is made easier by gridding the waste material and the selective application of adhesive. A pair of pliers and tweezers are still helpful, but SDL offers a significant improvement in user friendliness compared to previous LOM-based solutions¹.

3.1.2 Printing Speed

The time necessary to finish a build varies depending on the complexity, orientation and number of the model(s) to be printed. Since IRIS performs two operations per layers—cutting and gluing—one could expect that it requires more time than machines based on other methods, assuming the same layer thickness. As will be shown, this is not necessarily the case. Based on experience, each cycle can take from two to twelve minutes for typical models (3–0.6 mm/hour) and a full build anything from one to one hundred hours. More meaningful than these numbers are comparing IRIS's performance with other 3D printers', of which I had two available to me: Blueprinter (Figure 2-2), which uses selective heat sintering of nylon and 100 microns layer thickness (same as IRIS)[23]; and Ultimaker 2 (Figure 2-1), a filament

¹ Mcor's machines are often associated with Kira's (both use paper), whose de-cubing process was considered to be difficult. For a video demonstrating this, visit: <https://www.youtube.com/watch?v=V0neSBCbFyE>.

deposition machine typically printing with 50 microns layer thickness[24]. I compared three models with distinct characteristics to highlight the differences:

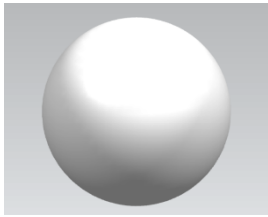
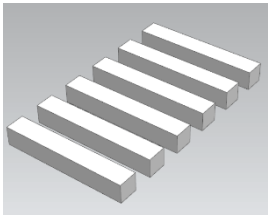
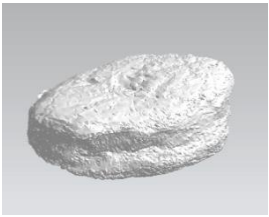
- 60 mm diameter sphere: simple shape, many layers.
- Six square 20 by 20 mm rods: few layers, high volume.
- Fishcake: high-detail, low volume.

Table 3-1 lists each machine's printing time for the three models. As seen, the print times for IRIS are absolutely comparable but vary much less than those of the two other. This is because IRIS is primarily dependent on the number of layers (the height of the build) as it cuts and applies glue to the entire sheet of paper regardless of the model's shape. Secondly, the total cut length increases with level of detail and number of shapes, explaining the relatively longer time to print the rods and the fishcake. The Blueprinter is similar in that it works with complete layers and is therefore dependent on model height. Additionally, it is largely independent of the number of shapes, but sensitive to finer details. As for the Ultimaker 2, build volume and detail level are the main contributors to building time (as they decide how much material is used) which is why the sphere, with its simple shape and medium volume, is built so efficiently.

Overall, the LOM-based IRIS performs averagely in terms of printing speed, although it is clear that this printing method compliment certain models exceptionally well—notably flat ones—making it a very situational but potentially attractive choice for 3D printing applications.

There was not opportunity for comparing with an SLM print in aluminium. It is however reasonable to expect that process to be far more time-consuming due to the necessary cooling time and heat-treatment.

Table 3-1 Comparing printing speeds

			
Models	Sphere	Six rods	Fishcake
Height	6.0 cm	2.0 cm	3.7 cm
Volume	113 cm ³	312 cm ³	46 cm ³
IRIS	13:10	8:45	13:15
Ultimaker	5:00	21:15	10:45
Blueprinter	28:15	11:00	23:00

3.2 Characteristics of Paper

In short, paper of all types are produced by either mechanically or chemically separating the cellulose fibres of wood, cotton or other organic materials, and mixing the fibres with water into *pulp*. The pulp is first directed through a vacuum dryer and then a series of rollers, gradually removing the water from the mixture by suction, pressing and heating, eventually resulting in a flat sheet of paper. In general, ordinary types of paper have three characteristic properties:

1. High in-plane tensile stiffness and strength
2. Low bending stiffness and high flexibility
3. Porous structure, meaning low density and weight

These properties are primarily decided by the type of fibres and their length, direction and intertwinement. Longer and more intertwined fibres make stronger and stiffer paper. Chemical pulping produces longer fibres than mechanical, which is a rougher process. Chemical pulp can also be *beaten*—a grinding process that “roughens” the fibres, making them more easily intertwined. The continuous production method aligns the fibres with the running direction, or *machine* direction (MD), giving the paper anisotropic properties. The degree of anisotropy can be varied to a certain degree by changing the speed and feed rate of the pulp, but strength and stiffness is generally always lower in the *cross* direction (CD) of the paper[26,27].

IRIS uses regular *bond* paper—more commonly referred to as office, copy or writing paper—of 0.1 mm thickness and 80 gsm (grams per square meter). 0.19 mm thick 160 gsm coloured paper can also be used to create solid colour models. Bond paper is made from over 90% chemical pulp and is durable, relatively stiff (but flexible enough for copier machines for example) and typically white, with a rough, permeable surface for writing and printing on. During this project, MultiCopy Original 80gsm copier paper has been used for all prints. Some characteristic values for this type of paper is listed in Table 3-2[28,29].

Table 3-2 Characteristic values for MultiCopy Original

Property	Value	Unit
Density	80	g/m ²
Thickness	0.1	mm
Tensile index (MD/CD)'	50/25	Nm/g
Tensile strength (MD/CD)'	4.0/2.0	kN/m
Breaking strain (MD/CD)'	1.8/4.7	%
Permeability	750	ml/min

'Hard to control; approximate values.

3.3 Characteristics of the 3D Printed Paper Material

It is perhaps not surprising that the solid paper models are wood-like—they are soft to the touch, light-weight and have a rough texture—and can be both sanded and coated like normal wood. They feel more natural and “warmer” than those of other 3D printers—a trait that has without a doubt also been a factor in why Mcor is so popular within its niche user group.



Figure 3-4 Lacquered bat and ball printed with IRIS

3.3.1 Mechanical Properties

Mcor's printers are able to compete with other additive manufacturing methods in terms of printing accuracy and speed, but the paper material it produces is not particularly resilient to mechanical deformation. As Mcor continuously emphasizes[30], the material *is* comparable to most plastics created with lower-budget FDM and SL printers. Even without coating, larger models (cross sections above 1-2 cm²) are stiff and durable enough for most decorative, educational and non-mechanical prototyping purposes—which is what the machines are designed for. The models can be made slightly more durable, and waterproof, by applying a coating, for example Mcor's FLEX. However, comparing strength with the metals, ceramics or high-strength polymers that can be printed using other methods, the paper models crinkle like, well, paper.

The material can best be described as a thick paper laminate. Each layer is glued to the neighbouring layers, thus utilizing the high in-plane stiffness of the paper sheets to create a moderately rigid material, despite each individual sheet's virtually non-existent stiffness. Using manual force to bend and twist material samples, some initial observations were made about its mechanical characteristics (a–c corresponds with Figure 3-5: a–c):

- (a) Bending stiffness in the laminate plane is low and the samples make an “S”-shape when bent (not clearly shown in Figure 3-5). Delamination occurs at high deformation.
- (b) Stiffness around the strong axis is good but the material buckles at low deformation.
- (c) Torsion stiffness is very low. Samples deform heavily before tearing.
- (d) Resistance to delamination and buckling increases rapidly with material thickness.
- (e) Failure from stress normal to the layers occurs within the paper sheets, not in the glue.

The difference in stiffness for case (a) and (b) was expected, as a result of the anisotropic structure. It is reasonable to assume that the high tendency to buckle is a result of the low bending stiffness and high tensile stiffness of the paper, which also causes the S-shape during bending, shown in Figure 5-8. The observations also show that the glue is somewhat elastic, allowing the layers to slide in relation to each other, causing the low torsional stiffness. When tensioning a rod with transverse layers, interlaminar failure occurred within the paper, not the glue.

Conclusively, three factors were identified that define the paper laminate's properties:

1. The flexible paper sheets offer very little resistance to buckling
2. The paper's porous structure is prone to interlaminar tearing
3. The glue is somewhat elastic

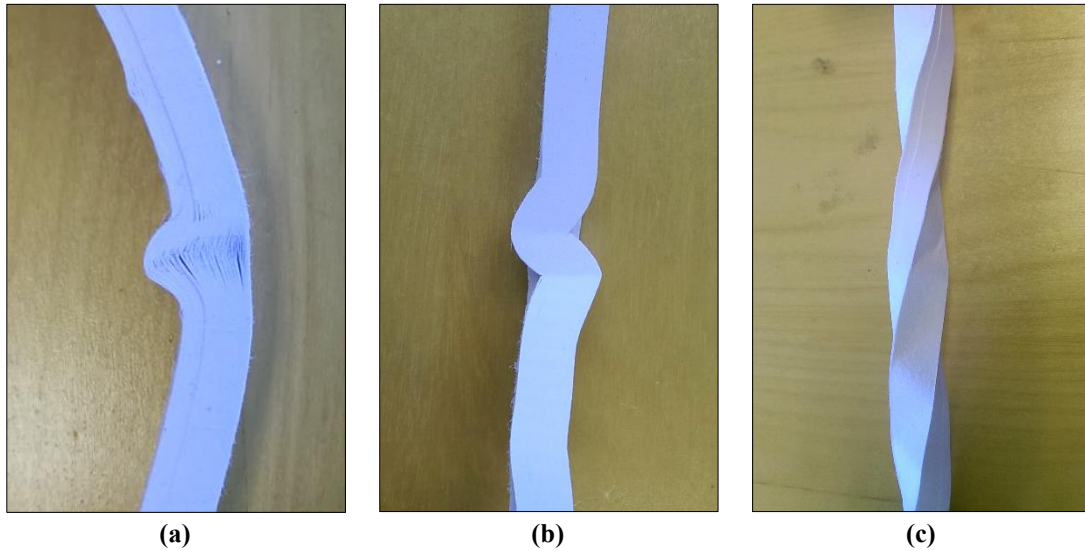


Figure 3-5 Manually deforming the paper material

These appeared to be the limiting factors and improving them would therefore be the goal when aiming to strengthen the paper material.

3.3.2 Creep

Paper has an innate tendency to deform over time—creep—even at low stress levels, caused by the fibres' ability to move within the loose structure and align themselves with the direction of the applied stress[31]. Combined with the observed elasticity of the glue, this could be a concern if using the paper material for structural purposes.

A very simple test was performed to see if the material would creep when exposed to low but long term stress. A 12 cm long, 1 cm wide square rod of the paper material was placed with the layers flat upon a fulcrum and loads of approximately 300 grams were applied on either side. After three weeks, no creep deformation was visible, indicating that the material is not as viscous as was feared. This does of course not rule out high creep rates at higher stress levels, which was in fact experienced during testing (chapter 5.6.1).

3.3.3 Truss-based Structures

As part of the initial thesis statement, beams with various truss-based hollow structures were produced to investigate the paper material's interaction with trusses. Four designs were made

and printed as 14 cm long, 3 cm tall and 1 cm wide beams. Observation (d) was that the resistance to buckling increases rapidly with increasing material thickness; a 2 cm thick rod appeared more resistant to buckling (and thus failing) than what was expected in comparison with a 1 cm thick rod for example. Based on this, it was hypothesized that a truss-based structure would not be as beneficial in use with the paper laminate as it can be for other materials. Manually deforming the beams reinforced this prediction, as the thin members buckled with little effort. These beams were however only 1 cm thick. It is possible that a better result would have been seen had they been wider and therefore more restrictive of laminar movement normal to the layers. Such samples would however be difficult to print and de-cube. More in-depth testing of truss-based structures was not performed due to time-constraints; investigating how to strengthen the material itself was deemed more important.

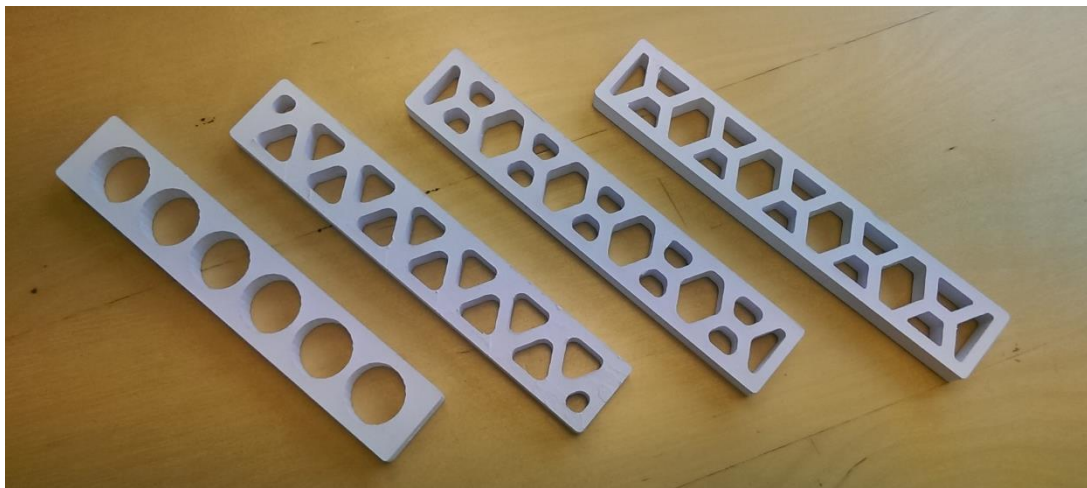


Figure 3-6 Beams with truss-based structures

4 Strengthening the Thick Paper Laminate

The most unique trait of the thick paper laminate from Matrix300+ and IRIS is the porous structure of the paper with which it is made. This enables the material to be infused with a liquid substance that solidifies, essentially creating a fibre-reinforced composite material. Polymers reinforced with fibres of carbon, glass or Kevlar (to name some typical ones) are commonly used in automotive, aerospace and other industries for their high strength-to-weight ratio and customizability. A popular method for producing high-quality parts of these materials is using vacuum to draw the liquid polymer through a laminate of the reinforcing fibres, laid-up in a mould and sealed inside a vacuum bag[32]. This is the process typically referred to as “vacuum infusion”, but it was evaluated to be unfit for the 3D printed paper models, for reasons covered below.

Wood-turners and carpenters utilize different a type of vacuum infusion when *stabilizing* soft or deteriorated pieces of wood to make them harder, more durable, moisture resistant and easier to turn and handle. The term simply refers to wood that has been made stable, meaning it will not deform over time, but is often used about a process where a vacuum chamber is used to essentially degas the wood and then, when pressure is reintroduced, saturate it with a stabilizing agent, like a sponge absorbing water. The agent hardens and keeps moisture out, hardening and preserving the wood[33–35].

Inspired by this practice, a similar treatment was applied to the wood-like paper laminate. As bond paper is designed to have good permeability, it was expected that the paper material would be similarly fit for vacuum infusion as wood. Hypothetically, the porous structure of the paper would allow for complete saturation with a hardening agent, which when solidified would dramatically improve the material’s strength, stiffness and durability.

Infusing the paper material in a vacuum chamber has three benefits over the more traditional vacuum infusion process: It is simple to set up and execute; it is faster due to low preparation time, especially for infusing several models; and most importantly, any shape can be infused as long as it fits in the chamber. Traditional vacuum infusion is typically only used for sheet-like structures, as controlling the flow of resin through the laminate of important to achieve a uniform result. The two primary drawbacks to using a vacuum chamber are however that there is no outer pressure holding the model together (like the bag does in traditional vacuum infusion), and if a curing agent is used (meaning the polymer will harden within a certain time) the polymer that is not absorbed by the models will be wasted. This excludes the

method for industrial purposes, but matters little in a prototyping setting, for which 3D printing and, considering the benefits, using a vacuum chamber is optimal. Hence, this method was chosen for infusing the specimens.

It was decided that the investigation would be carried out in two stages: first a “quantitative” series of tests to explore the effects of different hardening agents applied to the paper material using resin infusion and other methods. Five different agents were tested. The most effective agent was afterwards applied to a new set of larger specimen for “qualitative” testing, to more properly determine the effectiveness of the treatment.

4.1 Three-point Bending Tests

Three-point bending tests were performed to quantify the properties of and improvement made to the specimens. Measurements taken of the specimens and during the tests are illustrated in Figure 4-1. Table 4-1 lists the equations utilized to find the stiffness gradient, moment of inertia and maximum bending stress. During testing, the load force and deflection of the specimen were logged and plotted against each other in a force-deflection diagram, from which the gradient of the curve (the stiffness of the specimen) could be collected.

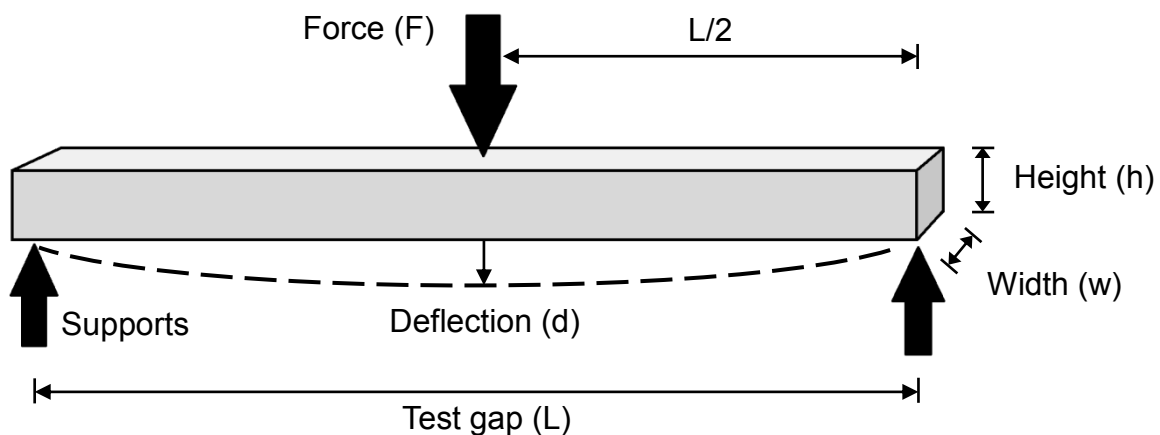


Figure 4-1 Measurements of a three-point bending test

4.1.1 Test Setup

Testing took place at the Material Engineering Laboratory at NTNU. The equipment utilized for all the bending tests are shown in Figure 4-2 and include a Würth 50 ton hydraulic press with foot control, a ± 20 kN load cell (AEP Transducers TS-C2[36]) and an inductive distance sensor. Load and deflection was logged through *Spider 8* data acquisition system using the



(a)



(b)

Figure 4-2 Three-point bending test equipment and setup
(a) Hydraulic press with foot control; (b) load cell, distance sensor and 3-point setup.

software *Catman Easy*, from HBM[37,38]. Both sensors were calibrated and manually checked before testing to ensure correct readings.

As extending the hydraulic piston was done by pumping with your foot, the deflection rate was difficult to keep steady and halted momentarily between every pump. Steadiness was improved by also displaying deflection over time in *Catman* and adjusting the speed accordingly. The deflection rate was to best ability kept around 2 mm per minute.

4.1.2 Equations

Table 4-1 lists relevant equations used for calculating the specimens' properties. Equation 3 provides the bending moment half way across the specimen, at $L/2$, where it is largest. The largest bending stress occurs here at the top (compression) and bottom (tensile) of the specimen, which is calculated using Eq. 4. This was used to find the stress level at which the ductile specimens would yield and the brittle specimens would break, referred to as the flexural strength.

Table 4-1 Bending test equations

Value	Equation	Unit	No.
• Stiffness gradient	$m = \frac{\Delta F}{\Delta d}$	N/mm	(1)
• Moment of inertia, square rod	$I = \frac{wh^3}{12}$	mm ⁴	(2)
• Max. bending moment	$M_{max} = M_{middle} = \frac{F_{max}L}{4}$	Nmm	(3)
• Max. bending stress	$\sigma_{B,max} = \frac{M_{max}y_{max}}{I} = \frac{3F_{max}L}{2wh^2}$	MPa	(4)

4.1.3 Stiffness, Shear and the Issue with Elastic Moduli

The standard property used to describe the stiffness of a material is its elastic moduli E (tensile) and G (shear). Two primary theories exist connecting these properties to the results of a bending test: classic (Euler-Bernoulli) beam theory, which treats the specimen as if only affected by bending stress; and Timoshenko beam theory, which is more intricate as it tries to account for the effect of shear forces within the material as well by expanding upon the classic theory. As the thickness of a specimen increases in relation to its length, so does the appearance of shear forces when bending it. Timoshenko's theory is therefore better suited for shorter, thicker specimens, whereas classic beam theory calls for length-to-thickness ratios typically well above 1:16[39]. The specimens created and tested for this project have ratios of 1:12 down to 1:5. However, Timoshenko's theory includes both E and G in its equation:

$$q(x) - EI \frac{\delta^4 w}{\delta x^4} = \frac{EI}{\beta GA} \frac{\delta^2 q}{\delta x^2} \quad (5)$$

For uniform, isotropic materials G relates to E through the simple relation

$$E = 2G(1 + \nu) \quad (6)$$

where ν is the material's Poisson's ratio (~0.35 for most aluminium alloys). The paper material however, untreated or treated, is highly anisotropic and thus does not adhere to this relation. Nor are the values for any of their material properties (E , G and ν for all three

dimensions) known, and would require extensive testing to find, which is beyond the scope of this thesis.

To evade this issue and still acquire meaningful conclusions from the tests, specimens of untreated paper and aluminium alloy (supposedly 6082-T6) were created and tested as well to construct a value range with which to compare the results for the treated specimens. The elastic properties of the aluminium alloy are well known, and corresponding stiffness values for any size specimen in a bending test can easily be derived using Timoshenko or classic beam theory to provide a meaningful comparison—a “benchmark”—for the paper specimens.

The ratio between the support span and thickness of the qualitative specimens for which this will be done is 1:10. Solving Timoshenko for a rectangular beam in a three-point bending test and separating out deflection (d) yields the following relation[40]:

$$d_{max} = d_{middle} = \frac{FL^3}{48EI} \left(1 + \frac{12EI}{\beta GAL^2} \right)$$

Removing the right part within the parenthesis would grant the relation according to classic beam theory. Entering the shape factor $\beta = 5/6$, the relation $A = wh$, eq. 2 for I and the relation between E and G into the equation we get:

$$d_{mid} = \frac{FL^3}{4Ewh^3} \left[1 + 2.4(1 + \nu) \left(\frac{h}{L} \right)^2 \right]$$

For $L/h = 10$, the deviation from classic beam theory is therefore $3(1+\nu)/124$, which rounds to 0.03 or 3% for aluminium. A deviation this small becomes insignificant in comparison to the uncertainties of the test results, and classic beam theory will therefore be utilized to compute theoretical stiffness values with which to compare the paper laminate.

5 Quantitative Tests

The first stage focused on outlining the effects on the paper material's properties when treated with different hardening agents. It was initially intended that five types of specimens should be treated with five different agents using three different methods, totalling 75 samples. However, not all treatments were possible, viable or considered necessary, resulting in 45 specimens eventually being produced and tested. In addition, similar specimens of untreated paper material and of aluminium alloy were also created and tested during this stage.

5.1 Test Specimens

For easy testing and calculation, the test specimens were created as 20 millimetre wide rectangular rods. Being a highly anisotropic material, it was natural to perform tests of both the weakest orientation of the paper laminate—layers oriented horizontally (flat) during testing—and the strongest orientation—vertically oriented (standing) layers. Testing specimen with layers oriented normal to the longitudinal axis (transverse layers), thus essentially only testing the strength of adhesion between the layers, was not performed.





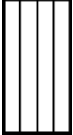
Initially, specimens of both orientations were created 10 mm thick and 140 mm long, which was the largest size that would fit inside the jar to be used as vacuum chamber. It was later hypothesized that the thickness of the specimens (i.e. the number of layers) might have an impact outside simply the different cross-sectional area, due to the layered structure. Specimens 5 and 20 millimetres thick were therefore created as well. It was quickly observed that the 5 millimetres thick specimens held minimal stiffness (they were easily deformed by hand) and were excluded from testing as being superfluous. Unfortunately, the 20 mm thick and 140 mm long specimens were too large for the vacuum chamber jar and could not be infused. Since the build area of IRIS is restricted to the 256 mm long A4 pages, lengths of 120 mm for the 20 mm specimen and 130 mm for the 10 mm specimens was eventually chosen, so that ten specimens could be printed at a time. Due to shear forces, the longer 140 mm long specimens would grant slightly higher stiffness values than those 130 mm when tested with the same setup. To save time, and because the purpose of the quantitative tests was to explore the effectiveness of the treatments, more than obtain accurate numbers, the 140 mm long specimens were still used.

An additional instance of the ten millimetre thick sample with horizontal layers was included to be tested standing, i.e. around the strong axis (specimen “10 II” in Table 5-1); a 10 mm

specimen with vertical layers tested around the weak axis (i.e. 10 l-) was considered unnecessary as the result would correspond with the similar 20 mm specimen.

The specimen types are noted by thickness, test orientation and layer orientation in relation to the test orientation, as shown in Table 5-1.

Table 5-1 Specimen types for quantitative testing

Illustration of cross-section					
Notation	20 -	20 l	10 =	10 -l	10 ll
Dimensions (h x w) [mm]	20 x 20	20 x 20	10 x 20	10 x 20	20 x 10
Weak/strong axis	Weak	Strong	Weak	Strong	Strong

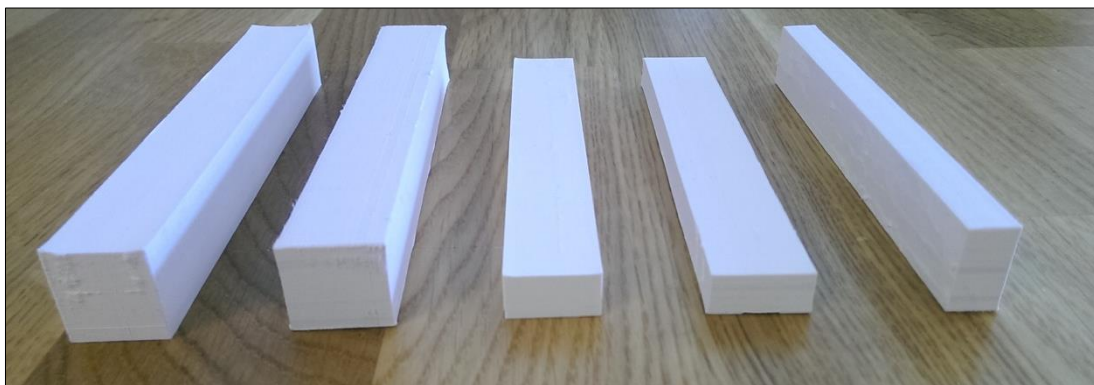


Figure 5-1 The five specimen types used for the quantitative tests
Corresponding with Table 5-1, from left to right: 20 -, 20 l, 10 =, 10 -l, 10 ll.

5.1.1 Initial Weight

It was expected that the effectiveness of the treatments would be dependent on the amount of hardening agent absorbed by the specimens. All specimens were weighed prior to any treatment to gauge how much of the hardening agents had been absorbed. On average, the untreated paper material had a volumetric weight of 0.83 g/cm³.

Below are the average weights from 20 of each specimen size, listed in gram as “average (min/max)”. The accuracy of the scale was 1 gram; if the measurement wavered between two numbers, the weight was noted as in between (.5), thus all weights are rounded to nearest half gram.

- 20 mm thick, 12 cm long specimens: 40.0 (38.5/42) g
- 10 mm thick, 13 cm long specimens: 21.5 (21/22.5) g
- 10 mm thick, 14 cm long specimens: 23.5 (22.5 /24.5) g

5.2 Hardening Agents

As the purpose of the first tests was to explore the effects of various hardening agents, a large variety in viscosity, chemical composition and hardening mechanism was desired. This was realized to some degree, but the set of agents used was ultimately influenced by availability. Five different hardening agents were tested:

- **EPIKOTE™ Resin MGS™ RIMR 135 lamination resin**

RIMR 135 is an epoxy resin designed for vacuum infusion of composite laminates. Mixed with 30 weight% of curing agent RIMH 137 it has a curing time of 6–8 hours[41]. When cured, the epoxy can be heat-treated at 60°C to reduce its brittleness, which is recommended. Properties of the cured and heat-treated epoxy are listed in Table 5-2 (The complete datasheet can be found in the appendix). The lamination resin was expected to provide the best result in terms of mechanical properties, but it is both expensive and environmentally hazardous. Other types of hardening agents were tested to see the effects of other types and less “forceful” agents.

Table 5-2 Typical properties of RIMR 135 lamination epoxy (Cured 24h at 23°C + 15h at 60°C) [41]

Density	1,18–1,20	g/cm ³
Modulus of elasticity	2,7–3,2	GPa
Flexural strength	90–120	MPa
Tensile strength	60–75	MPa
Compressive strength	80–90	MPa

- **Cascol Indoor PVA-based “wood glue”**

PVA, *Polyvinyl acetate*, is a thermoplastic polymer used primarily as adhesive or hardening agent for porous materials, for example paper, textiles, sandstone and wood[42]; hence it is often referred to as “wood glue”. Wood glue is readily available, designed for wood materials and biodegradable, which preserves the eco-friendliness of the models. It is water-soluble when liquid, has very high viscosity and hardens to

become plastic-like, but not brittle. It is water-resistant, but not waterproof. Mcor sells a PVA-based coating they developed themselves called FLEX, which makes the models more durable but is designed to facilitate flexibility[43]. Regular wood glue is however designed to prohibit movement and was expected to moderately improve the paper material's properties without compromising the economic and environmental benefits of the models.

- **Cascol Indoor, diluted 30 vol%**

Wood glue diluted to 30 volume percent water to increase infusibility and ease of application with lowered viscosity. Diluted wood glue is for example used for paper-mâché and was predicted to interact very well with the paper material.

- **Classic Uretan Lakk polyurethane-based wood lacquer**

Polyurethane is a versatile polymer used as hardening or binding agent in adhesives, insulation foam, wood panels and more[44]. As wood lacquer it is typically used on wooded floor boards to create a hard, durable surface. It has medium viscosity and makes the models waterproof.

- **Epolan V Epoxi Lakk epoxy floor finish**

2-component epoxy polymer utilized to create hard, industrial-grade finishes on concrete or wooden floors. It is water-based, but becomes completely waterproof when cured.



Figure 5-2 Hardening agents explored during the quantitative testing.
 Form the left: Casco Indoor, Classic Uretan Lakk, Epolan V Epoxi Lakk, RIMR 135 resin.



Figure 5-3 Vacuum infusion equipment for quantitative specimens

5.3 Vacuum Infusion

5.3.1 Equipment

Inspired by at-home wood stabilization methods[33,35], an ad hoc infusion chamber was built and used for the quantitative test specimens. As shown in Figure 5-3, the setup consisted of a glass jar as vacuum chamber, a hand-powered vacuum pump[45], and an intermediate container to stop spillage from ruining the pump. The handheld pump gave more control over the vacuum pressure compared to the on-or-off vacuum pump that was available at the laboratory, and the jar made an appropriately sized chamber for the specimens.

5.3.2 Infusion Process

All specimen treatments were carried out at the Polymers and Composites Laboratory at NTNU. The undiluted wood glue was excluded from the vacuum infusion treatment because of the high viscosity, and was only applied to the specimens as a coating (see subchapter 5.4). The four remaining agents were each infused into five specimens—one of each type mentioned in 5.1. The process was the same for all agents and was done as follows:

1. The glass jar was filled half-full with the hardening agent, the five specimens were added and the jar filled up to one cm above the specimens.
2. A piece of plastic was placed on top of the specimens to push them completely below the surface when the lid of the jar was attached.

3. The tube to the vacuum pump was connected and the vacuum increased steadily to around -23.5 inHg (approximately -0.80 bar) over 3–5 minutes, restricting the rate of frothing as to not cause spillage.
4. The vacuum was held stable for 1 hour, during which the chamber was shaken lightly from time to time to encourage air escaping the specimens.
5. After one hour the vacuum was released and the specimens left to soak in the agent for 1 more hour.
6. The specimens were retrieved from the jar and brushed off gently to remove excess agent. They were left to dry for 24 hours in 21°C under a low-set air suction vent and then at least 72 hours in a normally ventilated room at ~22°C, to ensure that the agents had hardened properly before testing. To counter the effect of gravity, all were flipped twice during the first hour and then every hour for three more hours, to achieve as uniform saturation as possible.

(Note: The specimens were **not** heat-treated after the initial 24 hours of curing, admittedly because the writer was not aware at the time that this was recommended.)



Figure 5-4 Vacuum infusing specimens with RIMR135 epoxy. The vacuum forces air out of the porous paper material, frothing the liquid agent—a good sign.

5.4 Supplementary Treatments

In addition to the vacuum infusion, specimens were also coated with and soaked in (at normal pressure) some of the hardening agents. Naturally, vacuum infusion was expected to achieve superior results, as the agent would permeate further into the specimens. One of the major

appeals of 3D printing is however its speed and simplicity, which does not resonate well with the vacuum infusion process. The two faster and quicker treatments were therefore applied, both for comparison with the vacuum infusion and to see what the simpler treatments, that someone using a 3D printer might be more willing to apply, may achieve in terms of strengthening the material. (These treatments however were considered to be of less importance and therefore not applied to all specimen types or with all agents for various practical reasons²). Method:

Coating: two thin coats were applied with a paint brush with about an hour to dry in between.

Soaking: specimens were submerged for 10 minutes. Excess agent gently brushed off.



Figure 5-5 Soaking specimens in Classic Uretan Lakk (left) and wood glue (right)

An unfortunate effect was observed with specimens that had been soaked or infused with the water based hardening agents, wood glue and Epolan V Epoxi—they wetted the paper. Figure 5-6 shows some examples. Just like you would expect regular paper to react when wetted, the specimens expanded and deformed as a result, especially in the corners. None of the other agents experienced this. The effect was strongest for specimens infused with the diluted wood glue (the agent with the highest water-content). The inevitable recommendation is that water based hardening agents should only be used as a coating, not applied in ways that allow for deeper penetration of the paper.

²Coating with normal wood glue was very troublesome due to the high viscosity and stickiness. The remainder of both epoxies had obtained an unusable viscosity after the infusion; there was some Epolan V Epoxy left to use during the infusion, but buying or mixing more to treat more specimens was considered wasteful and unnecessary.

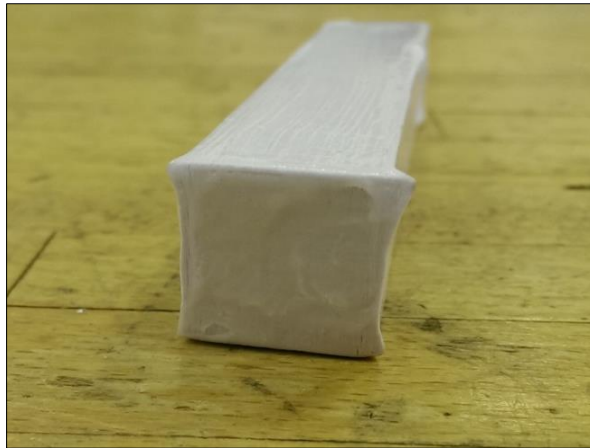


Figure 5-6 Specimen wetted by the diluted wood glue

5.5 Amount of Agent Absorbed

Specimens were weighed before and after treatment to see how much of the agents had been absorbed. Table 5-3 lists the average weight increases compared to the average initial weight, with the (biased) sample variances in italics[46]. Keep in mind that these are taken from only six or fewer specimens, so the individual numbers are not particularly meaningful. Those from only one or two specimens are marked with an apostrophe ('). When comparing the numbers however, some trends are visible: the infused specimens absorbed the most, which was expected, but the differences to the soaked specimens (which absorbed second most) are generally small. The infusion process appeared to have been much less effective than was initially hoped and predicted for. The lamination epoxy, which is of course designed for

Table 5-3 Specimens' average and variance in weight increase for each agent and treatment, in percent.

Agent	Treatment	$\bar{\Delta W}$ [%]	Var(W)
Wood glue	Soaking	11,5	3.8
Diluted wood glue	Coating	5.7	11.8
	Soaking	7.6	4.8
Classic Uretan Lakk	Infusion	8.5	7.0
	Coating	4.4'	3.8'
	Soaking	19.5	30.2
Epolan V Epoxi	Infusion	23.7	14.6
	Coating	3.0'	0.0'
	Soaking	6.0'	0.0'
RIMR135 epoxy	Infusion	12.0	3.6
		48.6	70.9
		45.1*	12.4*

'Very few specimens

*Excluding the high values of specimen "10-1"

vacuum infusion, penetrated much deeper into the specimens than the other agents, adding almost 50% to its specimens' weight. Notably, the epoxy seems to have penetrated primarily through the sides perpendicular to the layers (in other words in between, not through the sheets of paper), which explains why specimen "10-l" obtained the best saturation. This was true for several of the other agents as well, and should be kept in mind if vacuum infusion were to be used to strengthen a model.

Beside the lamination epoxy, Classic Uretan Lakk worked moderately well with almost 25% increase; the rest of the infusion results were however disappointing. It seems that unless an agent specifically designed for vacuum infusion is utilized, simply coating or soaking the model may be the preferred treatment for general applications.

5.6 Results of the Quantitative Bending Tests

Within this chapter the results from the quantitative test phase are presented and briefly discussed. Values for stiffness, maximum load and corresponding bending stress for the aluminium and untreated paper specimens are listed in Table 5-4. Table 5-5 contains the same for the treated specimens, with the addition of the individual specimen's weight-increase (compared to the average initial weight, which results in a slightly higher variance than in reality). Graphs for all tests are available in the appendix. Observations made during the testing are discussed in short in section 5.6.1.

Table 5-4 Stiffness and strength of the aluminium and untreated paper specimens

Material	Specimen type	Stiffness, m [N/mm]	Max load [N]	Max bending stress, $\sigma_{B,max}$ [MPa]
Untreated paper	10 =	88	ND	
	10 -l	400	228	
	10 ll	833	380	
	20 -	73	ND	
	20 -	97	ND	
	20 l	717	460	
	20 l	1 000	610	
Aluminium	5-	760	2 300	621
	5-	750	2 100	567
	5-	730	2 200	594
	10 -	4 350	8 700	587
	10 -	4 400	8 800	594
	10 l	8 830	18 000	608
	10 l	7 760	18 300	618
	20	15 750	Out of range	-
	20	14 500	Out of range	-

ND: Not Determinable, due to high creep rate even at low deformation

Table 5-5 Weight increase, stiffness and maximum strength for the treated specimens

Specimen/ Hardening agent	Treatment	Specimen type	Weight increase, %	Stiffness, <i>m</i> [N/mm]	Max load [N]
Wood Glue, diluted 30v%	Coating	20 –	3	98	ND
		20 I	5	1 700	940
		10 =	12	48	ND
		10 II	7	900	480
		10 –I	2	413	280
	Dipping	20 –	5	95	ND
		20 I	8	1 550	860
		10 =	7	Data lost ³	Data lost ³
		10 II	12	1 000	455
		10 –I	7	750	420
	Infusion	20 –	5	83	ND
		20 I	8	1 700	880
		10 =	12	43	ND
		10 II	7	775	630
		10 –I	12	400	425
Wood Glue	Dipping	20 I	10	1 230	1 170
		10 =	11	31	ND
		10 II	15	600	560
		10 –I	11	510	435
Classic Uretan Lakk	Coating	20 I	3	1 875	1 300
		10 –I	6	540	410
	Dipping	20 –	13	185	ND
		20 I	15	1 660	1 100
		10 =	23	53	ND
		10 II	19	1 100	830
		10 –I	28	625	415
	Infusion	20 –	25	140	ND
		20 I	28	2 800	1 100
		10 =	19	65	ND
10 II		19	830	520	
10 –I		28	530	520	
2K Epoxy Wood Lacquer	Coating	20 –	3	100	ND
		20 I	3	1 550	680
	Dipping	10 –I	6	382	320
	Infusion	20 –	10	107	ND
		20 I	13	780	680
		10 =	15	40	ND
		10 –I	11	338	370
RIMR135 EpoxyResin	Infusion	20 –	40	2 430	3 800
		20 –	45	3 140	4 150
		20 I	43	8600	6200
		10 =	49	767	1 870
		10 II	49	4 375	4 850
		10 –I	66	1 330	1 970

³ Unfortunately, one of the test results was lost due to user error.

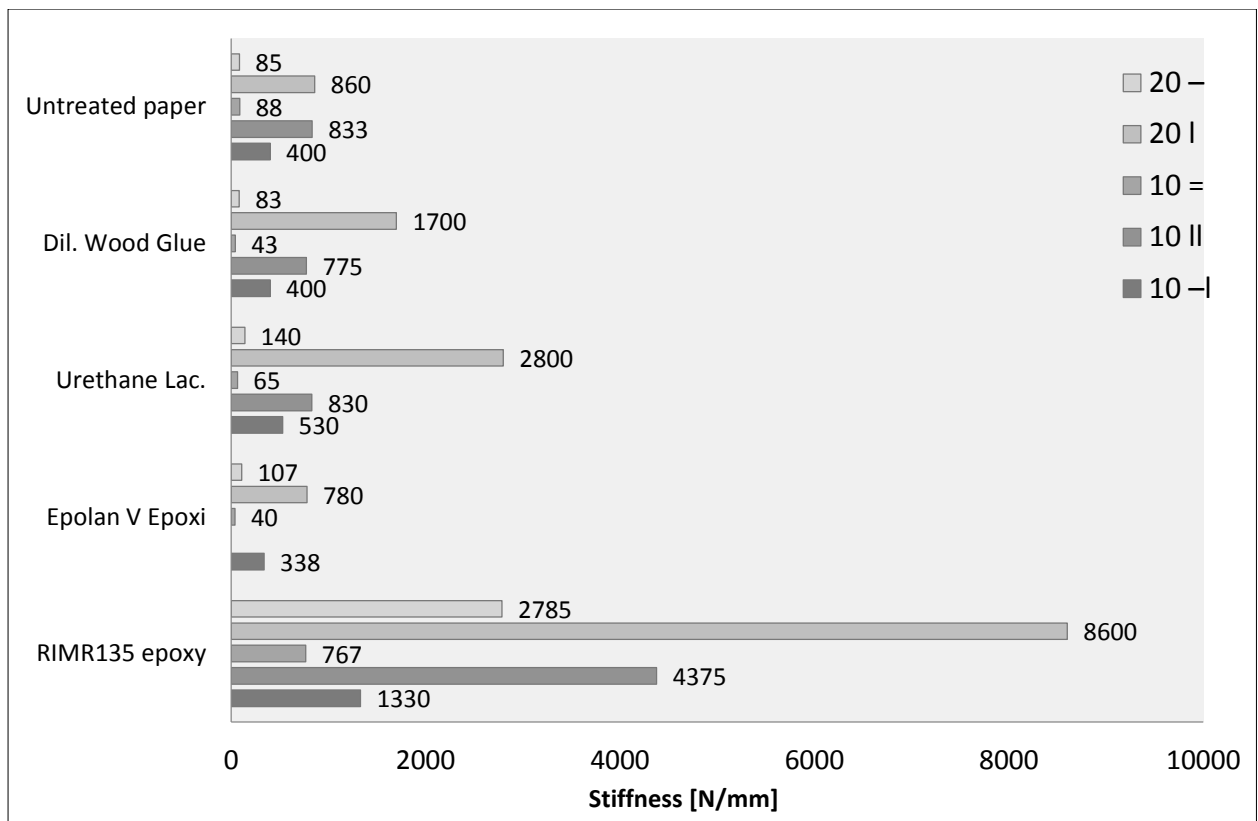


Figure 5-7 Stiffness measurements of the infused specimens

Figure 5-7 compares the stiffness measurements of all the infused specimens and the untreated paper. These and the numbers in Table 5-5 are all single-specimen results, so the numbers themselves are of course unreliable. It is nonetheless evident that, excluding the lamination epoxy, the treatments did improve the stiffness and strength of the paper, but not by much. Once again, the differences between the vacuum infusion and the other treatments are small, corresponding with the poor infusion results. It is possible that with lower pressure over longer time, and longer time soaking, the infusion process would be more effective and provide larger improvements.

The RIMR135 lamination epoxy however showed impressive results in the bending tests, with all specimens improving greatly upon both the stiffness and strength of the untreated paper. The specimens were still highly anisotropic, indicating that the strength of the paper itself still contributed significantly to the specimen's. Those with vertical layers performed around half as well as the similar aluminium specimens. However, accounting for the difference in density between aluminium (2.71 g/cm^3) and the infused paper laminate ($0.83 \times 1.45 = 1.2 \text{ g/cm}^3$) the stiffness of the paper was up to 1.28 times of the average for the aluminium!

5.6.1 Observations during Testing

As seen in Figure 5-8, the untreated specimens showed similar tendencies during the bending tests as they did during the initial observations of the material: the flat-layered specimens were very soft and bent into an S-shape, while the vertically layered specimens were much stiffer but buckled quickly. At large deformations, the latter would tear at the underside of the fold. All the untreated specimens also exhibited high creep rates, even at low deflection, which showed every time the deflection rate halted between pumps. This can be attributed to the flexibility of the glue for the specimens with flat layers and to the innate paper's ability to relax over time for the vertically layered.

Except for those infused with the lamination epoxy, all treated specimens exhibited the same deformations and failure mechanisms as the untreated ones, at varying degree. Figure 5-9 shows the S-shape of specimen "10=" and buckling of "10-l", both infused with Classic Uretan Lakk. Despite the generally disappointing results, the hardening agents did work well in preventing delamination of the paper sheets. Because of this, the improvements seen in the vertically layered specimens were much greater than the horizontal (some of which performed *worse* than the untreated paper).

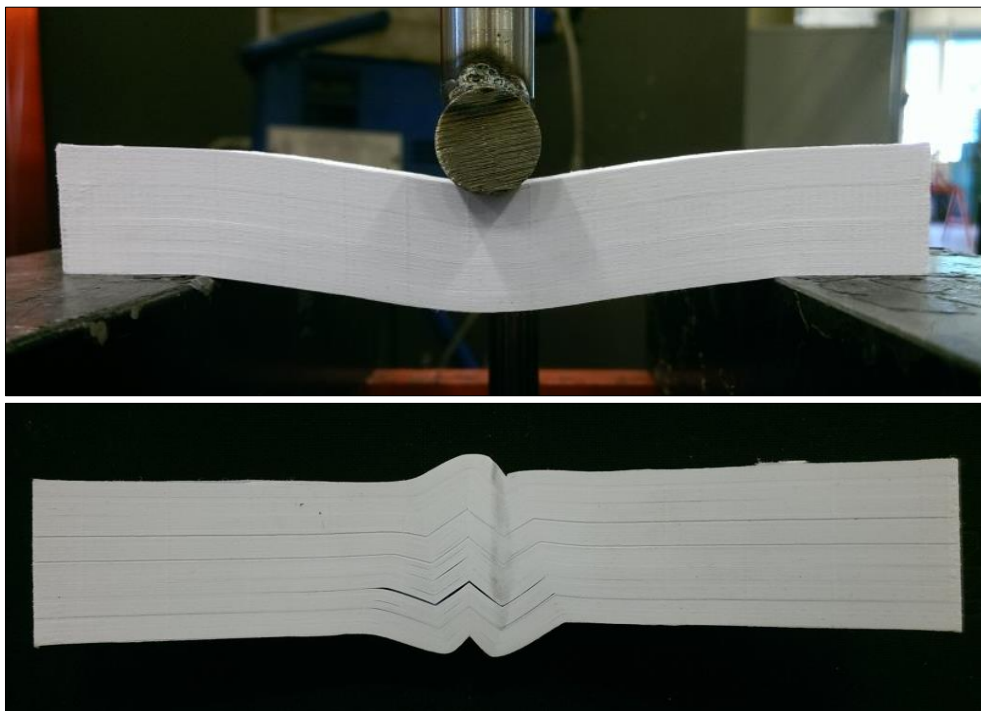


Figure 5-8 Deformation and buckling of the untreated paper laminate

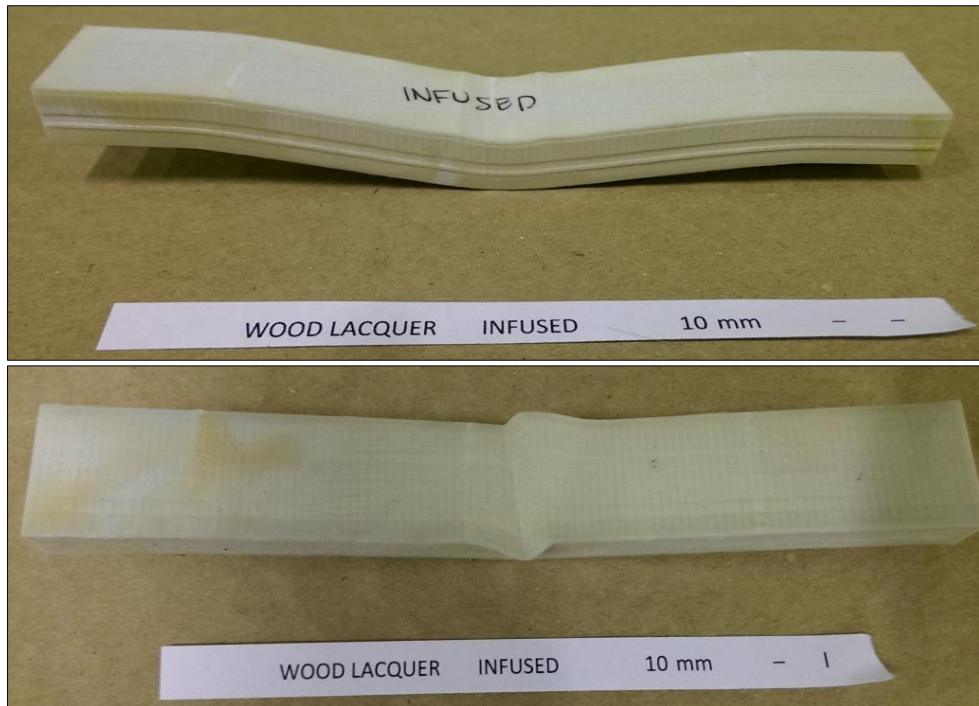


Figure 5-9 Specimens treated with urethane wood lacquer showing same type of deformations as the untreated specimens.

The specimens infused with lamination epoxy did not deform and buckle, but instead suffered brittle failures. It was clear that the thick, short specimens experienced large internal shear forces, which caused the horizontally layered specimens to fracture along the mid plane (as seen in Figure 5-10) where the shear forces are strongest[47]. With the vertically layered specimen however, the break could not tear through the layers and instead fractured across the specimen.

The clean breaks through the specimens revealed that the infusion process had in fact not fully saturated the paper material (see Figure 5-111), which could be the reason for the



Figure 5-10 Failure along the mid plane of epoxy infused specimen “20–”

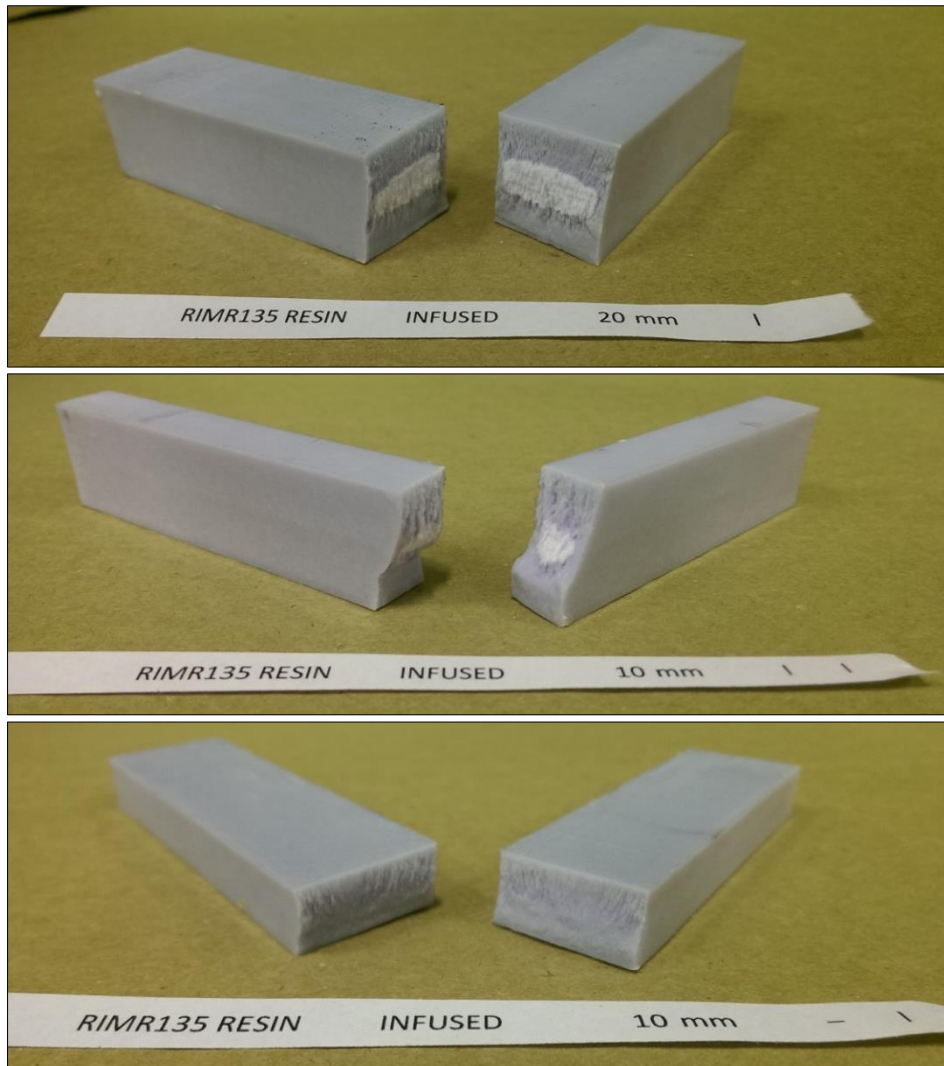


Figure 5-11 Brittle breaks of epoxy infused specimens with vertical layers

perceived anisotropy: the epoxy penetrated further into the sides of the laminate than through the paper sheets, giving the vertically layered specimens a more favourable infusion “profile”; looking at Figure 5-12, profile (v) has a higher moment of inertia around the horizontal axis than profile (h).

Specimen “10 -|” was fully infused, which accounts for the high relative weight increase.

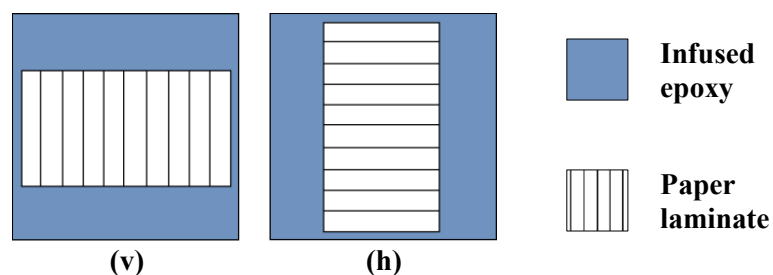


Figure 5-12 Vertically (v) and horizontally (h) layered specimen infusion profiles

6 Qualitative Testing

6.1 Qualitative Specimens

To achieve more reliable results than in the first series of tests, the qualitative specimens were created 24 cm long instead of 12, with a square 2x2 cm cross section. Ten rods were created—two to be tested untreated and eight (four tests per layer orientation) to be infused with RIMR 135 epoxy. The average weight of the untreated 24 cm specimens was unsurprisingly twice the weight of the twelve centimetre specimens: 80 grams (max.: 78 g; min.: 82 g).

6.2 Treating the Specimens

As these specimens were longer, the vacuum chamber jar used for the quantitative specimens was not large enough. Instead, the vacuum pump and degassing chamber available at the laboratory was utilized, and the risk of spillage from vigorous frothing was handled by infusing the specimens in a deep container. The setup and process can be seen in Figures 6-1 to 6-3. The metal wire visible in the pictures was folded in between each specimen to keep them apart and thus achieve proper infusion of them all. The process was done as follows:

1. Epoxy was poured into the container to about 1 cm above the specimens. Metal brackets were placed on top to keep the specimen submerged.
2. The container was sealed in the degassing chamber and the vacuum pump turned on.
3. The pressure sank quickly and was kept at about -26 inHg (-0.88 bar) for 1 hour.
4. The vacuum was released and the specimens left in the epoxy to soak for 1 more hour.
5. After soaking, the specimens cured on a rack for 20 hours. They were flipped over every half hour for two hours, after which the viscosity was high enough to prevent flow.

Noted: 1 litre of epoxy was poured over the specimens and 0.5 litres remained after infusion.

6. After the infusion and initial curing, the specimens *were* heat-treated in an oven at 60°C for 5 hours to reduce brittleness, after which they cooled in room temperature.

Summarized: 1 hour vacuum, 1 hour soaking, 20 hours curing at 21°C, 5 hours at 60°C.

The specimens were tested two days after the heat treatment.

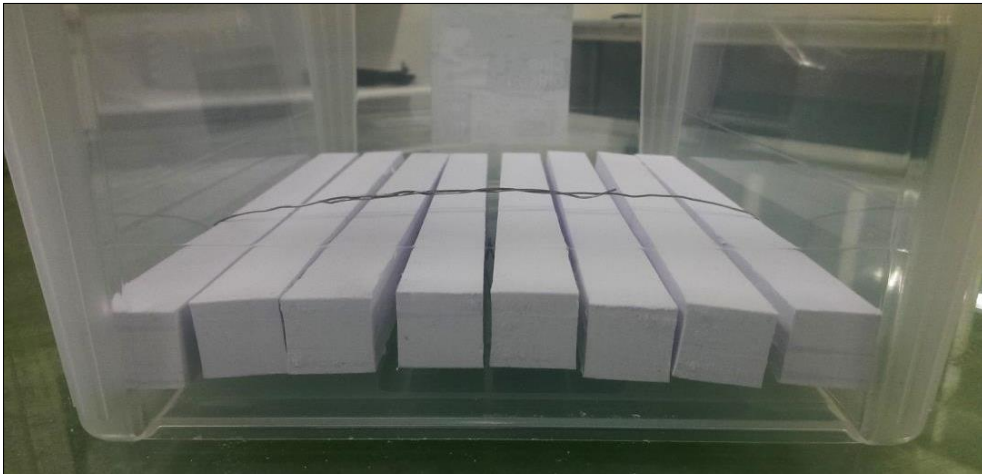


Figure 6-1 Specimens ready for infusion

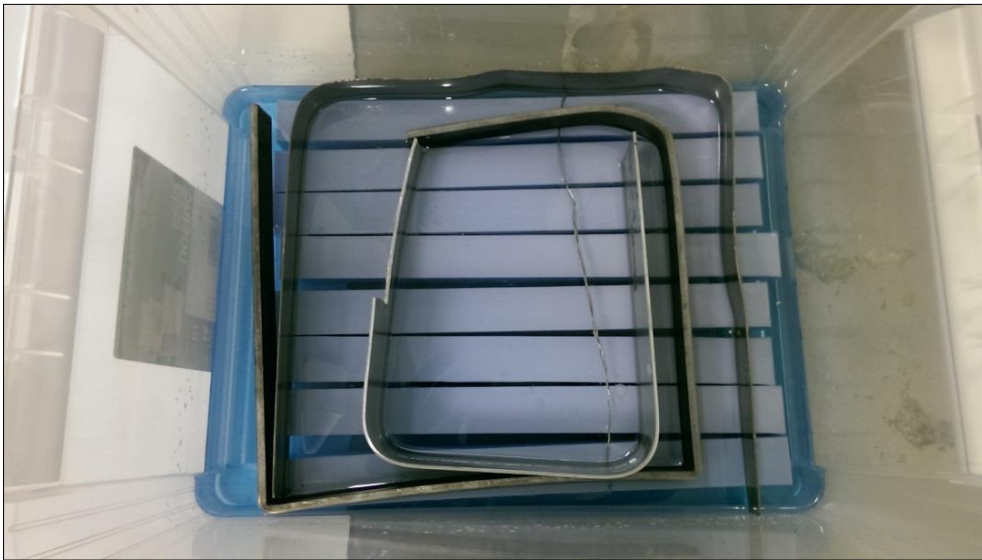


Figure 6-2 Specimens soaking up the epoxy after degassing

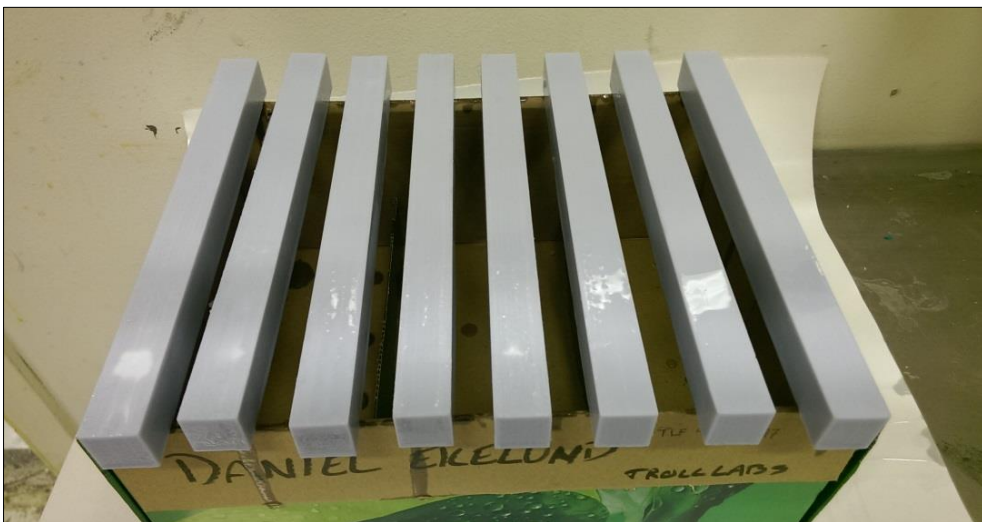


Figure 6-3 Curing the specimens

6.3 Testing

Testing was performed with the same equipment and deflection rate was again kept to best ability around 2 millimetres per minute. Setup was also similar, with the single point-load placed halfway between the two supports, except this time the support gap was 200 mm wide.

Curious about the infused material’s response to load cycles, two of the specimens (number 4 and 8) were loaded cyclically. Number 4 was loaded to 2 mm deflection, released after 30 seconds to 0 mm, then loaded to 4 mm, released again after 30 sec., then loaded to failure. The same was intended with specimen 8, but it failed during the second cycle, at 3.9 mm. The graph for specimen 4 is shown in Figure 6-6.

6.4 Results for the Qualitative Specimens

Table 6-1 lists the results obtained for the 24 cm long specimens—Number P1 and P2 were of untreated paper while 1–8 were infused with RIMR135 lamination epoxy. Figure 6-4 shows that this time the vacuum infusion was able to fully saturate the specimens (except for the very centre of specimen 8). Viewing the test results, the difference between the horizontal and vertical layers was in this case much smaller for both stiffness and maximum load. A larger sample size is required to conclusively tell if there is a definite difference or if the variations found here are simply due to statistical variance. It is possible that the epoxy, and its chemically harsh curing process, deteriorates the paper to such degree that the anisotropic property of the paper laminate is practically lost. Some situations might however benefit from a highly anisotropic structure, in which case a partial infusion of the model can provide this.

Table 6-1 Results from the bending tests of the qualitative specimens

No.	Layer orientation	Agent absorbed [g]	Weight increase, %	Stiffness [N/mm]	Max load [N]	Flexural strength [MPa]
P1	–	0	0	53	Est. <20	<0.75
P1		0	0	308	270	10.1
1	–	57.0	42	Data lost	Data lost	N/A
2	–	55.0	41	567	2 470	92.6
3	–	60.0	43	571	2 630	98.6
4	–	58.5	42	627	3 710	139.1
5		57.5	42	668	3 200	120.0
6		58.0	42	675	3 300	123.8
7		58.5	42	725	2 780	104.3
8		56.5	41	693	2 250	84.4



Figure 6-4 Fracture surfaces of qualitative specimens 5–8

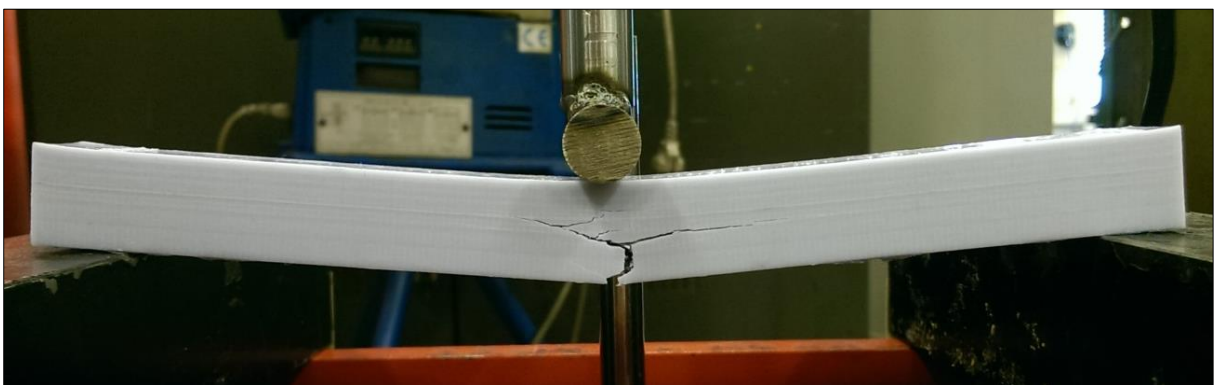


Figure 6-5 Failure of qualitative specimen with flat layers

An interesting observation is the deviating results in strength of the cyclically loaded specimens 4 and 8. The vertically layered specimen 8 performed significantly worse than the rest, not only in terms of breaking load but also breaking strain (3.9 mm versus 5–6 mm for the other specimens). This can be explained by the fact that specimen 8 was the only specimen not fully saturated by the vacuum infusion. Specimen 4 on the other hand, performed considerable better than the rest, both in terms of max load and strain, breaking at an impressive 7.95 mm deflection. This could be due to mechanical conditioning effects from the cyclic loading, increasing the paper sheet's tensile strength, which have been observed[48,49].

As indicated by Figure 6-4, the vertically layered specimens once again suffered brittle fracture transverse to their length, splitting them completely in two. Probably due to a combination of reduced shear effects and the epoxy penetrating into the centre, the long horizontal specimens also fractured through the thickness, not along the mid-plane like the shorter specimens. However, as the crack propagated from the bottom and through the material, it had to break through each layer one by one, which gradually depleted its energy.

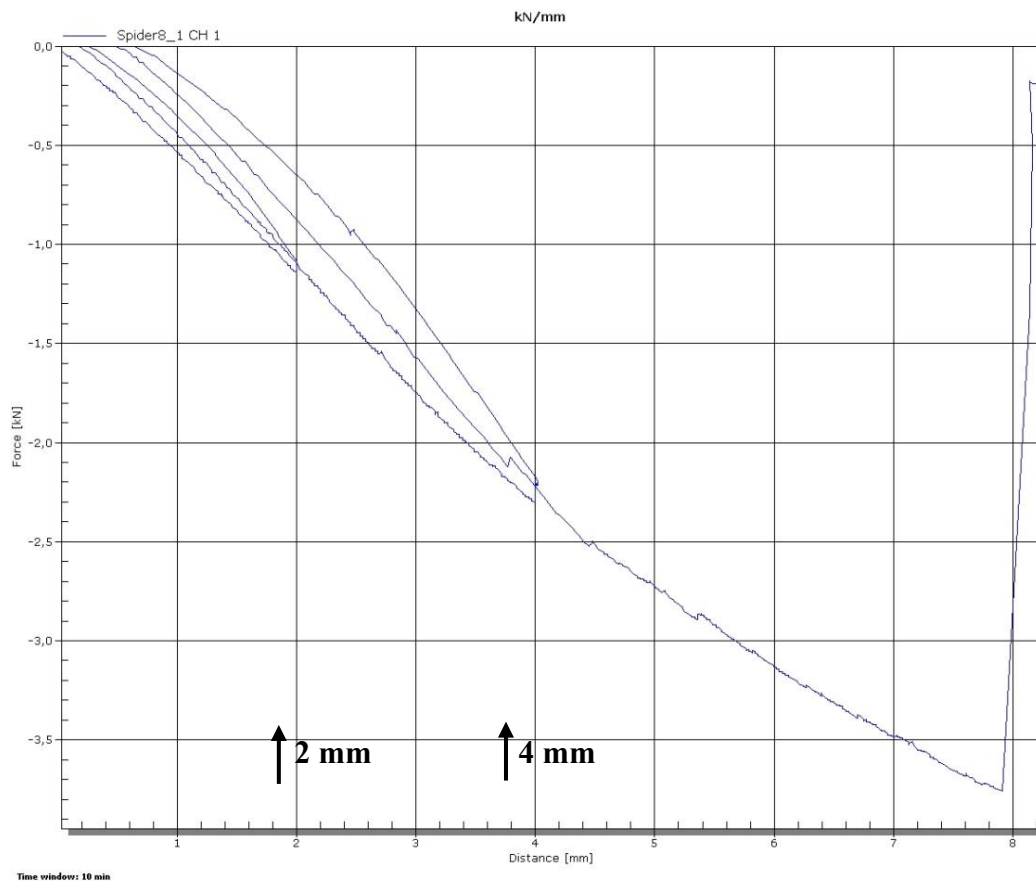


Figure 6-6 Cyclic loading of specimen 4. Force on vertical axis; deflection on horizontal. 2 and 4 mm deflection has been marked for clarification.

In other words, although the stiffness and strength of the horizontally layered specimens were slightly lower, their fracture toughness was higher, and as a result they did not break through-and-through.

6.4.1 Comparing with Aluminium and Pure Epoxy

As discussed in chapter 4.1.3, to draw meaningful conclusions from the stiffness values found in the tests, similar specimens of aluminium are used for comparison. The same is done with pure epoxy (whose properties are listed in Table 5-2) to check if the paper laminate actually contributes positively to the material's properties or if one should rather just create parts purely of the lamination epoxy. To calculate stiffness values for theoretical specimens of the same dimensions, tested in the same setup as the infused paper, classic beam theory is used. The theoretical elastic modulus of 6082 aluminium alloy is 71 GPa[50]; RIMR135's properties are listed in Table 5-2. Classic beam theory states that for a rectangular specimen under three-point bending, the deflection halfway between the supports is given by equation 7.

$$d_{middle} = \frac{FL^3}{48EI} \quad (7)$$

Substituting in $I = wh^3/12$ (eq. 2) and solving for $m = F/d$, we get, with our specimen size:

$$m = 4Ew \left(\frac{h}{L}\right)^3 = 3E \cdot 20 \left(\frac{20}{200}\right)^3 = 0.08E \quad (8)$$

Entering the properties for aluminium and for pure epoxy in equation 8, gives us numbers for stiffness and strength that can be compared with, as listed in Table 6-2. For the infused paper laminate, the values are listed as the average of specimens 2–3 / average of specimens 5–7 (i.e. horizontal / vertical layers).

Table 6-2 Comparing infused paper laminate, epoxy and aluminium

Material	Density [g/cm]	Stiffness [N/mm]	Flexural or yield strength [MPa]	Stiffness/density [Nm ² /kg]	Strength/density [Nm/kg]
Infused paper laminate	1.43	569 / 690	95.6 / 116	398 / 483	66.9 / 81.1
RIMR 135 Epoxy	1.19	216–256	90–120	181–215	75.6–101
6082-T6 aluminium	2.71	568	270	210	99.6

As can be seen, the infused paper material specimens were stiffer than the theoretical aluminium alloy. Accounting for the difference in density, the paper specimens' stiffness was 1.9–2.3 times higher than the aluminium's! The aluminium was however superior in terms of strength, holding over twice the load of the infused paper and the pure epoxy before yielding. Both materials performed better than the pure lamination epoxy alone.

Using vacuum infusion and heat treating of lamination epoxy, 3D printed paper material was able to become stiffer than aluminium, twice as stiff compared to its weight, as well as over two thirds as strong if accounting for the lower density. Considering the immense difference in cost between the equipment and material needed to 3D print similar models in the two materials, epoxy infused paper laminate is definitely a very strong option to aluminium, if not superior in many situations.

7 Conclusion

3D printing enables the creation of objects with complex shapes—*any* shape—from virtual models to physical ones, at a reasonable speed and price. This combination makes it an ideal production method for prototyping, hobby-projects and manufacturing of very complex shapes and frequently changed shapes. There exist plenty of different printers using different methods to print with a wide range of materials, from plastics to metals to composites. Mcor Technologies' printers Matrix300+ and Mcor IRIS uses ordinary, cheap office paper to create models in a material that can be described as a thick paper laminate and in many ways mimics wood.

This project has explored the possibilities and potential for improving the mechanical properties of this material, primarily by utilizing the porosity of the paper to infuse it with lamination epoxy, essentially creating a fibre-reinforced composite. The investigation consisted of two phases: the first explored the effects of infusing, soaking and coating material specimens with five different hardening agents—wood glue, diluted wood glue, urethane wood lacquer, epoxy wood finish and the lamination epoxy. All specimens were tested in three-point bending tests, with which the stiffness gradient and breaking or yield strength were determined from the load-deflection plots. The second phase aimed for more reliable measurements of stiffness and strength using longer specimens of the paper material infused with epoxy, which had also been heat-treated after curing to reduce its brittleness.

Infusion was done using a vacuum chamber to drive air out of the specimens while submerged in epoxy, which then soaked up the epoxy like a sponge when pressure was reintroduced. This method combines very well with 3D printing as it can be utilized with any shape. Full saturation of 2 by 2 cm square specimen was achieved with 1 hour at -0.88 bar vacuum and 1 hour soaking at normal pressure. Larger models can become fully saturated using lower pressure and longer time; how large remains to be determined. Other, more permeable types of paper would likely increase this limit, if there is one. The paper material from IRIS absorbed up to 66% of its weight in epoxy, but more typically around 45%, which increased its density from 0.83 to 1.45 g/cm³.

None of the four “secondary” hardening agents infused well into the material, nor did they perform well during testing. There was an improvement in the material's ability to resist buckling and delamination, resulting in improved stiffness and strength for bending in the already strong orientation, but practically no improvement on bending properties for the weak

orientation. Furthermore, infusing and soaking caused the water-based wood glue and epoxy wood finish to wet the paper material, deforming it. Water based solutions are therefore recommended to only be used as a thin coating.

The shorter specimens infused with lamination epoxy in the first phase were not fully saturated, and as the epoxy permeated easier into the “sides” of the material than through the layers, the uneven distribution of epoxy was more favourable for bending around the strong axis than the weak. However, both orientations improved greatly: the former obtained around half the stiffness of the similar aluminium alloy specimens that were tested, and the latter one third of that.

Following up, eight longer specimens were created and this time fully saturated with epoxy from the vacuum infusion. They were also heat-treated at 60°C for five hours to reduce brittleness. The results from bending these specimens were compared to theoretical specimens of 6082-T6 aluminium alloy and of pure lamination epoxy, whose stiffness and breaking or yield strength was calculated using classic Euler-Bernoulli beam theory. The paper material infused with lamination epoxy and then heat-treated was in fact stiffer than the aluminium alloy (and the pure epoxy)! Accounting for its lower density, the infused paper specimens were twice as stiff and over two-thirds as strong as the aluminium.

Considering the much lower cost of equipment and material, epoxy-infused 3D printed paper laminate is a strong option to other 3D printed materials and deserves to be explored further.

7.1 Further Work

The possibilities for further investigations are many, but three primary areas are here highlighted as being particularly valuable from a 3D printing and production perspective:

1. Vacuum chamber infusion—its capabilities in terms of speed and model size, using other resins and hardening agents; varying pressure, time, volume, etc.
2. Mechanical properties of infused paper laminate—elaborating upon the results found within this project, exploring the capabilities of the material itself.
3. Other types of paper or resin—how well can different types of paper (whose structure, strength, permeability, etc. are unlike office paper) or resins perform using this infusion treatment. Not all resins cure with time but with heat, which would make them more viable for industrial vacuum infusion treatment.

8 References

- [1] "Ultimaker 2", Ultimaker.com [Picture]. Taken from: <https://ultimaker.com/en/products/ultimaker-2-family/ultimaker-2>. [Accessed: 26-Jun-2015].
- [2] "Blueprinter", Inspire3D.ie [Picture]. Taken from: <http://www.inspire3d.ie/products/3d-printers/blueprinter/>. [Accessed: 24-Jun-2015].
- [3] "Mcor IRIS", McorTechnologies.com [Picture]. Taken from: <http://mcortechnologies.com/3d-printers/iris/>. [Accessed: 6-Jul-2015].
- [4] "Colour models created with IRIS", McorTechnologies.com [Picture]. Taken from: <http://mcortechnologies.com/3d-printers/iris/>. [Accessed: 6-Jul-2015].
- [5] Chowdhry, A., 2013, "What Can 3D Printing Do? Here Are 6 Creative Examples," Forbes.com [Online]. Available: <http://www.forbes.com/sites/amitchowdhry/2013/10/08/what-can-3d-printing-do-here-are-6-creative-examples/>. [Accessed: 18-Jun-2015].
- [6] "Fused Filament Fabrication," RepRap.org [Online]. Available: http://reprap.org/wiki/Fused_filament_fabrication. [Accessed: 14-Jun-2015].
- [7] "FDM Technology," Stratasys.com [Online]. Available: <http://www.stratasys.com/3d-printers/technologies/fdm-technology>. [Accessed: 14-Jun-2015].
- [8] 2012, "Fused Deposition Modeling," Additive3D.com [Online]. Available: <http://www.additive3d.com/fdm.htm>. [Accessed: 15-Jun-2015].
- [9] 2012, "Laser Sintering," Additive3D.com [Online]. Available: <http://www.additive3d.com/sls.htm>. [Accessed: 15-Jun-2015].
- [10] 2012, "Stereo Lithography," Additive3D.com [Online]. Available: <http://www.additive3d.com/sl.htm>. [Accessed: 15-Jun-2015].
- [11] Buchbinder, D., Schleifenbaum, H., Heidrich, S., Meiners, W., and Bültmann, J., 2011, "High Power Selective Laser Melting (HP SLM) of Aluminum Parts," Proceedings of the Sixth International WLT Conference on Lasers in Manufacturing, Elsevier Ltd., Munich, Germany, pp. 271–278.
- [12] Krishnan, M., Atzeni, E., Canali, R., Manfredi, D., Calignano, F., Ambrosio, E. P., and Iuliano, L., 2013, "Influence of post-processing operations on mechanical properties of AlSi10Mg parts by DMLS," High Value Manufacturing: Advanced Research in Virtual and Rapid Prototyping: Proceedings of the 6th International Conference on Advanced Research in Virtual and Rapid Prototyping, Leiria, Portugal, 1-5 October, 2013, P.J. da S. Bartolo, A.C.S. de Lemos, A.M.H. Pereira, A.J.D.S. Mateus, C. Ramos, C.D. Santos, D. Oliveira, E. Pinto, F. Craveiro, H.M.C. da R.T.G. Bartolo, H. de A. Almeida, I. Sousa, J.M. Matias, L. Durao, M. Gaspar, N.M.F. Alves, P. Carreira, T. Ferreira, and T. Marques, eds., CRC Press, pp. 243–248.
- [13] Manfredi, D., Calignano, F., Krishnan, M., Canali, R., Ambrosio, E. P., and Atzeni, E., 2013, "From Powders to Dense Metal Parts: Characterization of a Commercial AlSiMg Alloy Processed through Direct Metal Laser Sintering," *Materials*, **6**(3), pp. 856–869.
- [14] 2013, "Laminated Object Manufacturing and related technologies," Additive3D.com [Online]. Available: http://www.additive3d.com/com4_lks.htm. [Accessed: 22-Jun-2015].
- [15] "3D Printer Uses Standard Paper," RapidToday.com [Online]. Available: <http://www.rapidtoday.com/mcor.html>. [Accessed: 17-Apr-2015].
- [16] "LOM Rapid Prototyping," CubicTechnologies.com [Online]. Available: <http://www.cubictechnologies.com/Helisys.htm>. [Accessed: 15-Jun-2015].
- [17] 2012, "Laminated Object Manufacturing," Additive3D.com [Online]. Available: <http://www.additive3d.com/lom.htm>. [Accessed: 14-Apr-2015].

- [18] Shiri Habib-Valdhorn, "3D printer co Solido lays off entire workforce," *Globes.co.il*. [Online]. Available from: <http://www.globes.co.il/en/article-1000615567>. [Accessed: 22-Jun-2015].
- [19] 2015, "Solido SD300 pro," *SolidModelUSA.com* [Online]. Available: <http://www.solidmodelusa.com/collections/solido>. [Accessed: 22-Jun-2015].
- [20] Brooke, R., 2014, "Mcor reports 'extraordinary' growth," *TCTMagazine.com*. [Online]. Available from: <http://www.tctmagazine.com/3D-printing-news/mcor-reports-extraordinary-growth/>. [Accessed: 24-Jun-2015].
- [21] Martin, S., 2015, "Mcor Technologies Closing in on \$20M+ Funding with Annual Sales Up +600% on Paper-Based 3D Printers," *SolidSmack.com*. [Online]. Available from: <http://www.solidsmack.com/fabrication/ces-2014-mcor-technologies-closing-20m-funding-annual-sales-600-paper-based-3d-printers/>. [Accessed: 20-Jun-2015]
- [22] "3D Printers - Mcor IRIS - Review," *Aniwaa.com* [Online]. Available: <http://www.aniwaa.com/product/mcor-iris/>. [Accessed: 22-Jun-2015].
- [23] "Blueprinter," *Blueprinter-Powder-3dprinterco.uk* [Online]. Available: <http://blueprinter-powder-3dprinter.co.uk/>. [Accessed: 18-May-2015].
- [24] "Ultimaker 2 | Ultimaker," *Ultimaker.com* [Online]. Available: <https://ultimaker.com/en/products/ultimaker-2-family>. [Accessed: 18-May-2015].
- [25] 2015, "10 Reasons Paper-based 3D Printing is Better." *Mcor Technologies [White Paper]*. Available from: <http://mcor technologies.com/resources/white-papers/>. [Accessed: 22-Jun-2015].
- [26] 2015, "Paper making," *PaperOnline.com* [Online]. Available: <http://www.paperonline.org/paper-making/paper-production>. [Accessed: 26-Jun-2015].
- [27] Ekelund, D. I., 2015, Visit at Peterson paper factory, [Personal notes].
- [28] Ling, A., 2015, "Re: Porosity and tensile strength of Multicopy Original 80gsm." [E-mail] Receiver: Ekelund, D.I. [Received: 25-May-2015].
- [29] "Physical properties," *PaperOnWeb.com* [Online]. Available: <http://www.paperonweb.com/paperpro.htm>. [Accessed: 22-Jun-2015].
- [30] Reece, J., 2014, "Dispelling myths about Mcor's paper-based 3D printing," *McorTechnologies.com* [Online]. Available: <http://mcor technologies.com/dispelling-myths-about-mcors-paper-based-3d-printing-blog/>. [Accessed: 21-Jun-2015].
- [31] Farebrother, T. H., 1944, "Stress/Strain Curves of Boards," *Proc Papermak. Assoc. GBI*, **25**, p. 216. As sited in Rance, H.F., 1954, "The Mechanical Properties of Paper," [s.1.]
- [32] "Vacuum Infusion - The Equipment and Process of Resin Infusion," *FibreGlast.com* [Online]. Available: <http://cdn.fibreglast.com/downloads/vacuuminfusion.pdf>. [Accessed: 03-Jun-2015].
- [33] 2014, "Wood Stabilizing," *Craft Supplies USA* [Online]. Available: <http://blog.woodturnerscatalog.com/2014/02/wood-stabilizing-v-2/>. [Accessed: 27-Jun-2015].
- [34] "Information about stabilized woods," *BurlSales.com* [Online]. Available: <http://burlsales.com/stabilized.html>. [Accessed: 27-Jun-2015].
- [35] D. Comeau, "Wood Stabilization," *Comeau Cust. Knives* [Online]. Available: <http://dcknives.blogspot.no/p/wood-stabilization.html>. [Accessed: 27-Jun-2015].
- [36] "AEP Tranducer TS C2," *AEPTransdcers.com* [Online]. Available: <http://www.aeptransducers.com/load-cells/82-ts.html>. [Accessed: 26-Jun-2015].
- [37] "Spider 8, HBM," *HBM.com* [Online]. Available: <http://www.hbm.com/en/menu/products/measurement-electronics-software/specialized-data-acquisition-systems/spider8/>. [Accessed: 30-Jun-2015].
- [38] "HBM catman - Professional Data Acquisition Software" [Online]. Available: <http://www.hbm.com/en/menu/products/software/data-acquisition-software/catman/>. [Accessed: 30-Jun-2015].

- [39] Adams, D., 2010, "The short beam shear test," CompositesWorld.com [Online]. Available: <http://www.compositesworld.com/articles/the-short-beam-shear-test>. [Accessed: 28-Jun-2015].
- [40] Sideridis, E., and Papadopoulos, G. A., 2004, "Short-beam and three-point-bending tests for the study of shear and flexural properties in unidirectional-fiber-reinforced epoxy composites," *J. Appl. Polym. Sci.*, **93**(1), pp. 63–74.
- [41] 2006, "Technical Data Sheet, EPIKOTE™ Resin MGS™ RIMR 135," Hexion.com [Online]. Available: <https://www.hexion.com/Products/TechnicalDataSheet.aspx?id=8246>. [Accessed: 05-Jun-2015].
- [42] Gettens, R. J., and Stout, G. L., 1966, *Painting Materials: A Short Encyclopaedia*, Dover Publications, New York, USA.
- [43] 2014, "Mcor Technologies introduces new finishing option for IRIS and Matrix line of 3D printers, Mcor FLEX," McorTechnologies.com [Online]. Available: <http://mcor technologies.com/mcor-technologies-introduces-new-finishing-option-for-iris-and-matrix-line-of-3d-printers-mcor-flex-2/>. [Accessed: 24-Jun-2015].
- [44] 2015, "Polyurethane Applications," Polyurethane.AmericanChemistry.com [Online]. Available: <http://polyurethane.americanchemistry.com/Introduction-to-Polyurethanes/Applications>. [Accessed: 29-Jun-2015].
- [45] "Vakuumtester/bremsluftingssett - Testinstrument - Biltema" [Online]. Available: <http://www.biltema.no/no/Bil---MC/Verktoy-og-verkstedutstyr/Testinstrument-og-Elektronikk/Vakuumtesterbremsluftingssett-2000022139/>. [Accessed: 29-Jun-2015].
- [46] Weisstein, E. W., "Sample Variance," Mathworld--Wolfram Alfa [Online]. Available: <http://mathworld.wolfram.com/SampleVariance.html>. [Accessed: 04-Jul-2015].
- [47] Haukaas, T., "Timoshenko Beams," InRisk UBC [Online]. Available: http://www.inrisk.ubc.ca/files/2012/11/Timoshenko_Beams1.pdf. [Accessed: 25-Jun-2015].
- [48] Gibbon, S. K., 1944, "Stress/Strain Curves of Paper," *Proc Papermak. Assoc. GBI*, **25**, p. 199.
- [49] Steenberg, B., 1947, "Paper as a Visco-elastic Body - II," *Sven. Papperstidn*, **50**, p. 346.
- [50] 2015, "6082-T6 Aluminum," MakeItFrom.com [Online]. Available: <http://www.makeitfrom.com/material-properties/6082-T6-Aluminum/>. [Accessed: 03-Jul-2015].

Appendix

Included in the appendix:

Risk Assessment of Experimental Work

Resin RIMR135 and curing agent RIMH137 Technical Data Sheet, Hexion

Bending Test Plots, Catman Easy

NTNU	Kartlegging av risikofylt aktivitet			Utarbeidet av	Nummer	Dato
				HMS-avd.	HMSRV2601	22.03.2011
HMS				Godkjent av Rektor		Erstatter 01.12.2006

Enhet: IPM

Linjeleder: Torgeir Welo

Deltakere ved kartleggingen (m/ funksjon): **Martin Steinert (veileder), Daniel Ihlen Ekelund (student)**
(Ansv. veileder, student, evt. medveiledere, evt. andre m. kompetanse)

Kort beskrivelse av hovedaktivitet/hovedprosess: Masteroppgave Daniel Ihlen Ekelund: 3D-Printed Paper as Structural Material

Er oppgaven rent teoretisk? (JA/NEI): NEI



Signaturer: Ansvarlig veileder:

Student: *Daniel Welo Ekelund*

Dato: 4.2.2015

ID nr.	Aktivitet/prosess	Ansvarlig	Eksisterende dokumentasjon	Eksisterende sikringstiltak	Lov, forskrift o.l.	Kommentar
1	Styrkeprøving av prøver i aluminium, 3D printet papir og behandlet 3D printet papir (se 2).	D. Ekelund		Vernebriller		
2	Dyppe papirprøver i trelim.	D. Ekelund		Plasthansker		
3	3D printing av papirmodeller	D. Ekelund		Ingen		

Issued: August 2006

EPIKOTE™ Resin MGS™ RIMR 135 and EPIKURE™ Curing Agent MGS™ RIMH 134–RIMH 137

CHARACTERISTICS

Approval	German Lloyd
Application	Specially designed for infusion processes (RMT, SCRIMP/VARI); rotor blades for wind turbines, boat and shipbuilding, sports equipment
Operational Temperature	-60 °C up to +50 °C (-76 °F up to 122 °F) without heat treatment -60 °C bis +80 °C (-76 °F up to 176 °F) after heat treatment
Processing	At temperatures between 10 °C and 50 °C (50-122 °F) due to the very low mixing viscosity especially suited for infusion, injection and pultrusion
Features	Very low viscosity, excellent initial curing properties at room temperature, pot life from approx. 0,5 hours to approx. 4 hours, short curing times at high temperatures
Storage	Shelf life of 24 months in originally sealed containers

APPLICATION

Very low viscosity laminating resin system with different pot lives for processing of glass, carbon and aramide fibers. Due to its good mechanical properties, this system is suitable for the production of components featuring high static and dynamic loadability.

The range of pot lives is between approx. 0,5 hour and 3-4 hours. The parts can be worked and demoulded after curing at room temperature. Curing at higher temperatures (up to approx. 80-100 °C, 176-212 °F) is possible, depending on layer thickness and geometry of the parts to be manufactured. The curing times can be reduced to a few minutes by this.

Adding internal parting agents, such as zinc stearate, etc., has proven useful for pultrusion processes. Profiles with good surface qualities are obtained. Depending on profile geometry, mould temperatures in the range of 180-230 °C (356-446 °F) are possible, thus permitting high drawing speeds.

The mixing viscosity is very low, which is especially advantageous for infusion and injection processes. It may be lowered to approx. 150 mPas by heating the resin mass (see diagram). This means that even complicated molded parts with long flow paths can be easily infused. The temperature rise with hardener RIMH 137 remains very low up to a mold temperature of approx. 30 °C, so that even parts of greater thickness can be produced at elevated temperatures.

The infusion resin system does not contain any unreactive components. The raw materials used feature a

very low vapor pressure. This permits processing of the material under vacuum even at elevated temperatures (VARIM process). Compatibility problems are not to be expected in combination with UP gelcoats, various paints (e.g. PUR-based), etc. However, comprehensive tests are indispensable.

The relevant industrial safety regulations for the handling of epoxy resins and hardeners and our instructions for safe processing are to be observed.

The resin and hardeners can be stored for at least 24 months in their carefully sealed original containers. The resin and hardeners may crystallise at temperatures below +15 °C (59 °F). The crystallisation is visible as a clouding or solidification of the contents of the container. Before processing, the crystallisation must be removed by warming up. Slow warming up to approx. 50-60 °C (122-140 °F) in a water bath or oven and stirring or shaking will clarify the contents of the container without any loss of quality. Use only completely transparent products. Before warming up, open containers slightly to permit equalization of pressure. Caution during warm-up! Do not warm up over an open flame! While stirring up, use safety equipment (gloves, eyeglasses, respirator).

SPECIFICATIONS

		Infusion Resin RIM 135
Density	[g/cm ³]	1,13 - 1,17
Viscosity	[mPas]	700 - 1.100
Epoxy equivalent	[g/equivalent]	166 - 185
Epoxy value	[equivalent/100g]	0,54 - 0,60
Refractory index		1,548- 1,552

		Hardener RIMH 134	Hardener RIMH 137
Density	[g/cm ³]	0,93 - 1,00	0,93 - 0,98
Viscosity	[mPas]	10 - 80	10 - 50
Amine Value	[mg KOH/g]	550 - 700	400 - 600
Refractory index		1,4900 - 1,5000	1,460 - 1,463

Measuring conditions: measured at 25 °C / 77 °F

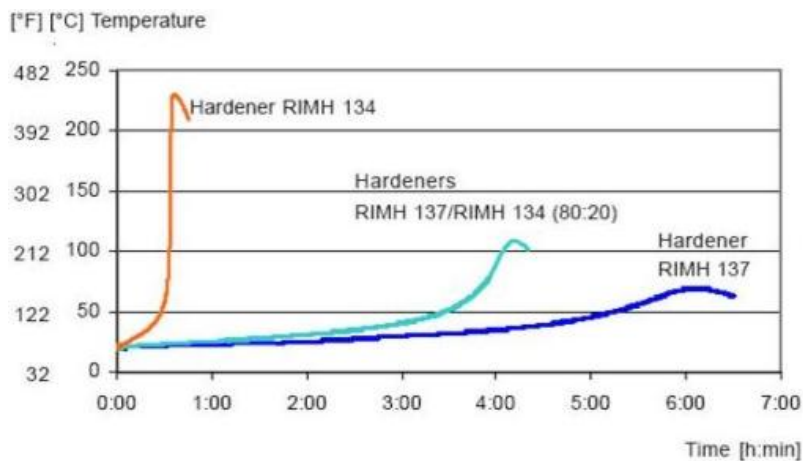
PROCESSING DETAILS

	Infusion Resin RIMR 135	Hardeners RIMH 134-137
Average EP - Value	0,56	-
Average amine equivalent	-	52

MIXING RATIOS

	Infusion Resin RIMR 135 : Hardener RIMH 134 – RIMH 137
Parts by weight	100 : 30 ± 2
Parts by volume	100 : 36 ± 2

The specified mixing ratios must be observed as exactly as possible. Adding more or less hardener will not effect a faster or slower reaction - but in incomplete curing which cannot be corrected in any way. Resin and hardener must be mixed very thoroughly. Mix until no clouding is visible in the mixing container. Pay special attention to the walls and the bottom of the mixing container.

TEMPERATURE DEVELOPMENT

Quantity: 100 g / 20 °C (77 °F)

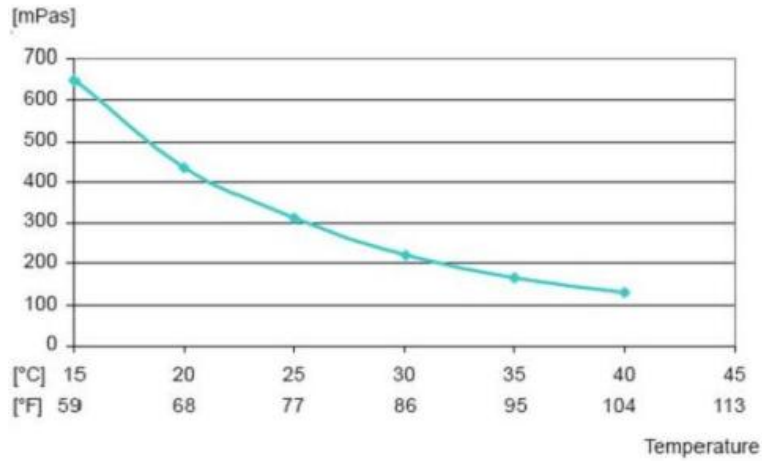
The optimum processing temperature is in the range between 20 °C and 25 °C (68-77 °F). Higher processing temperatures are possible, but will shorten pot life. A rise in temperature of 10 °C (50 °F) will halve the pot life. Water (for example very high humidity or contained in fillers) causes an acceleration of the resin/hardener reaction. Different temperatures and humidities during processing have no significant effect on the strength of the hardened product.

Do not mix large quantities - particularly of highly reactive systems - at elevated processing temperatures. The heat flow from the mixing container is very low, so the contents will heat up fast because of the dissipating reaction heat (exothermic resin-hardener reaction). This can result in temperatures of more than 200 °C (392 °F) in the mixing container, which may cause smoke-intensive burning of the resin mass.

VISCOSITY

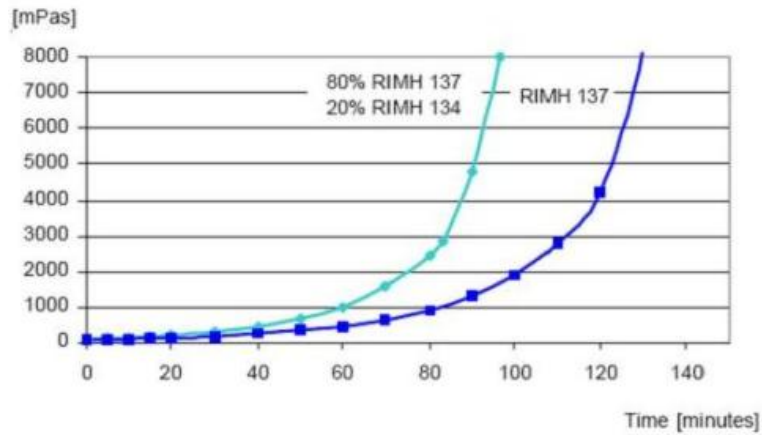
Viscosity of mixture at different temperatures

Infusion resin RIM 135 with mixture of Hardeners RIMH 137 (80 %) /RIMH 134 (20 %)



Viscosity development

Infusion resin RIM 135 with mixture of Hardeners RIMH 137 (80 %) /RIMH 134 (20 %) and Hardener RIMH 137



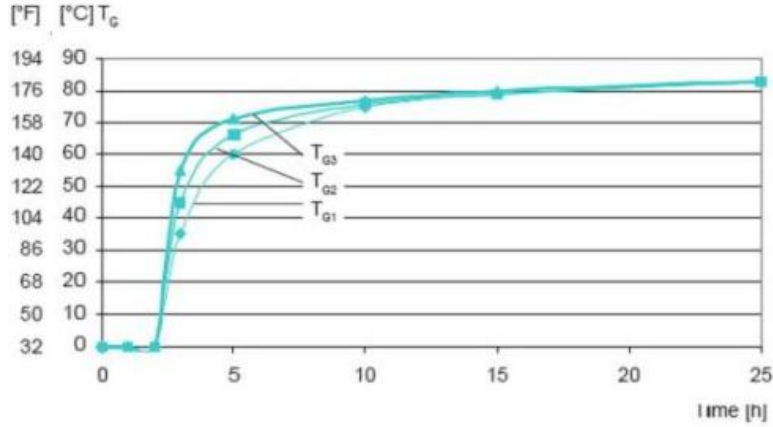
Measuring conditions:

Temperature: 40°C (104 °F); measuring gap 0,2 mm

T_g DEVELOPMENT

Development of glass transition temperature (T_g) at 60 °C

Infusion resin RIM 135 with mixture of Hardeners RIMH 137 (80 %) /RIMH 134 (20 %)

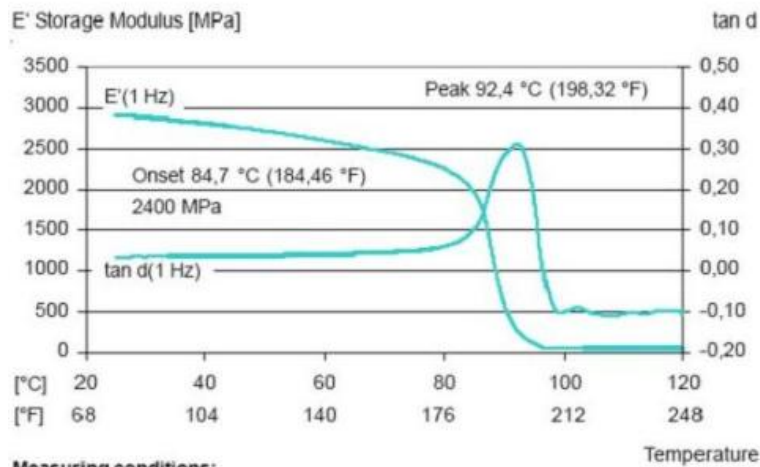


DMA

DMA Measuring after heat treatment

DMA-T_g (peak) tan delta

Infusion resin RIM 135 with mixture of Hardeners RIMH 137 (80 %) /RIMH 134 (20 %)



Measuring conditions:
 Sample thickness: 2 mm
 Heat rate: 2 K/min

MECHANICAL DATA

Mechanical Data of Neat Resin		
Density	[g/cm ³]	1,18 - 1,20
Flexural strength	[N/mm ²]	90 - 120
Modulus of elasticity	[kN/mm ²]	2,7 - 3,2
Tensile strength	[N/mm ²]	60 - 75
Compressive strength	[N/mm ²]	80 - 90
Elongation of break	[%]	8 - 16
Impact strength	[KJ/m ²]	70 - 80
Water absorption at 23 °C	24 h [%]	0,10 - 0,20
	7 d [%]	0,20 - 0,50
Fatigue strength under reversed bending stresses acc. to DLR Brunsw.	10%	exp. > 1 x 10 ⁶
	90%	exp. > 2 x 10 ⁶
Curing: 24 h at 23° C (74° F) + 15 h at 60° C (140° F), partly cured/full cure		
Typical data according to WL 5.3203 Parts 1 and 2 of the GERMAN AVIATION MATERIALS MANUAL		

Advice: Mechanical data are typical for the combination of laminating resin RIMR 135 with hardener RIMH 137. Data can differ in other applications.

Data of Reinforced Resin – Static Tests Standard Climate

Reinforced with:		GRC Glass Fibre	CRC Carbon Fibre	SRC Aramide Fibre
Flexural strength	[N/mm ²]	510 - 560	720 - 770	350 - 380
Tensile strength	[N/mm ²]	460 - 500	510 - 550	400 - 480
Compressive strength	[N/mm ²]	410 - 440	460 - 510	140 - 160
Interlaminar shear strength	[N/mm ²]	42 - 46	47 - 55	29 - 34
Modulus of elasticity	[kN/mm ²]	20 - 24	40 - 45	16 - 19
<p>GRC samples: 16 layers of glass fabric, 8H satin, 296 g/m² (8.7 oz/sq.yd.), 4 mm (0.16 in) thick CRC samples: 8 layers of carbon fabric, plain, 200 g/m² (5.9 oz/sq.yd.) 2 mm (0.08 in) thick SRC samples: 15 layers of aramide fabric, 4H satin, 170 g/m² (5.0 oz/sq.yd.) , 4 mm (0.16 in) thick</p> <p>Fibre content of samples during processing/testing: 40-45 vol% Data calculated for fibre content of 43 vol%</p> <p>Typical data according to WL 5.3203 Parts 1 and 2 of the GERMAN AVIATION MATERIALS MANUAL</p> <p>Sample Preparation: Curing: 24 h at 23 °C (74 °F) +15 h at 80 °C (180 °F)</p>				

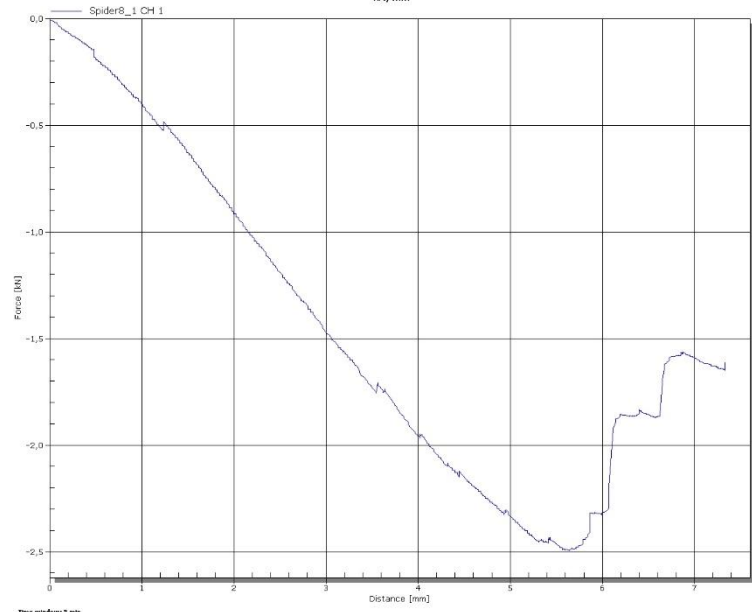
® and ™ Licensed trademarks of Hexion Inc.

DISCLAIMER

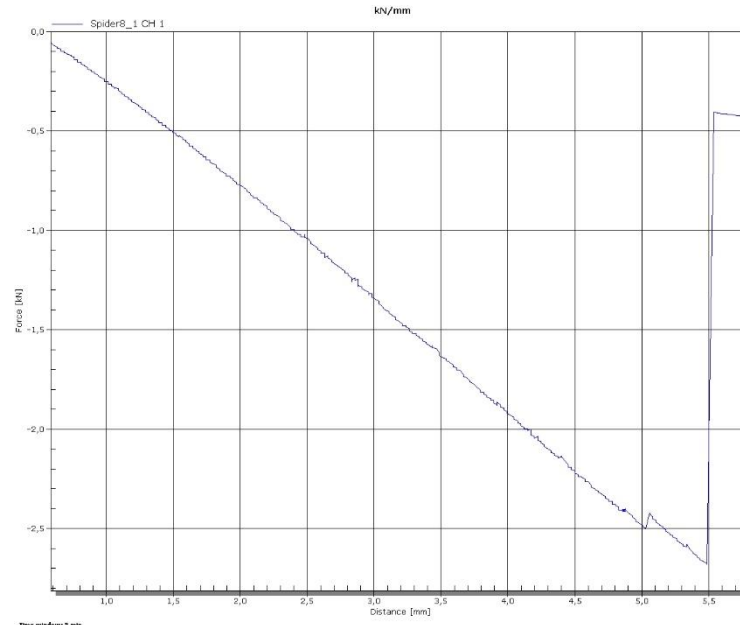
The information provided herein was believed by Hexion Inc. ("Hexion") to be accurate at the time of preparation or prepared from sources believed to be reliable, but it is the responsibility of the user to investigate and understand other pertinent sources of information, to comply with all laws and procedures applicable to the safe handling and use of the product and to determine the suitability of the product for its intended use. All products supplied by Hexion are subject to Hexion's terms and conditions of sale. **HEXION MAKES NO WARRANTY, EXPRESS OR IMPLIED, CONCERNING THE PRODUCT OR THE MERCHANTABILITY OR FITNESS THEREOF FOR ANY PURPOSE OR CONCERNING THE ACCURACY OF ANY INFORMATION PROVIDED BY HEXION,** except that the product shall conform to Hexion's specifications. Nothing contained herein constitutes an offer for the sale of any product.

PDS-8246- (Rev.6/28/2015 2:42:03 PM)

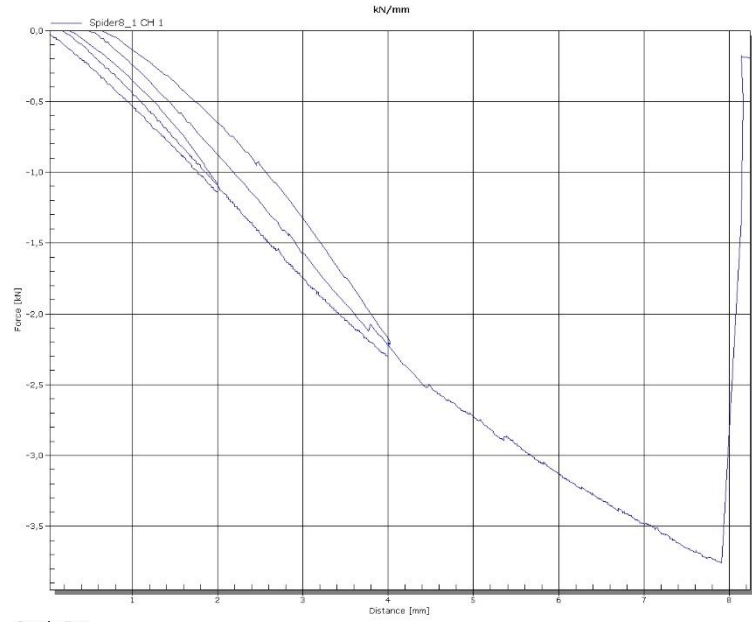
Graphs: 240mm specimens RIMR134 Resin L=200mm



2-: Time window: 5 min

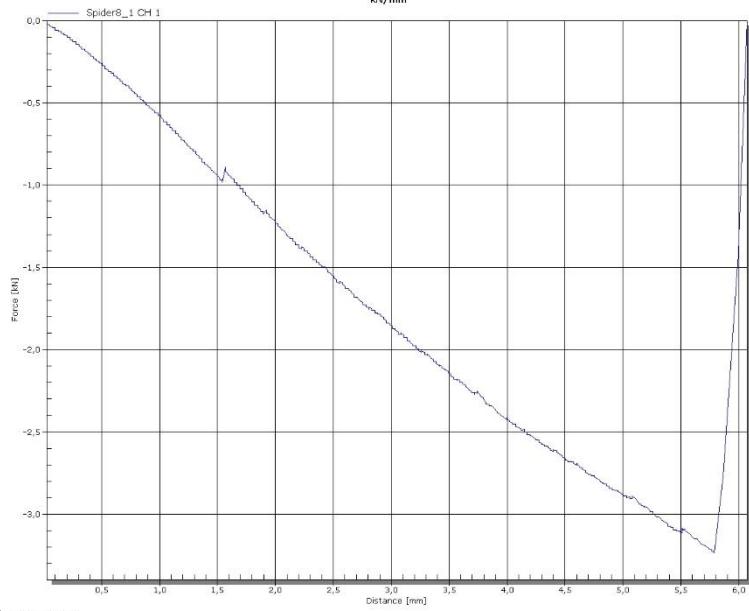


3-: Time window: 5 min

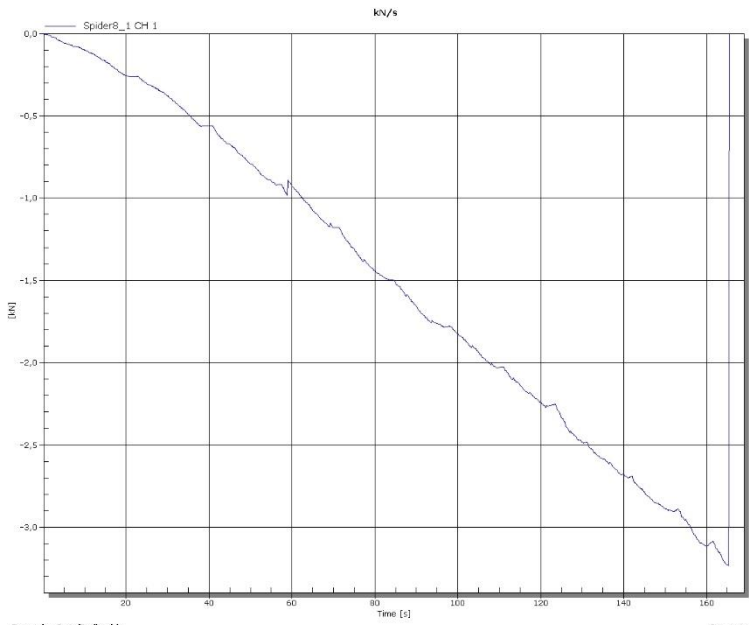


4-: Time window: 10 min

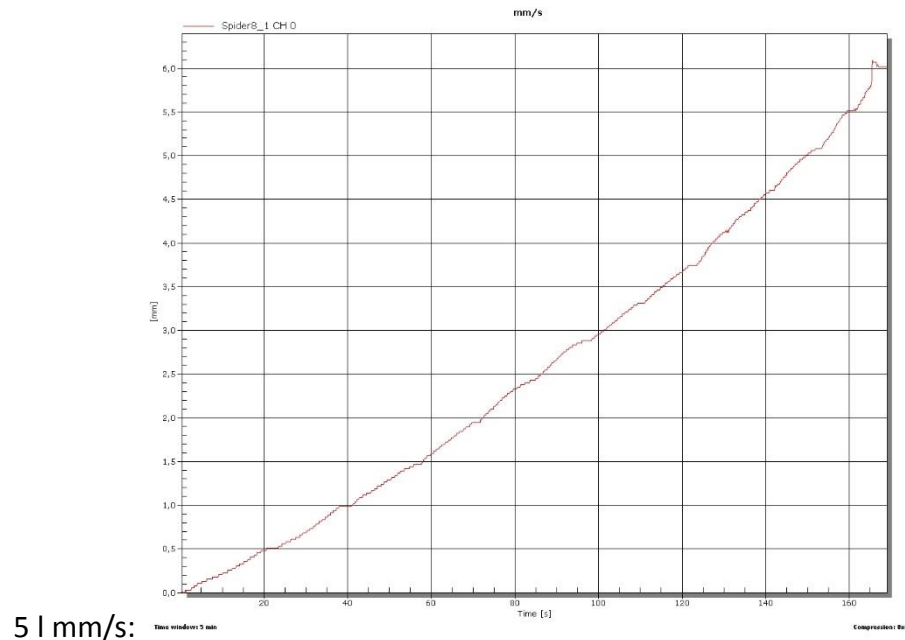
Graphs: 240mm specimens RIMR134 Resin L=200mm



51 F/mm:

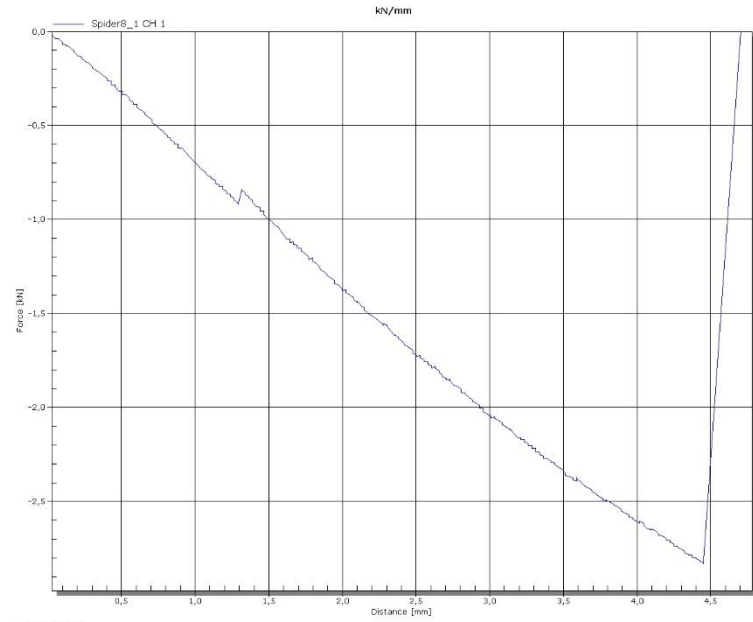
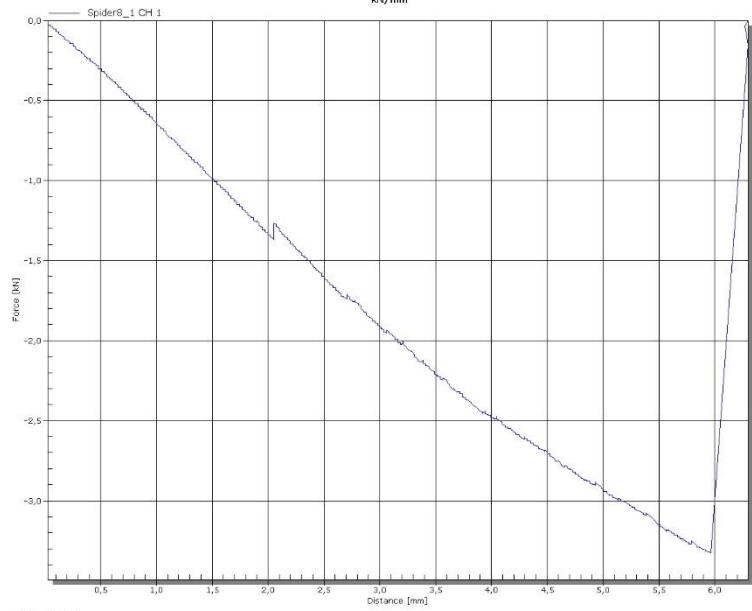


51 F/s:

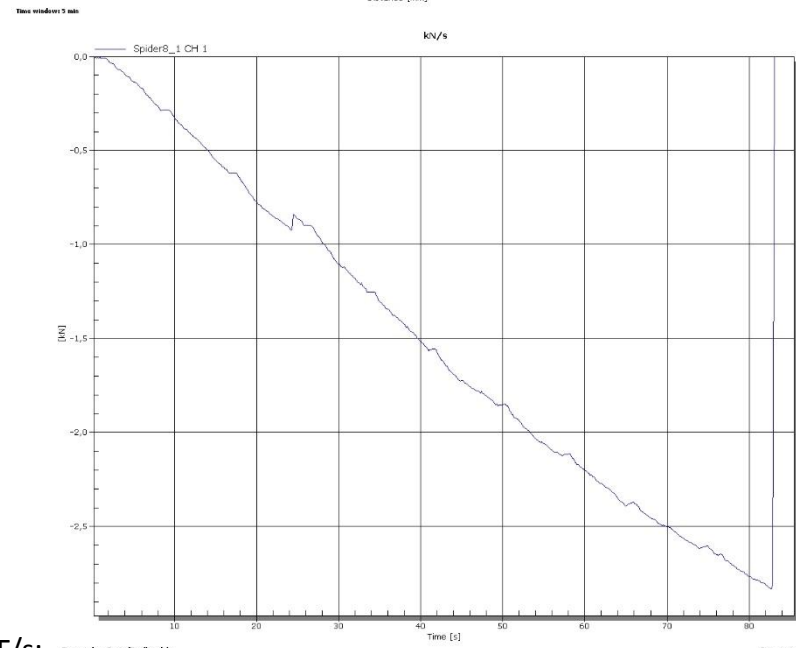


51 mm/s:

Graphs: 240mm specimens RIMR134 Resin L=200mm

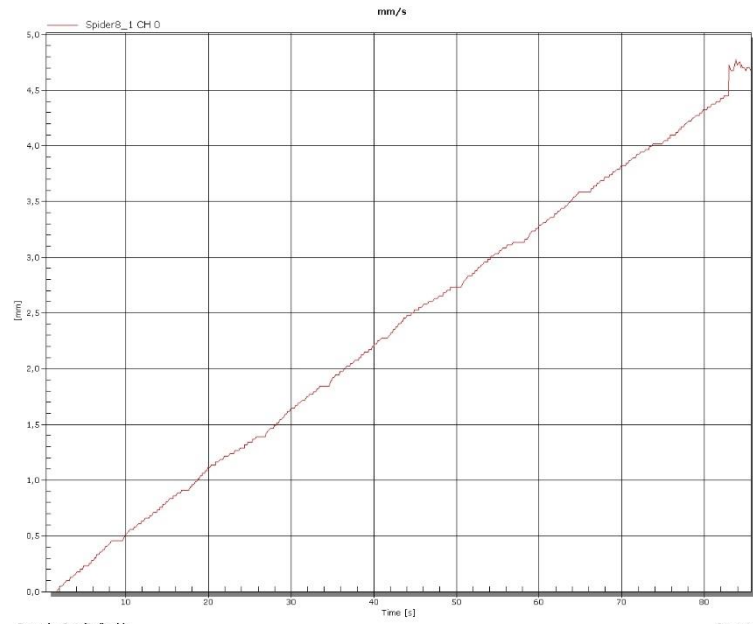


6 l:



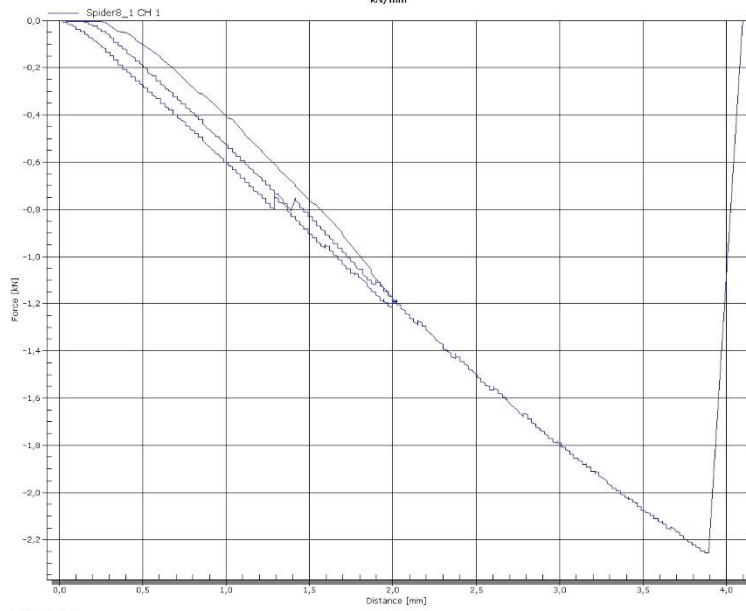
7 l F/s:

7 l F/mm:

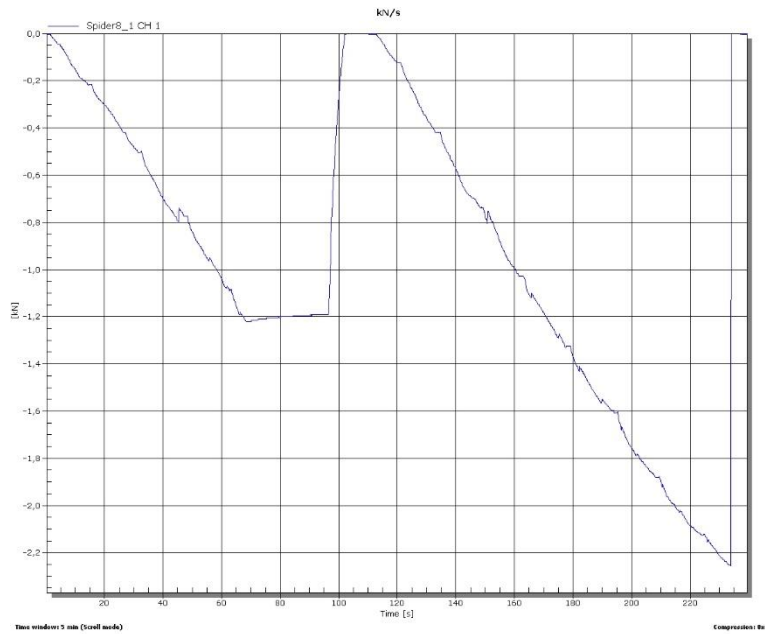


7 l mm/s:

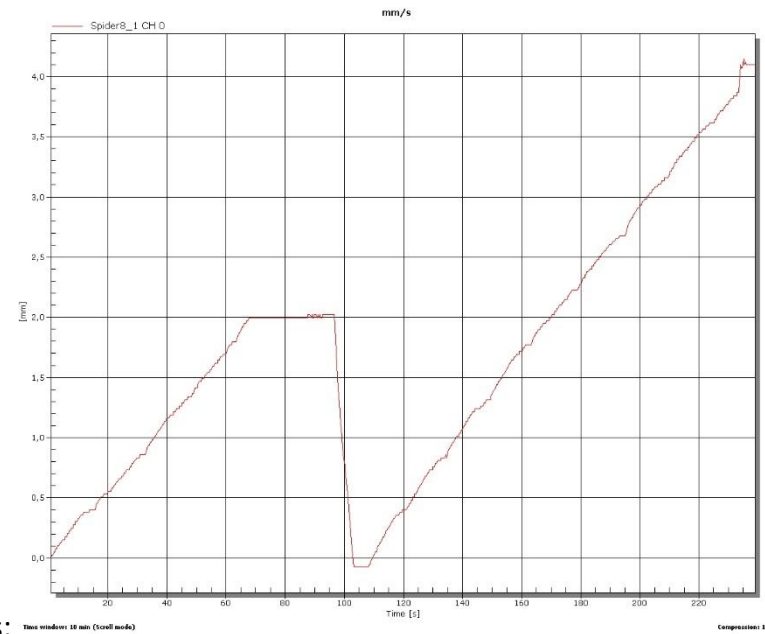
Graphs: 240mm specimens RIMR134 Resin L=200mm



8 l F/mm:

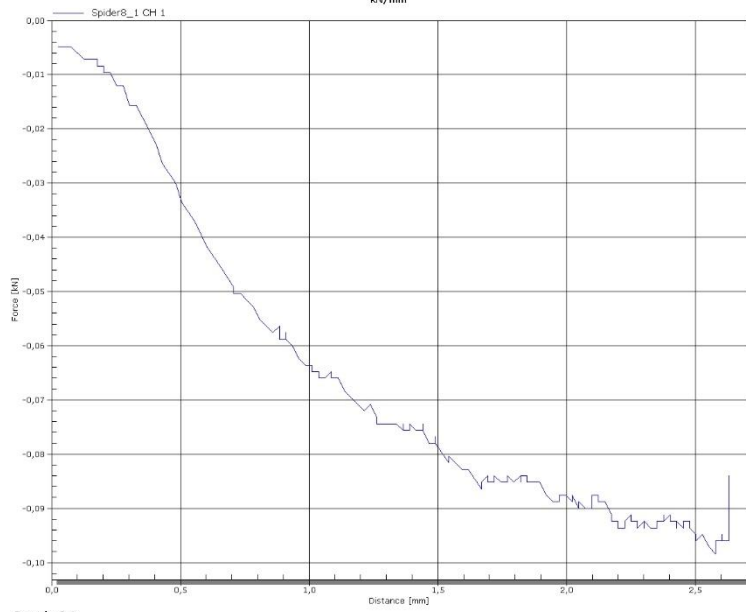


8 l F/s:

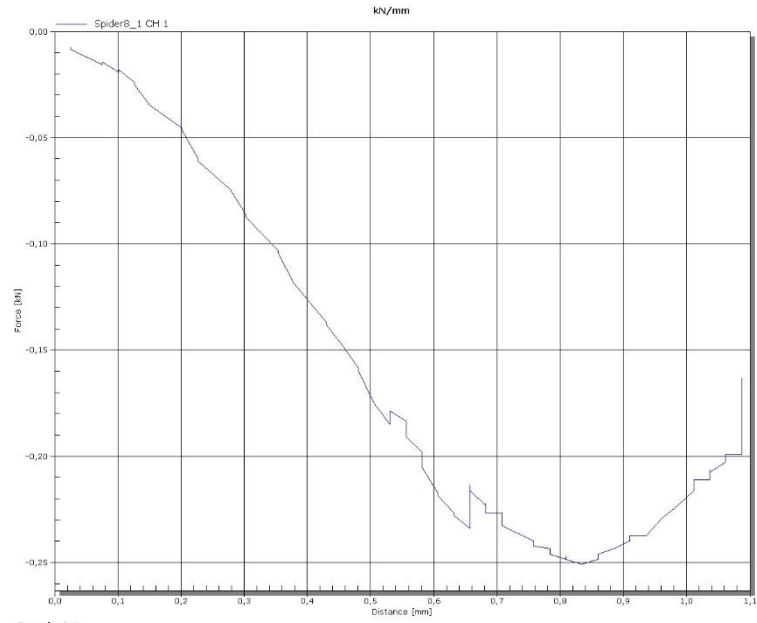


8 l mm/s:

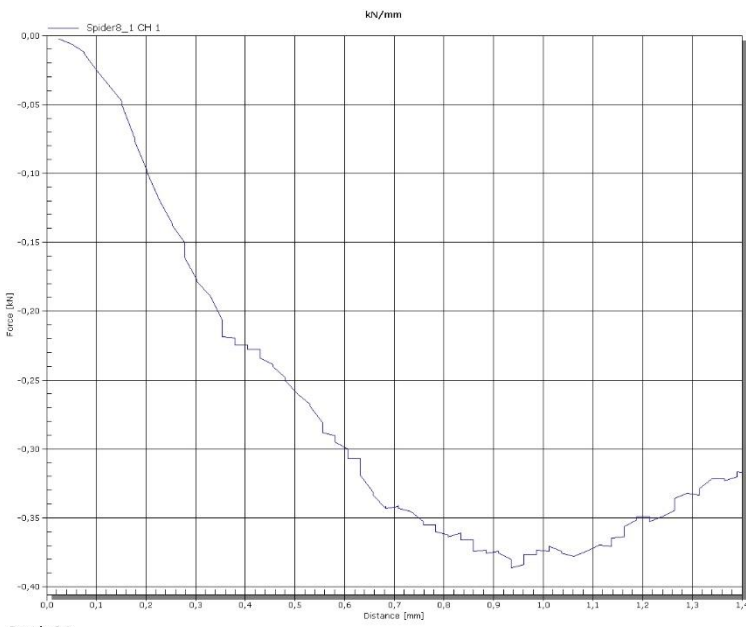
Graphs: Paper Vanilla L=90mm/200mm



10 --:

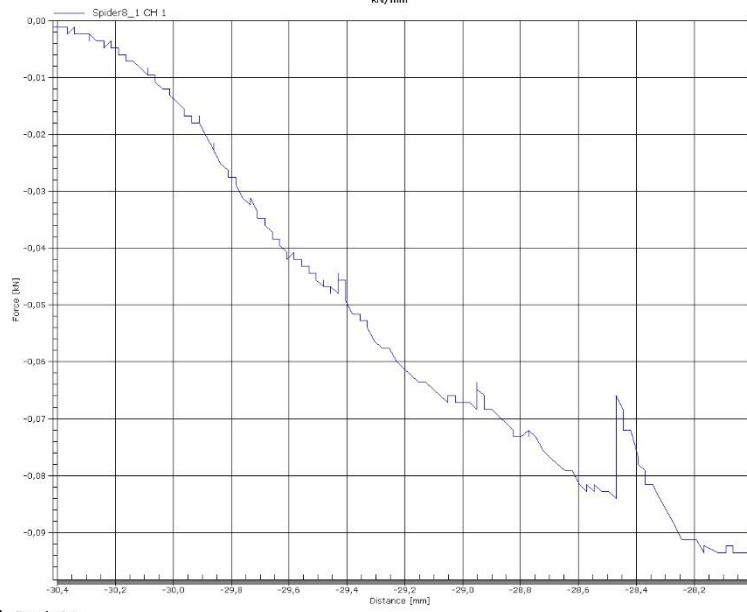


10 -I:

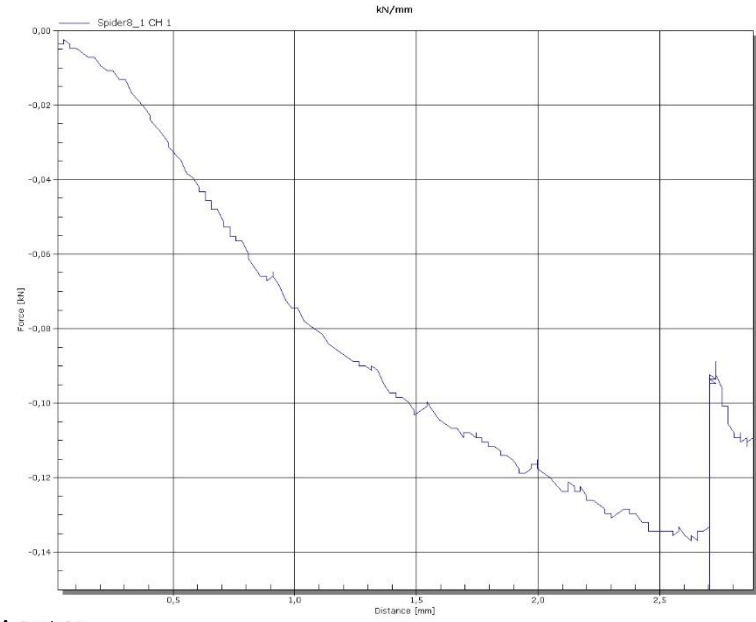


10 II:

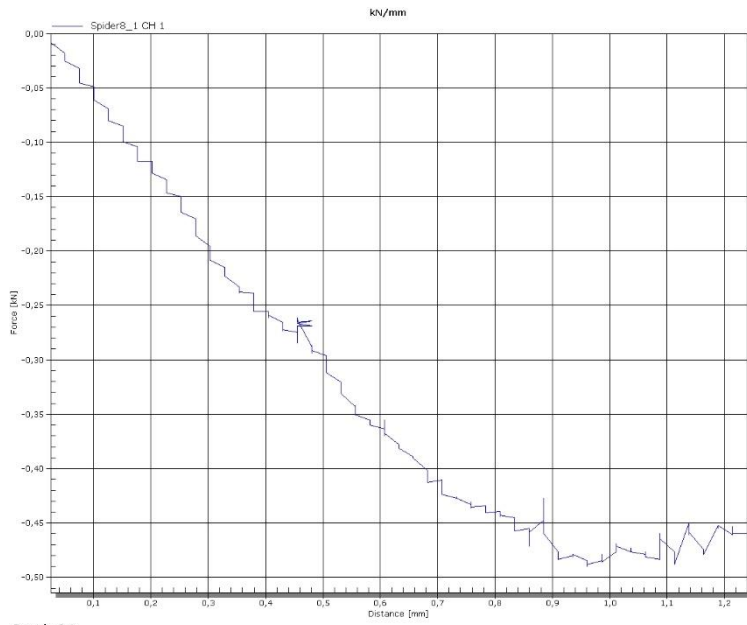
Graphs: Paper Vanilla L=90mm/200mm



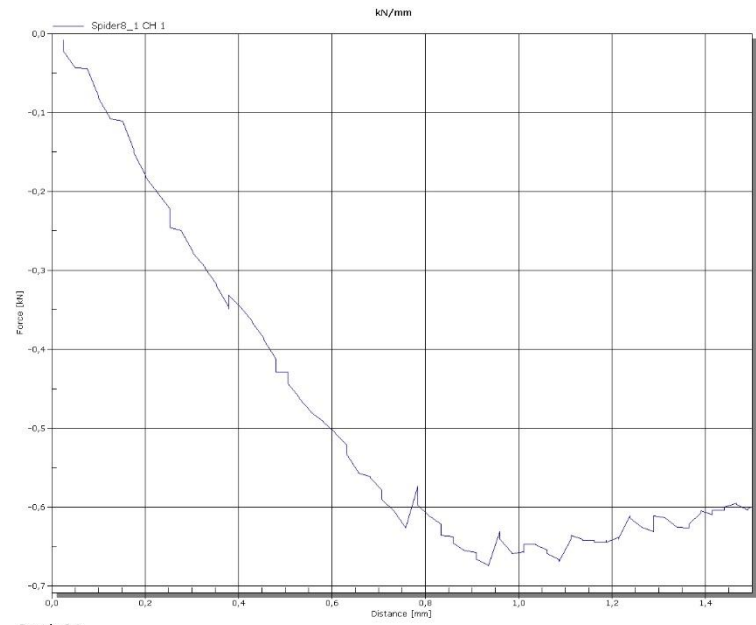
20 – (1):



20 – (2):

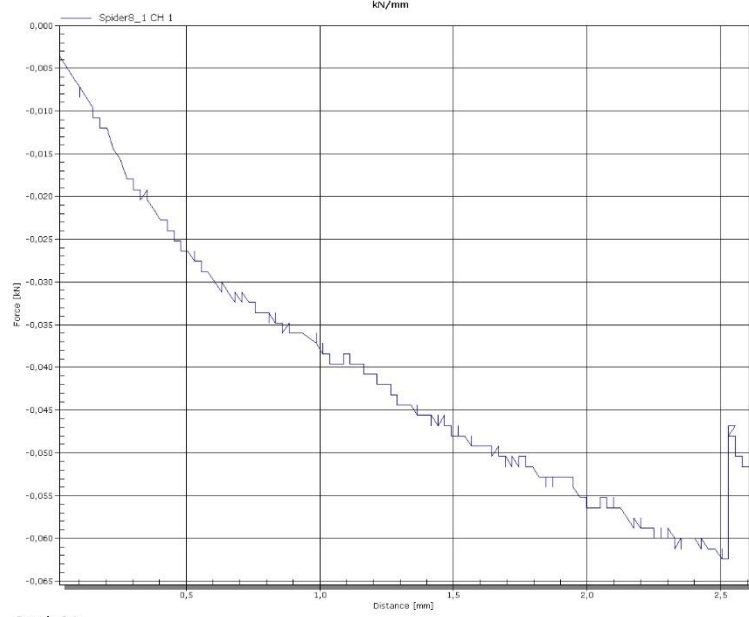


20 I (1):

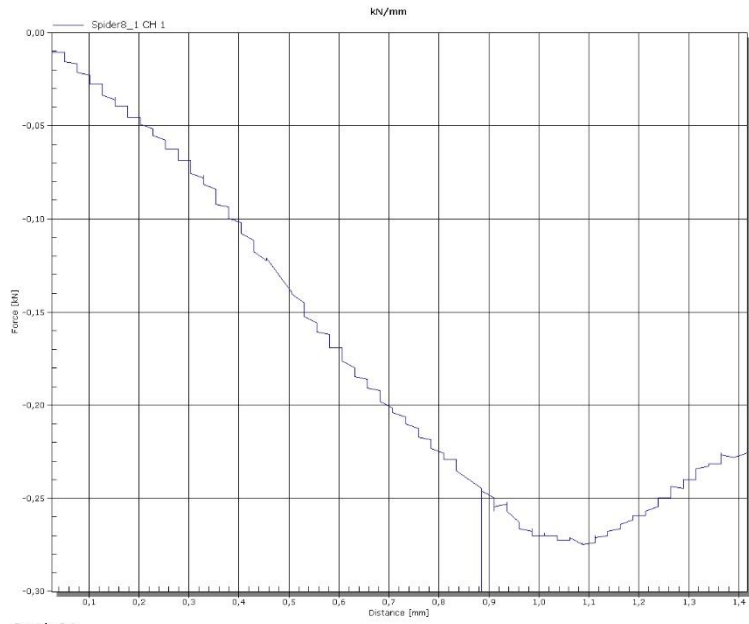


20 I (2):

Graphs: Paper Vanilla L=90mm/200mm

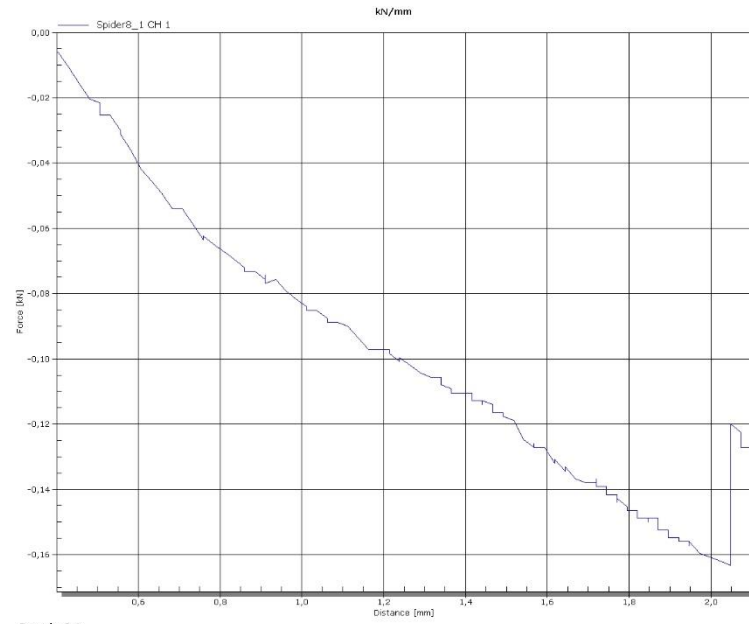


20 -:



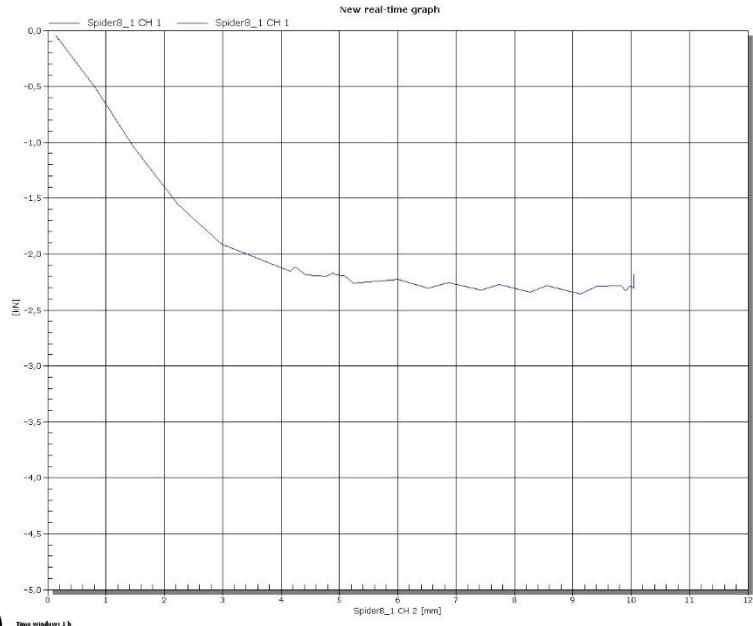
20 I:

LONG SAMPLES

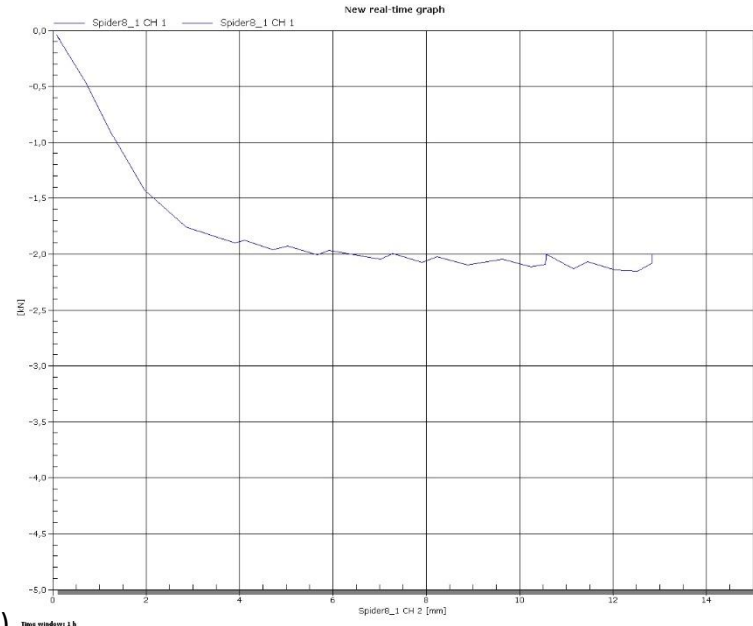


20 I, round 2:

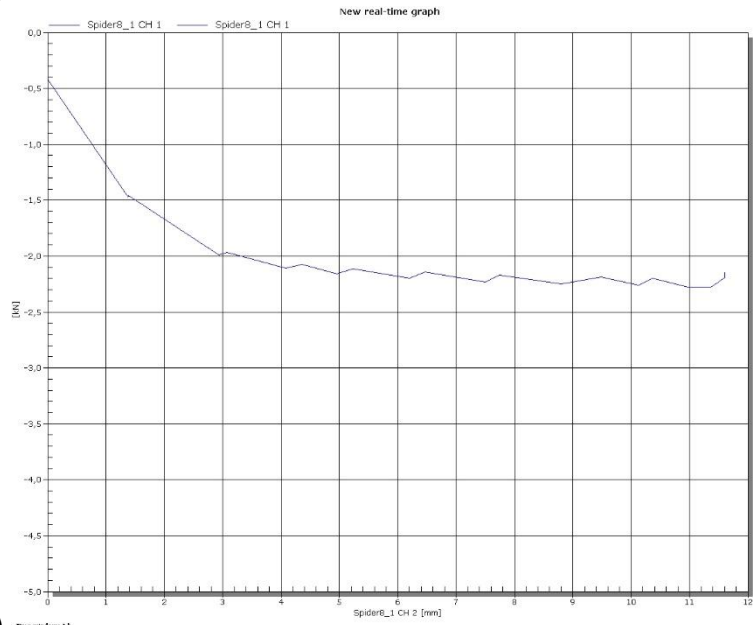
Graphs: Aluminum L=90mm



5 - (1)

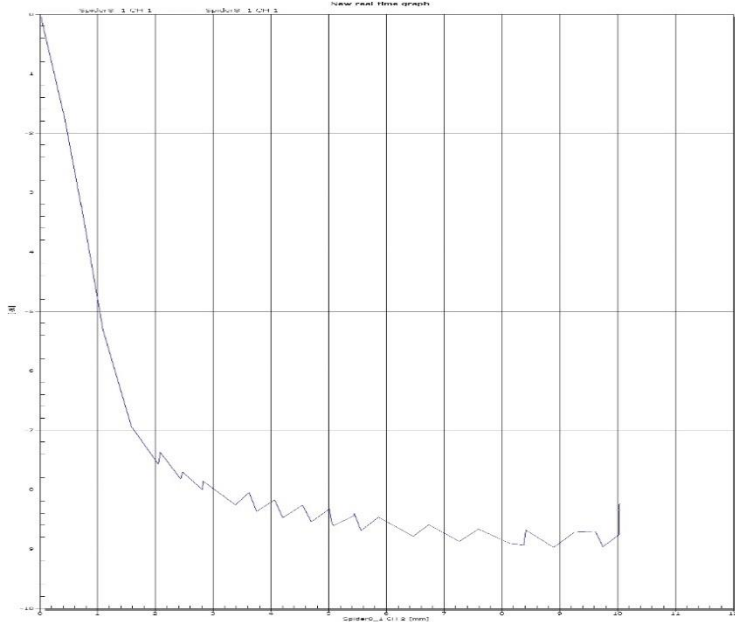


5 - (2)

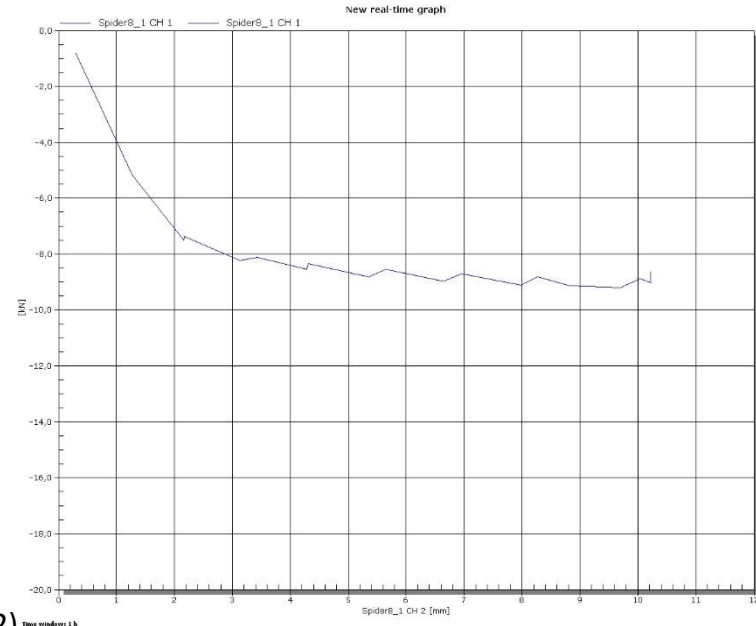


5 - (3)

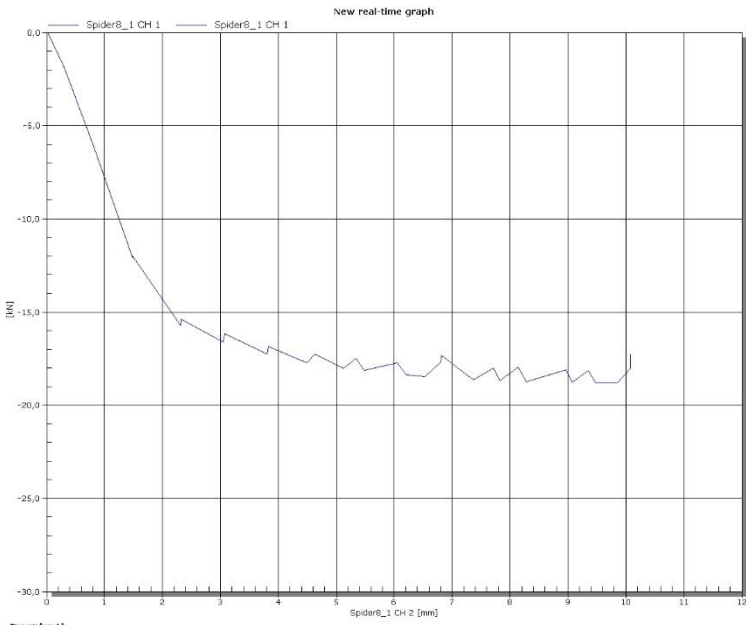
Graphs: Aluminum L=90mm



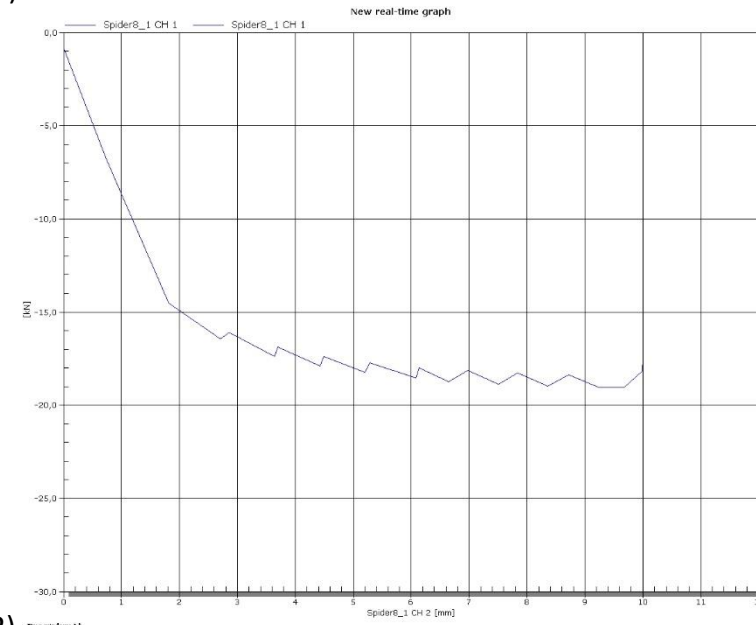
10 - (1)



10 - (2)

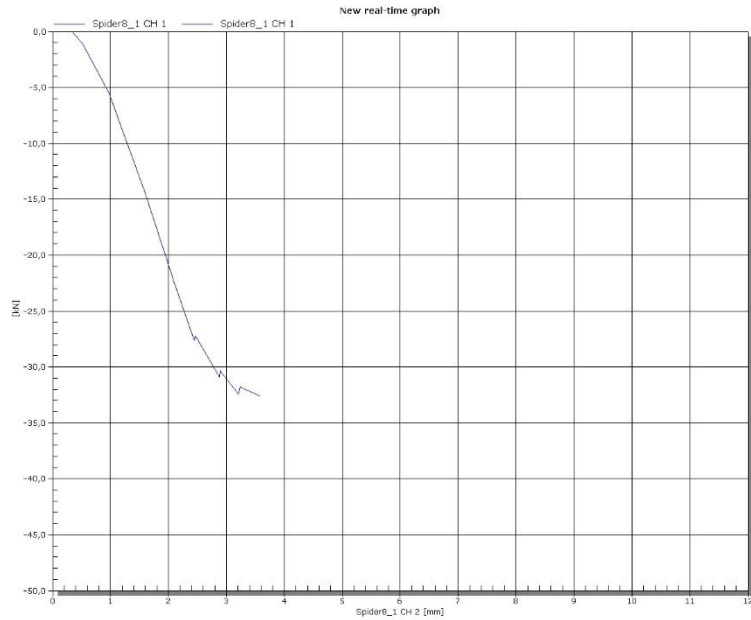


10 | (1)

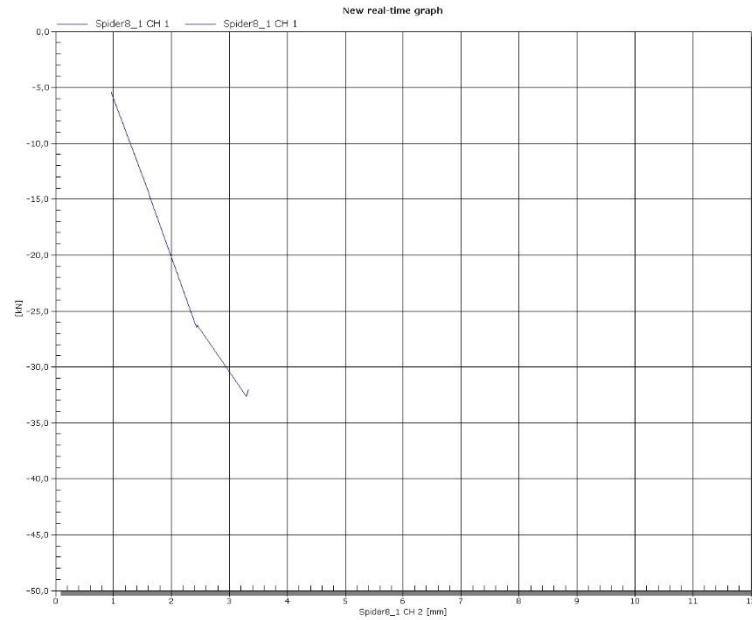


10 | (2)

Graphs: Aluminum L=90mm

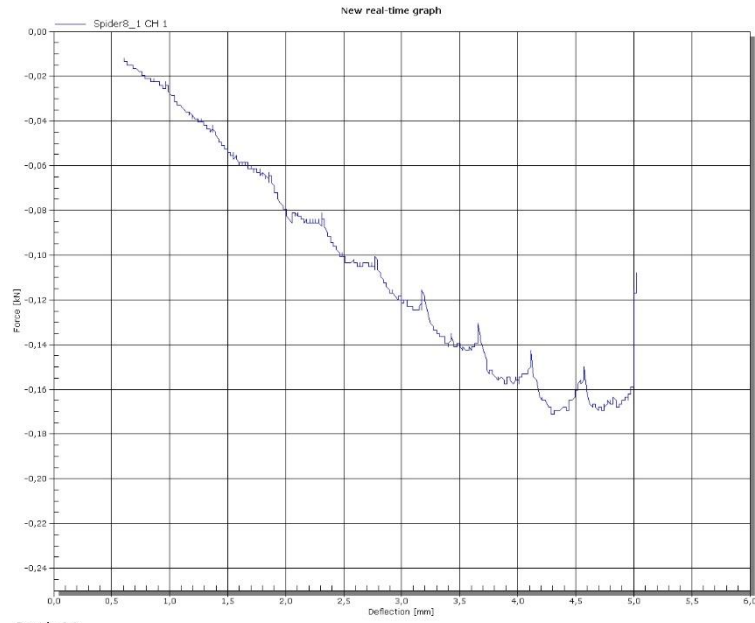


20 (1)

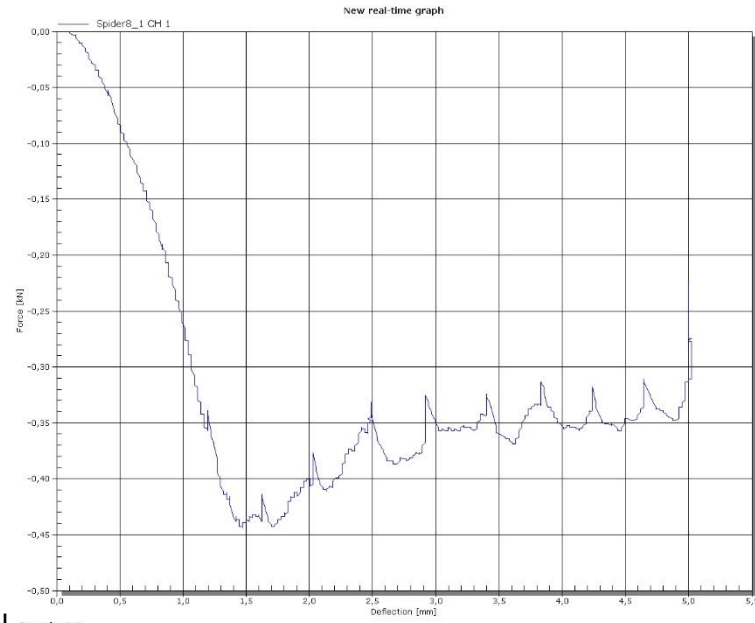


20 (2)

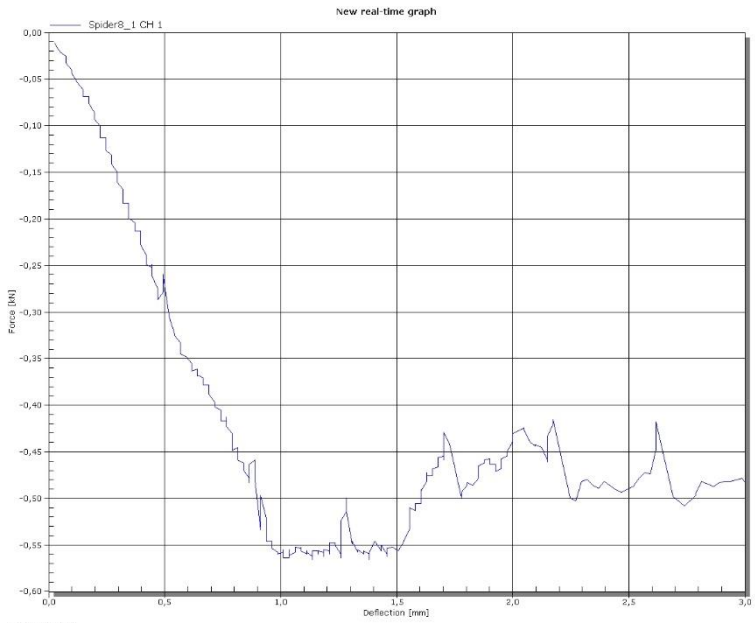
Graphs: Wood Glue L=90mm



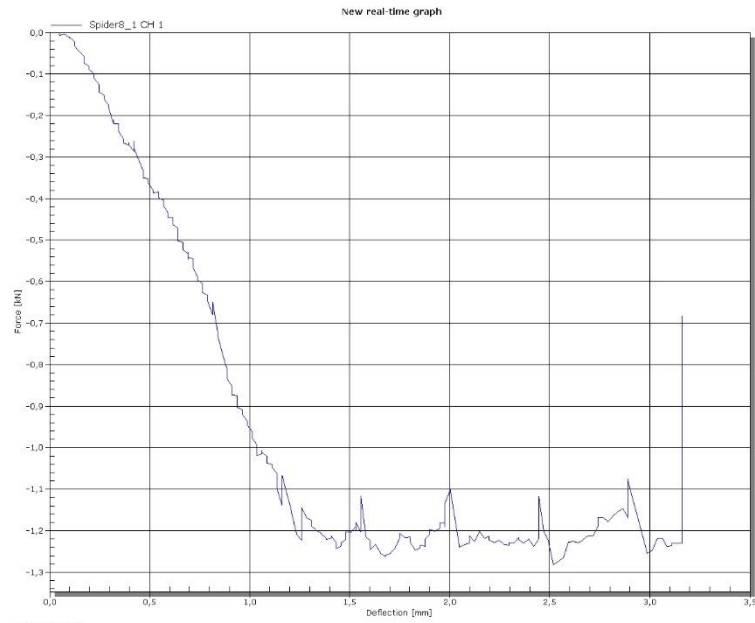
Dip 10 --



Dip 10 - I

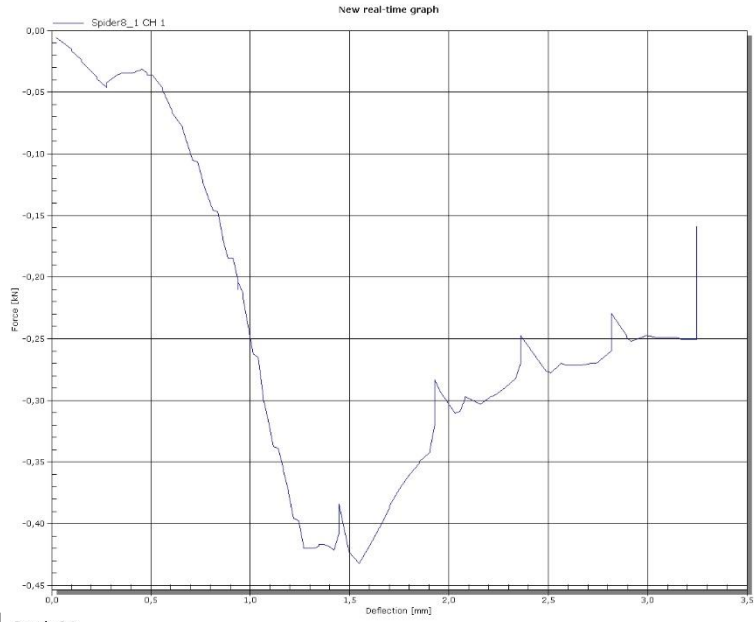


Dip 10 II

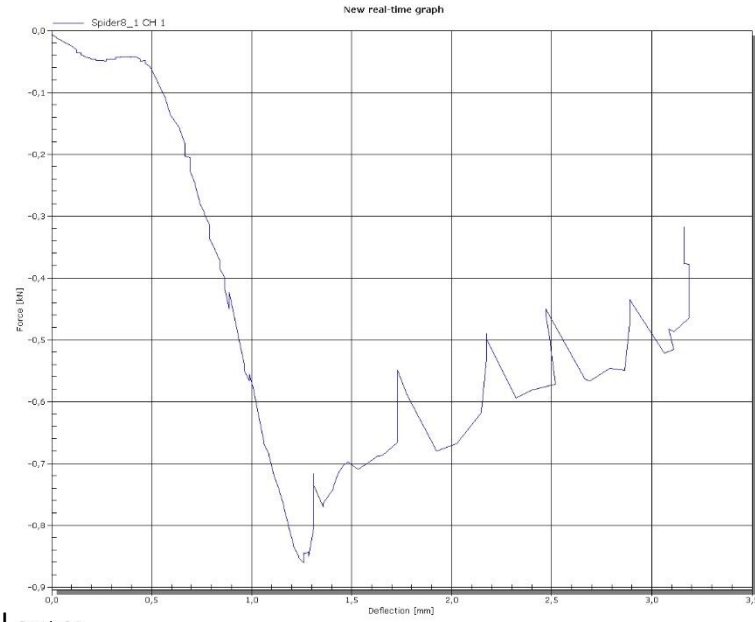


Dip 20 I

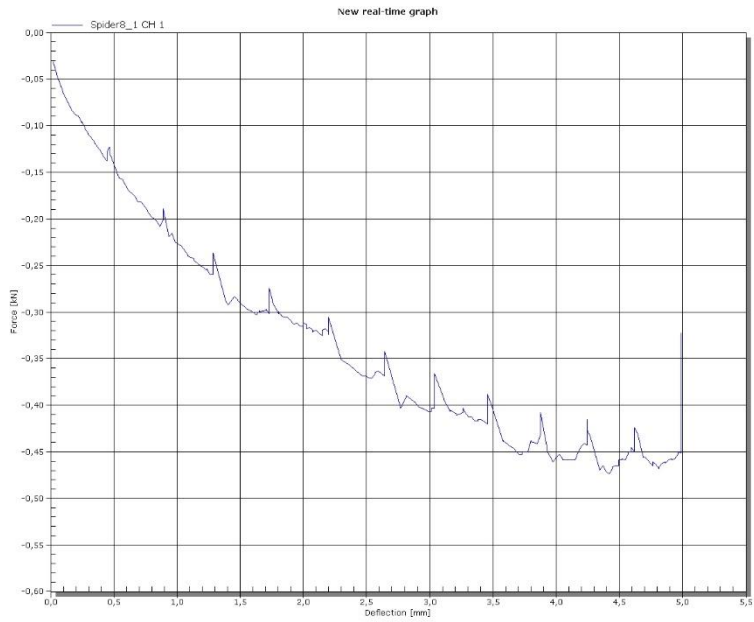
Graphs: Wood Lac. L=90mm



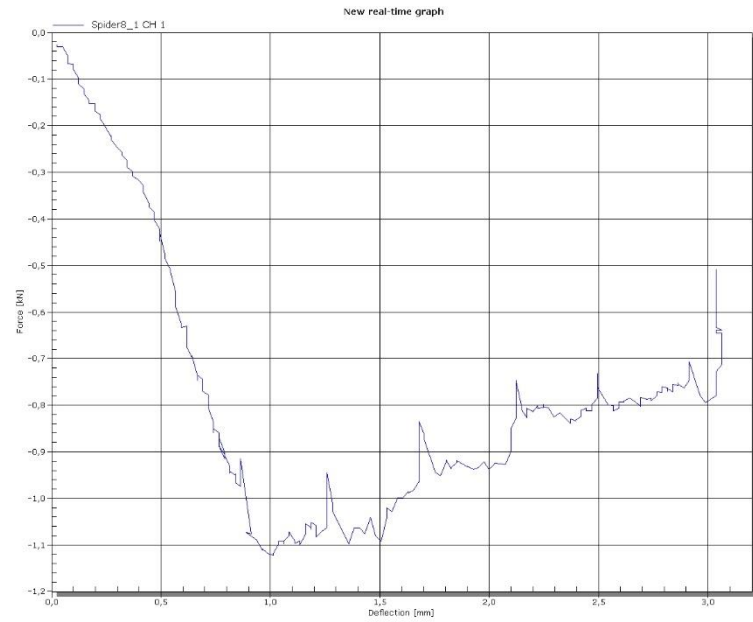
Dip 10 - I



Dip 10 II

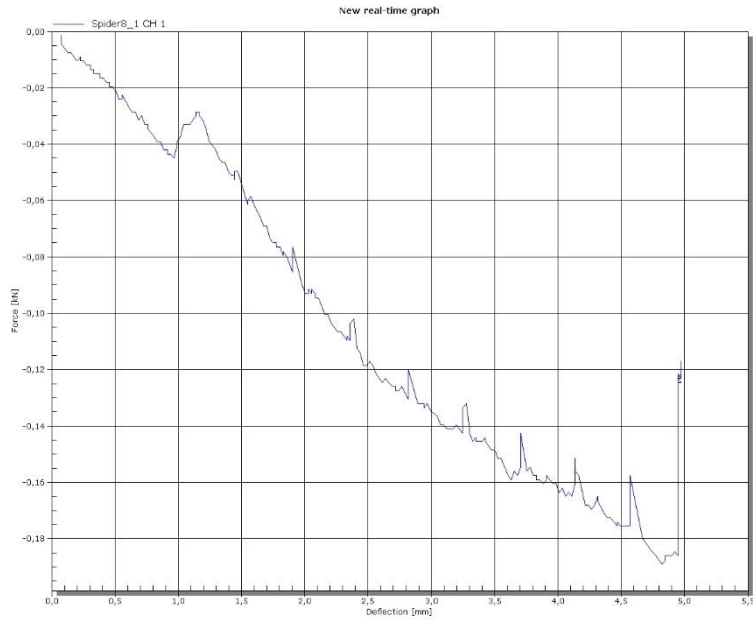


Dip 20 -

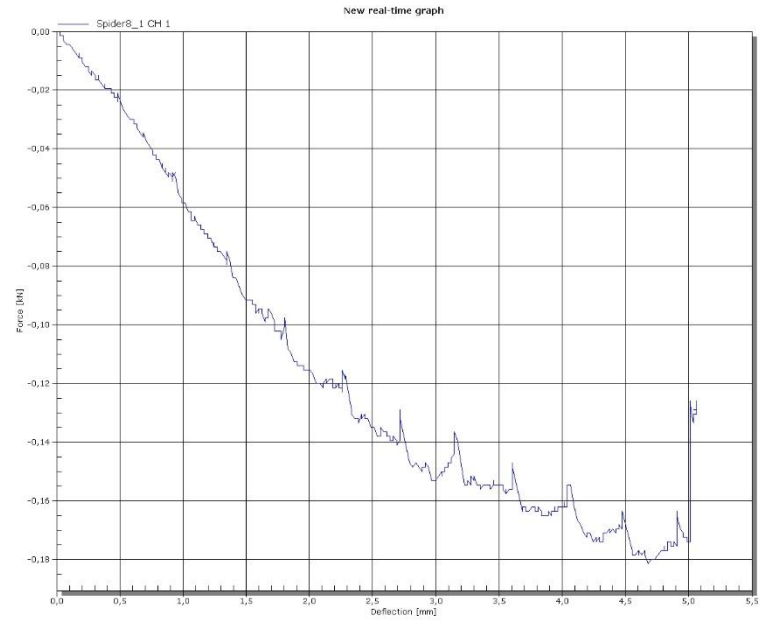


Dip 20 I

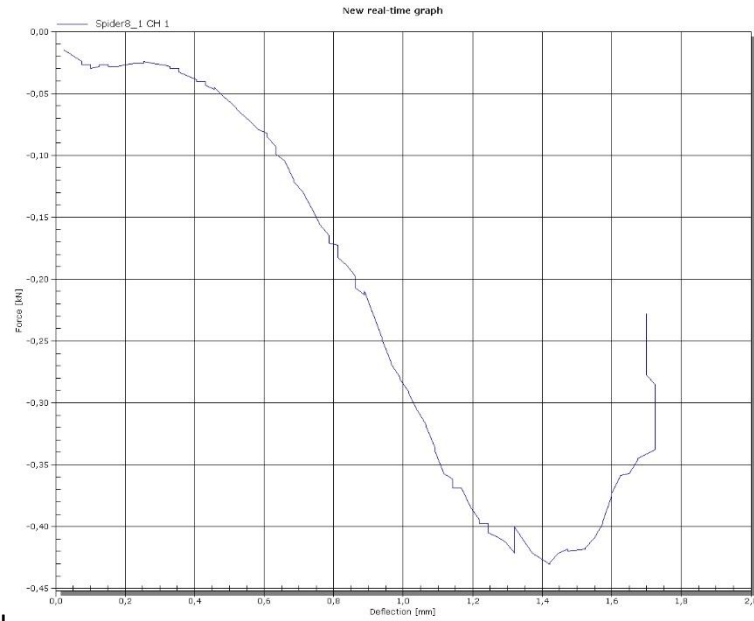
Graphs: Wood Lac. L=90mm



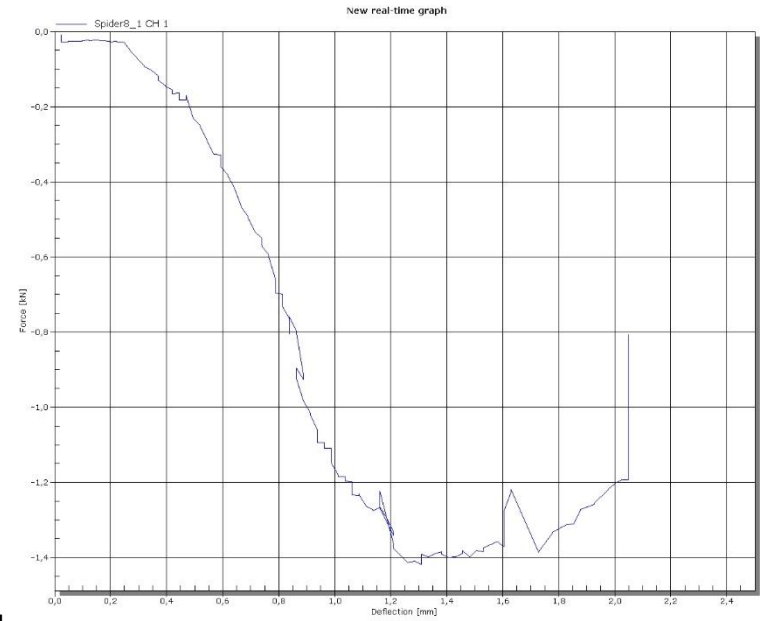
Dip 10 --



Inf 10 --

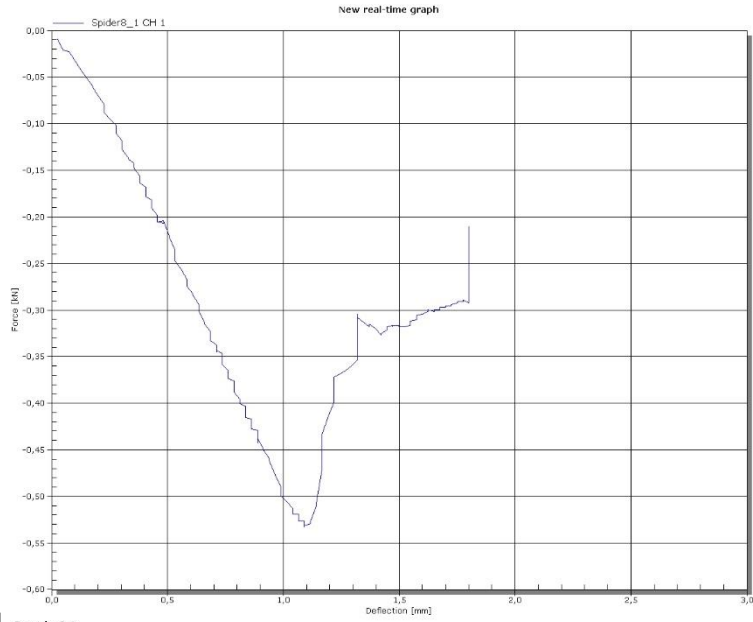


Coa2 10 - |

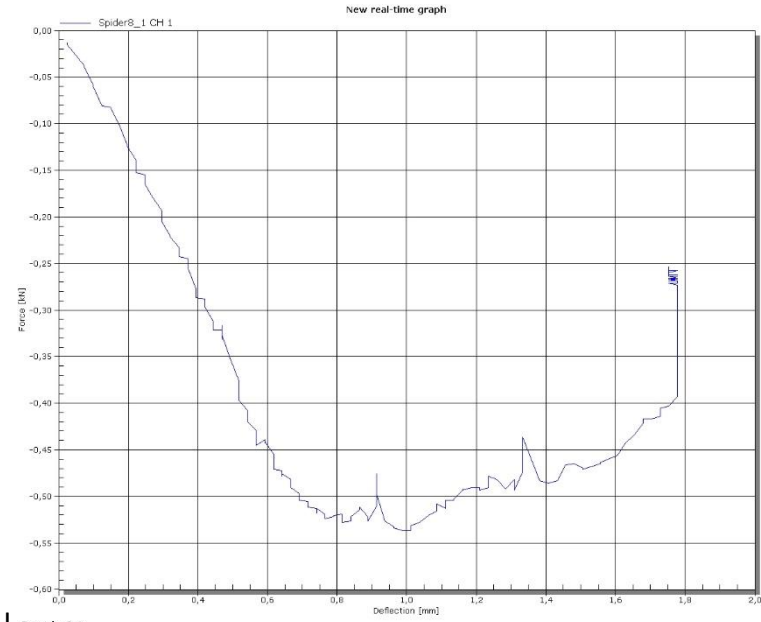


Coa 20 |

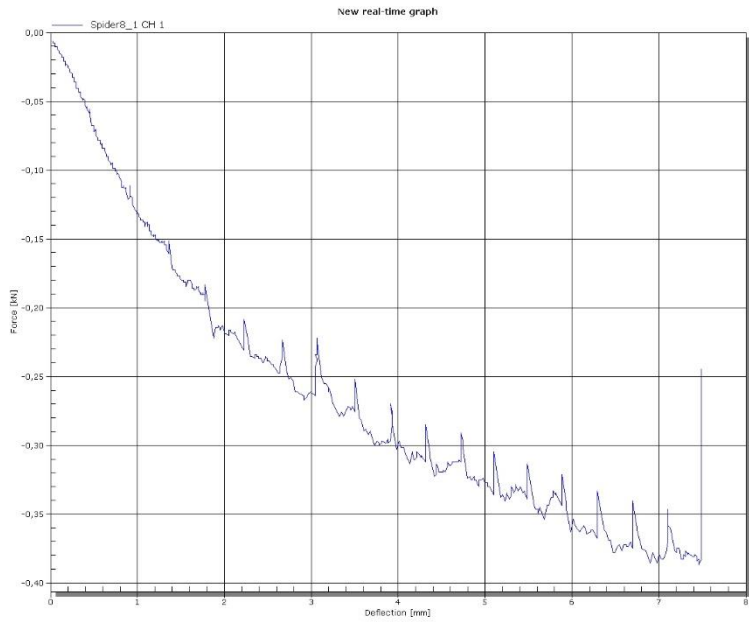
Graphs: Wood Lac. L=90mm



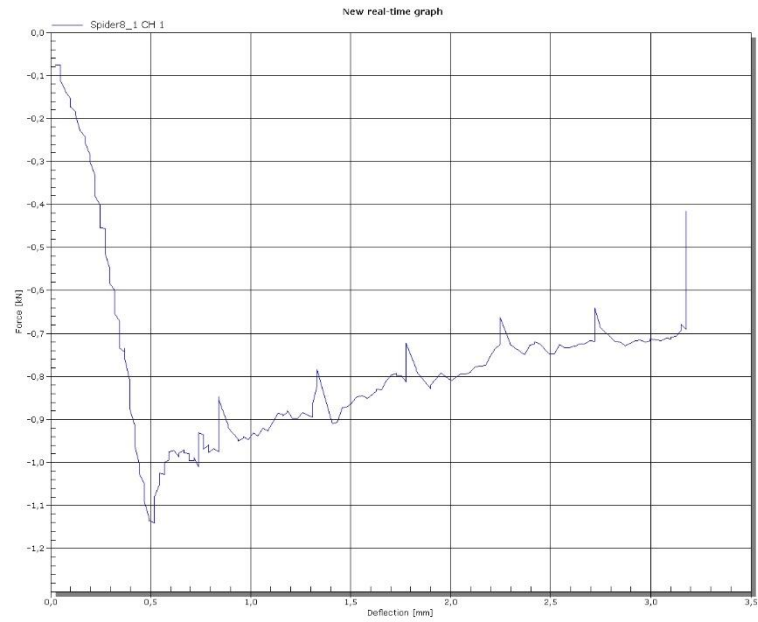
Inf 10 - I



Inf 10 II

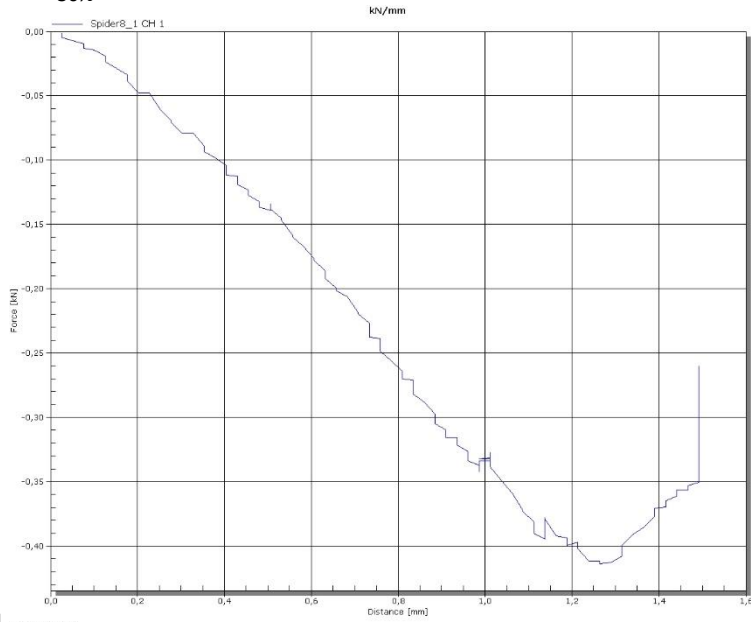


Inf 20 -

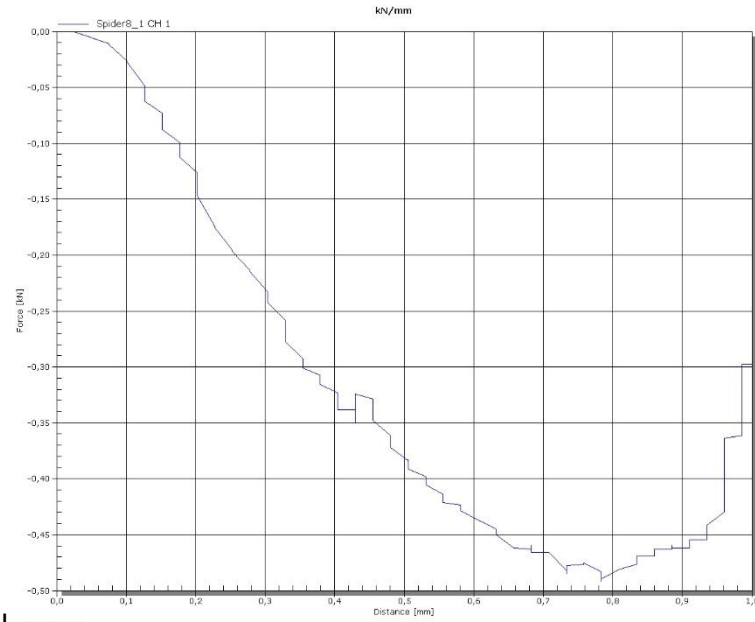


Inf 20 I

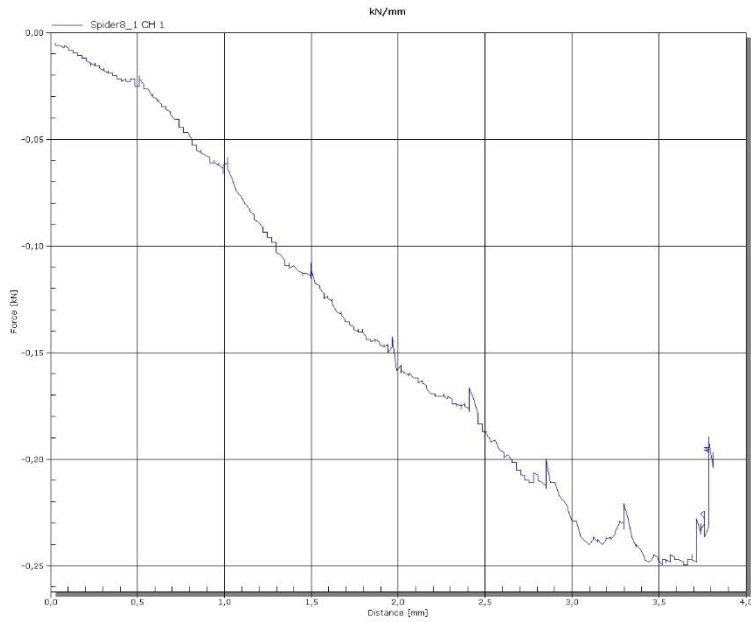
Graphs: DWG_{30%} L=90mm



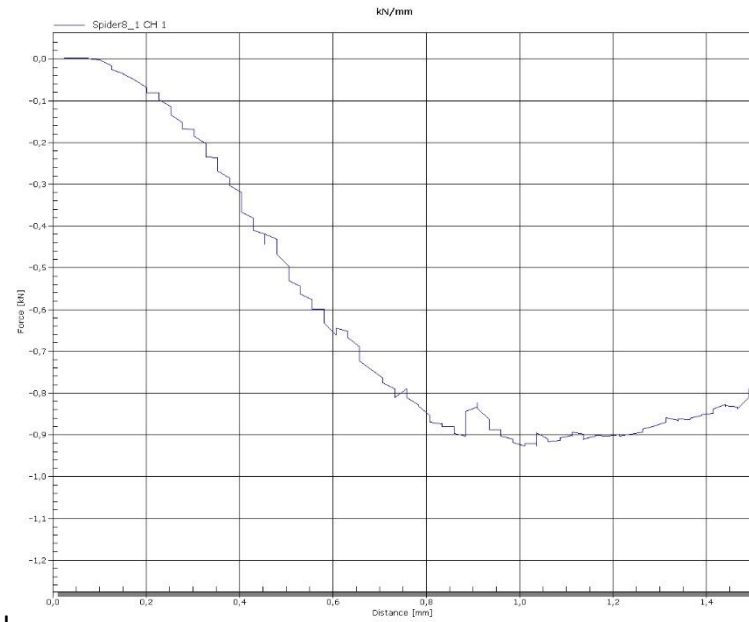
Dip 10 - I



Dip 10 II

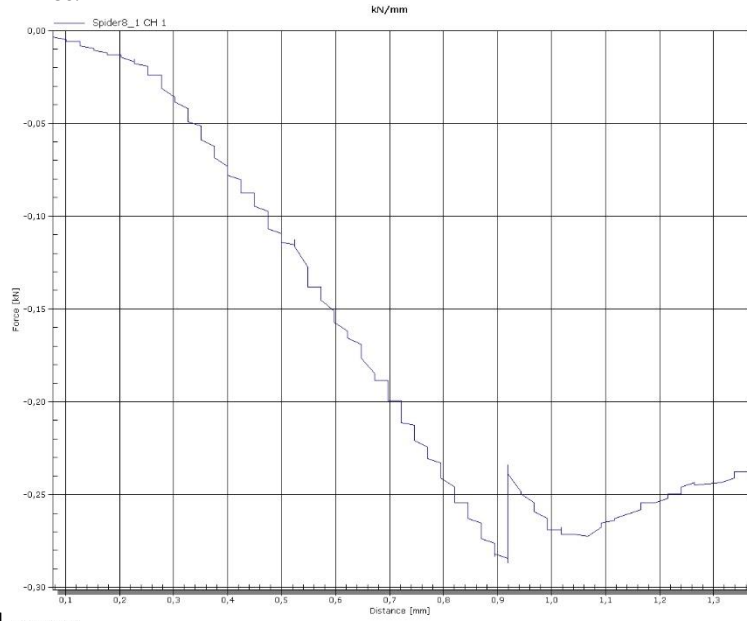


Dip 20 -

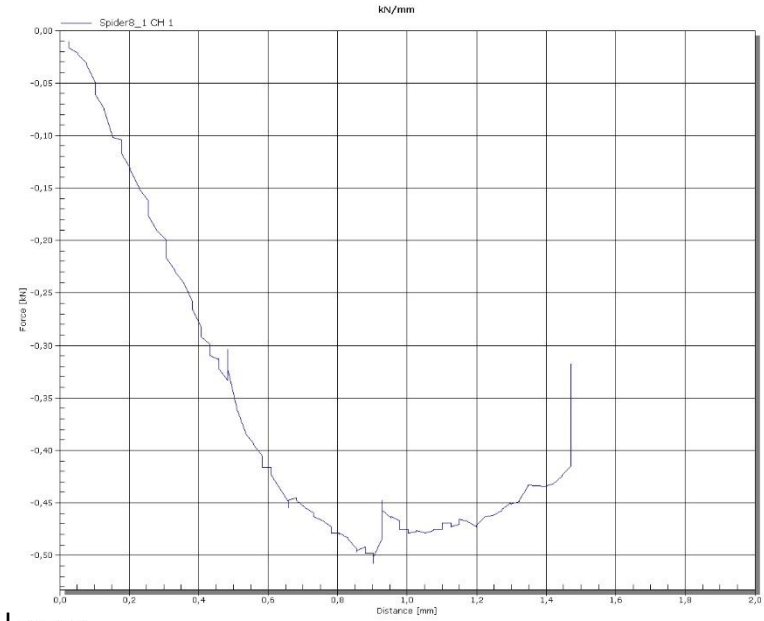


Dip 20 I

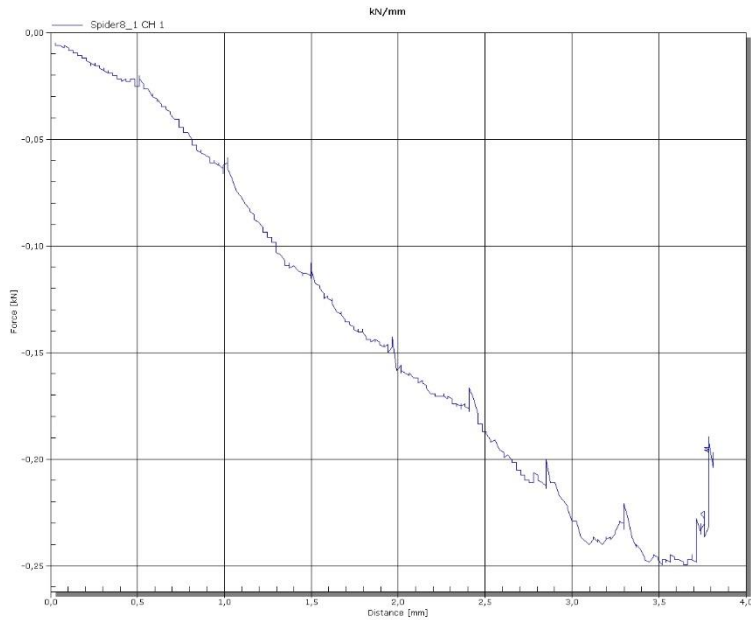
Graphs: DWG_{30%} L=90mm



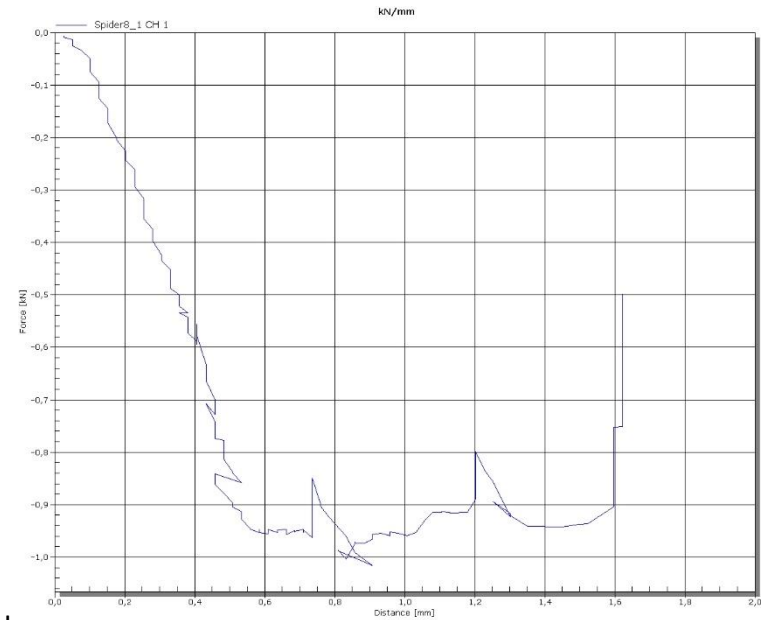
Coa 10 - I



Coa 10 II



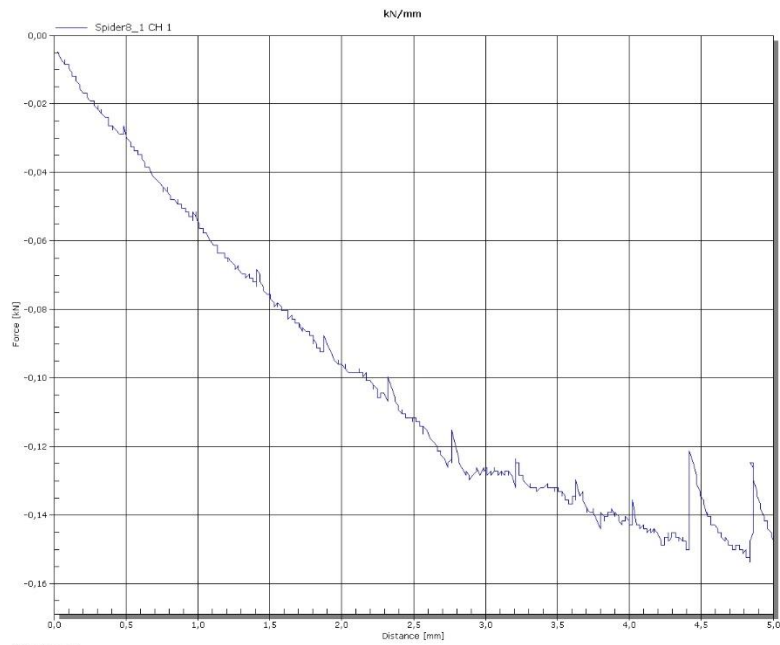
Coa 20 - I



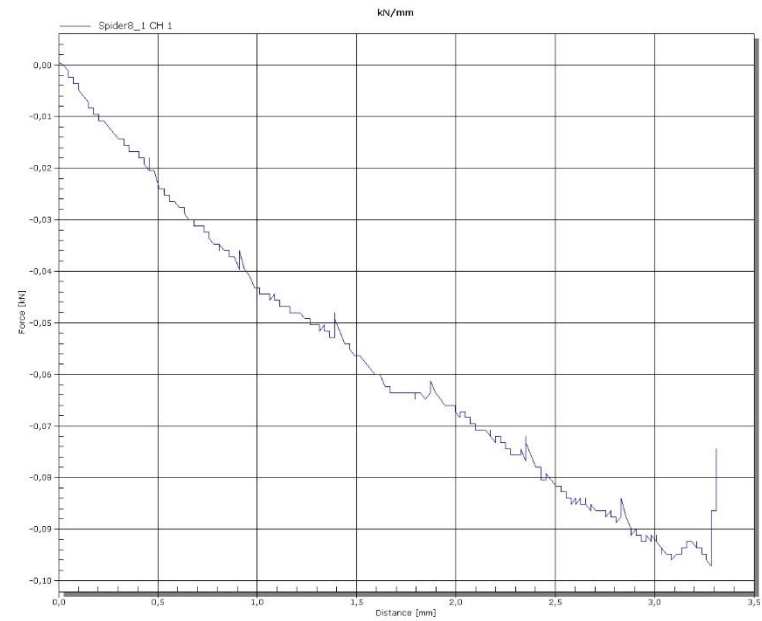
Coa 20 II

Graphs: DWG_{30%}

L=90mm

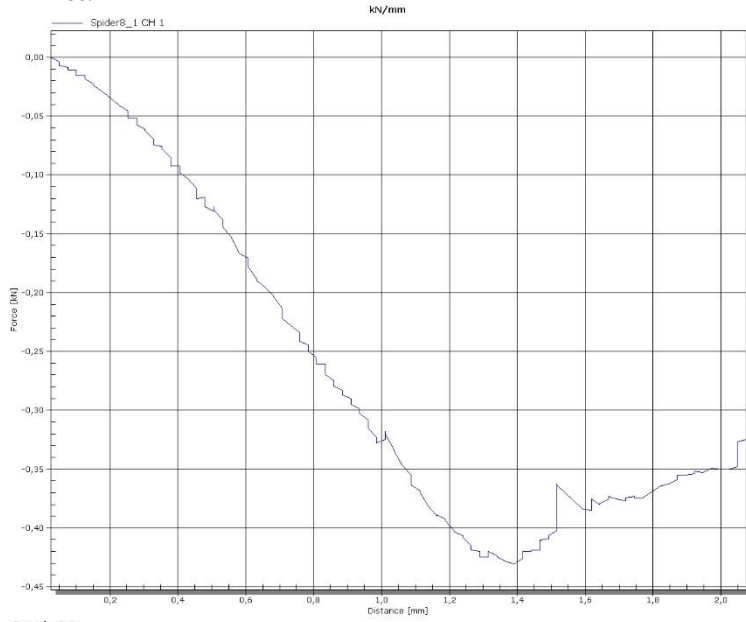


Coa 10 - - Time window: 5 min

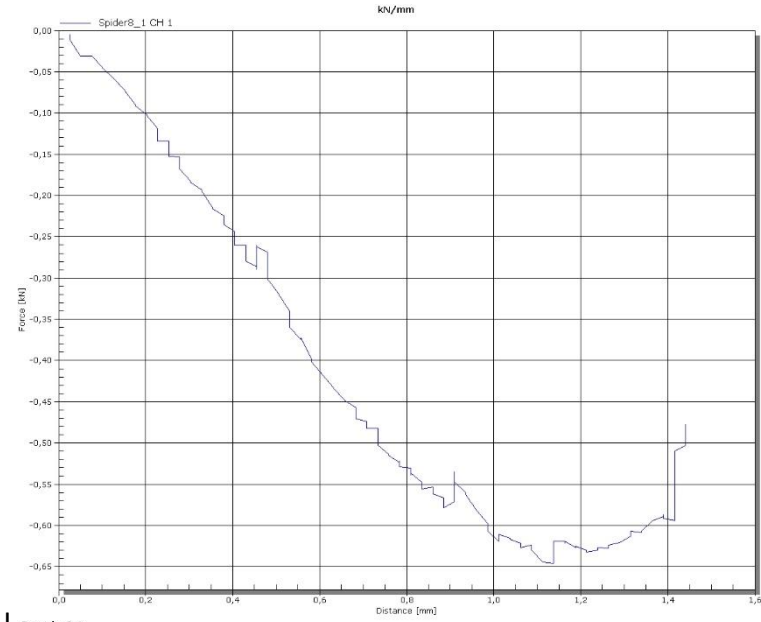


Inf 10 - - Time window: 5 min

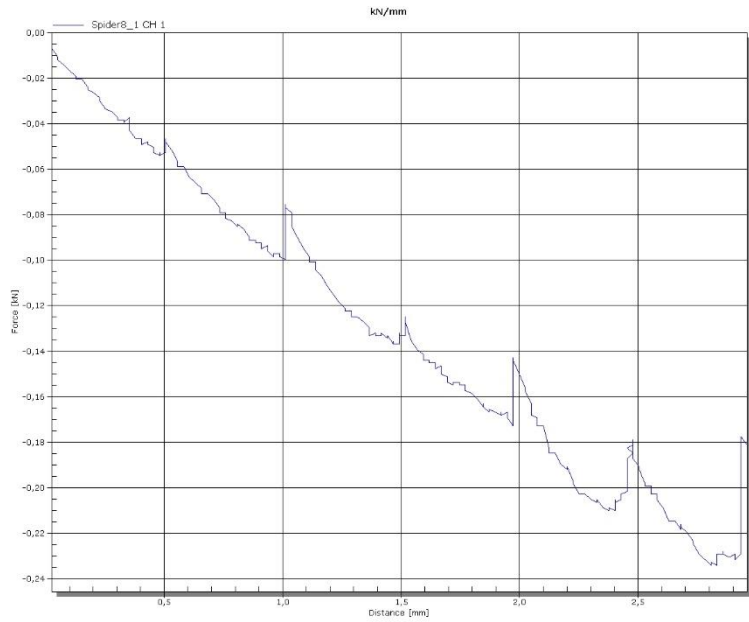
Graphs: DWG_{30%} L=90mm



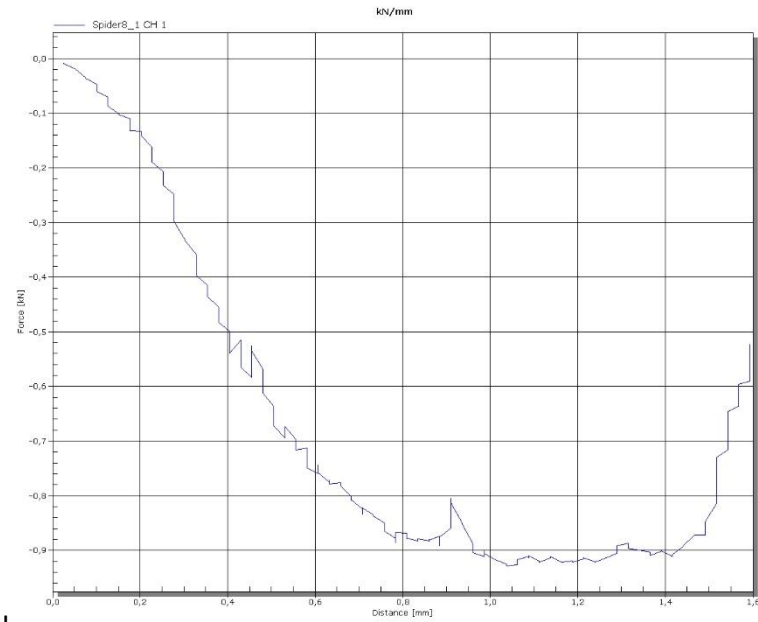
Inf 10 – I
Time window: 5 min



Inf 10 II
Time window: 5 min

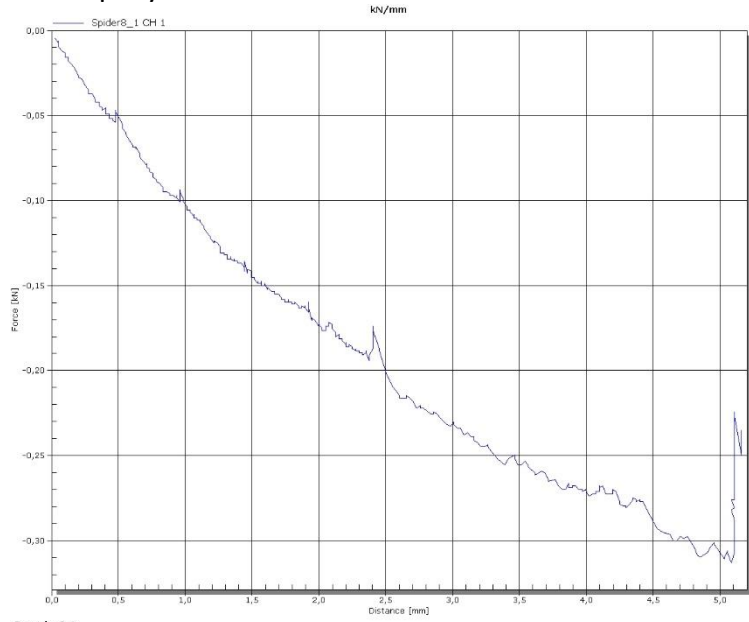


Inf 20 –
Time window: 5 min

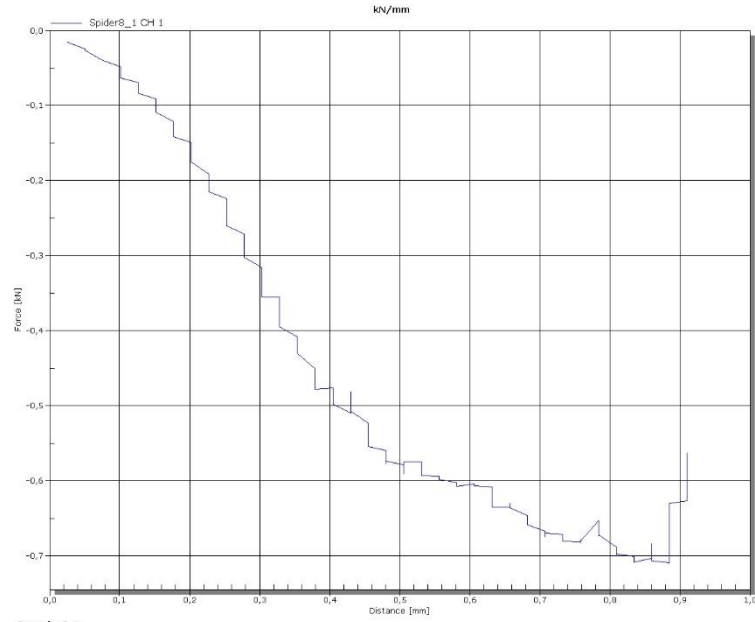


Inf 20 I
Time window: 5 min

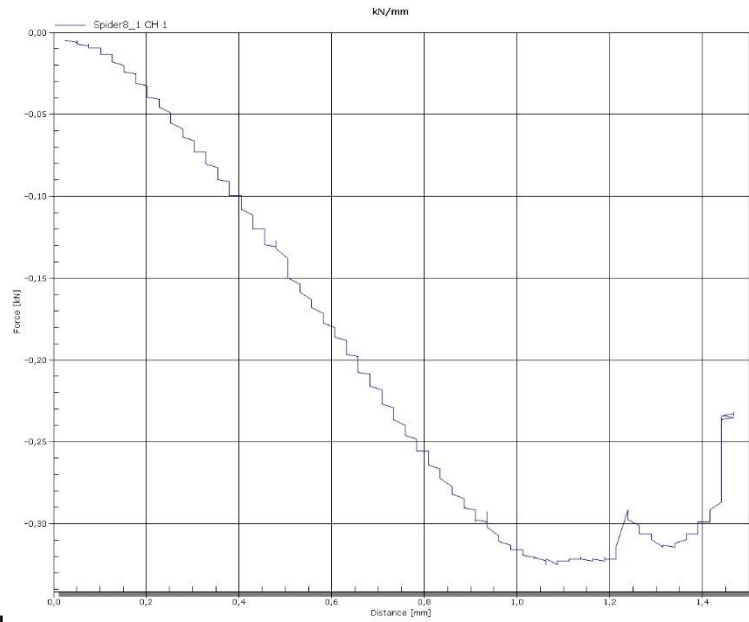
Graphs: Wood epoxy L=90mm



Coa 20 -
Time window: 2 min

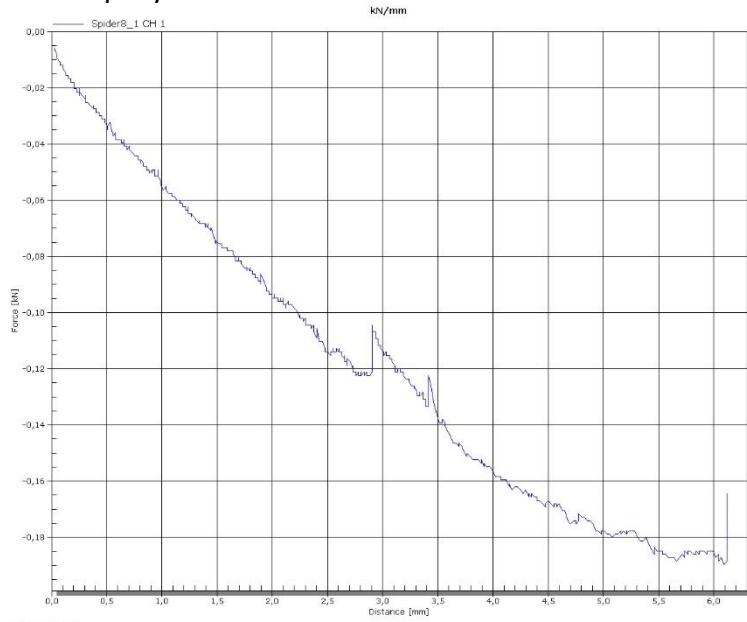


Coa 20 I
Time window: 2 min

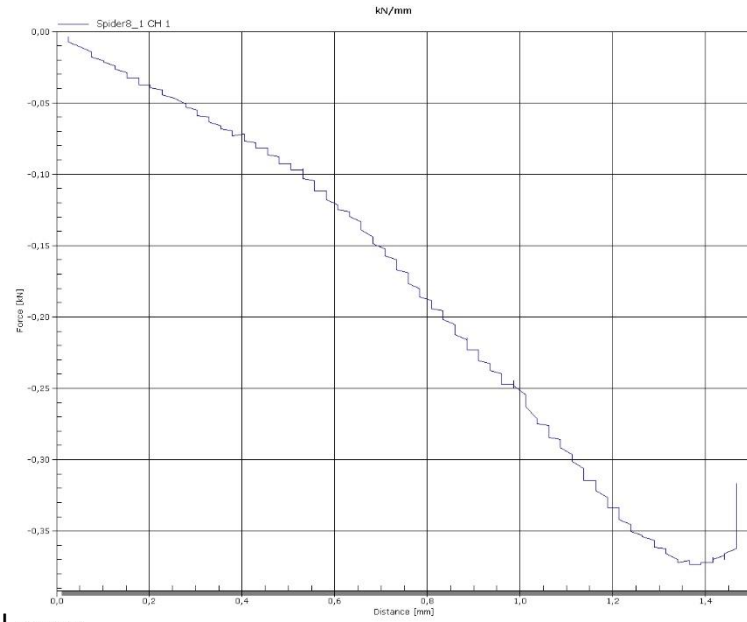


Dip 10 - I
Time window: 2 min

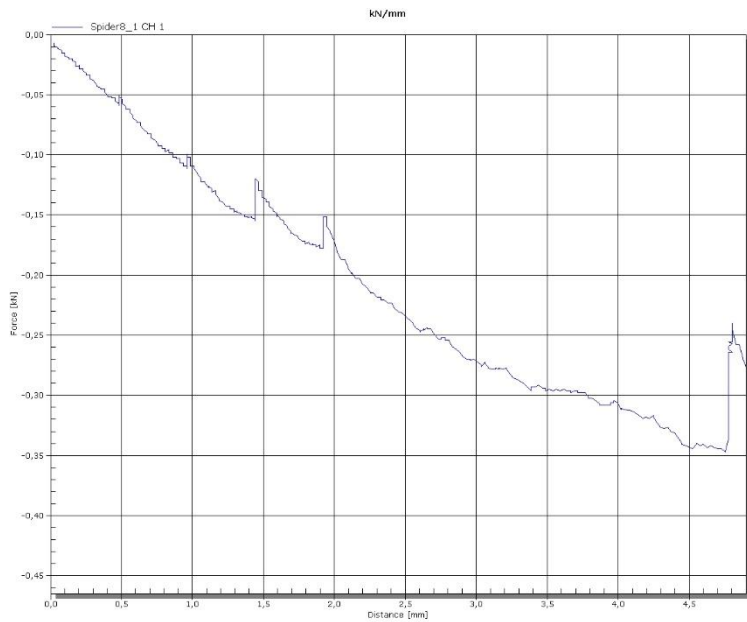
Graphs: Wood epoxy L=90mm



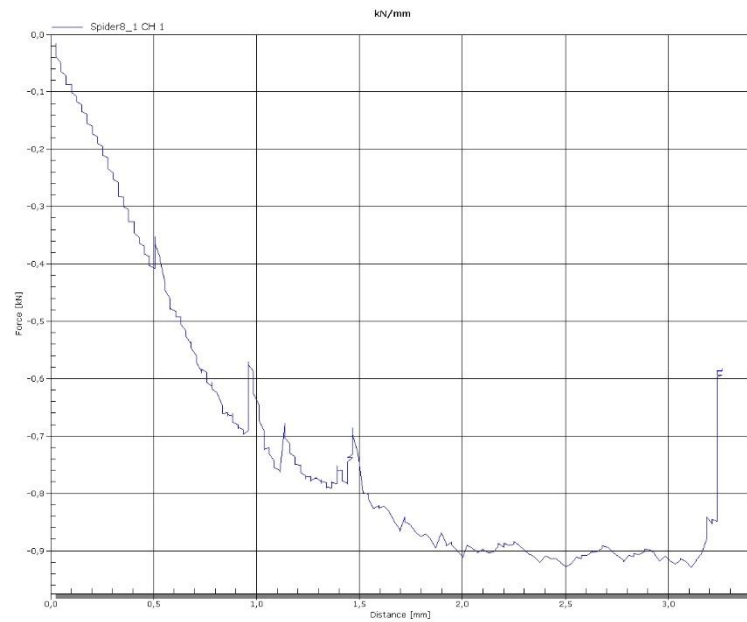
Inf 10 - -



Inf 10 - I

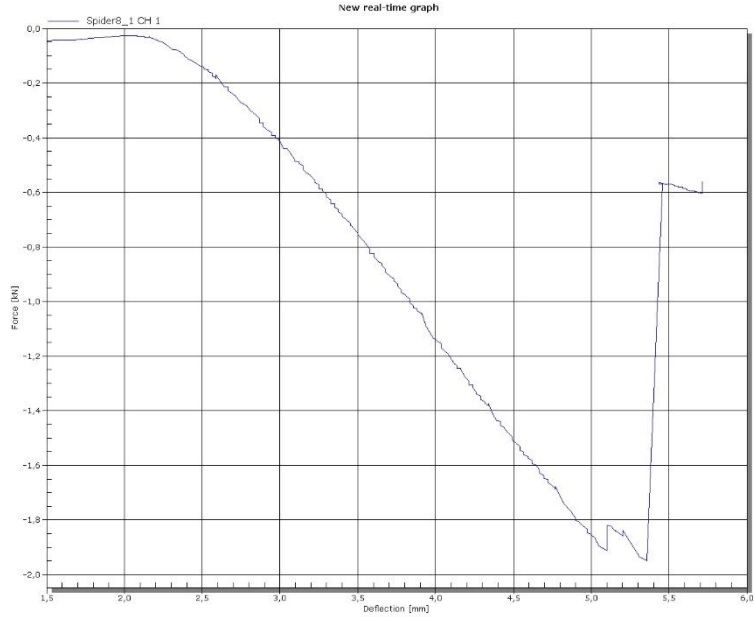


Inf 20 -

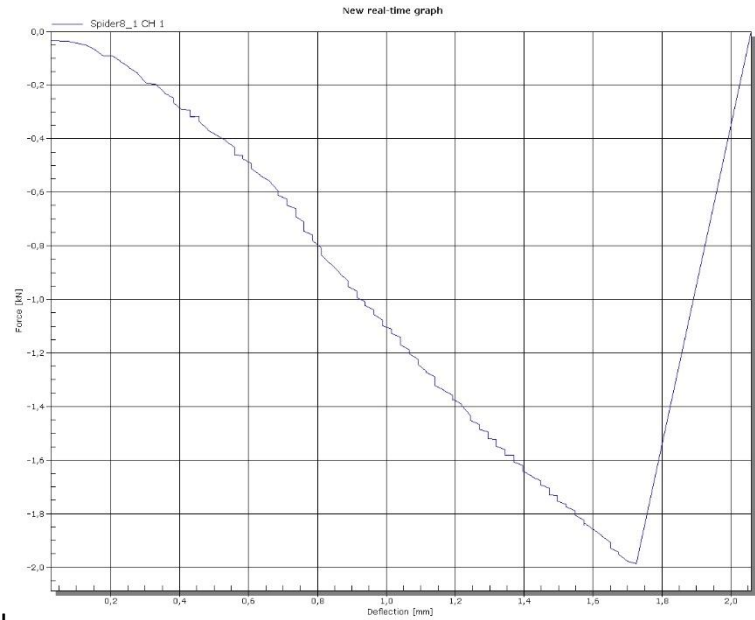


Inf 20 I

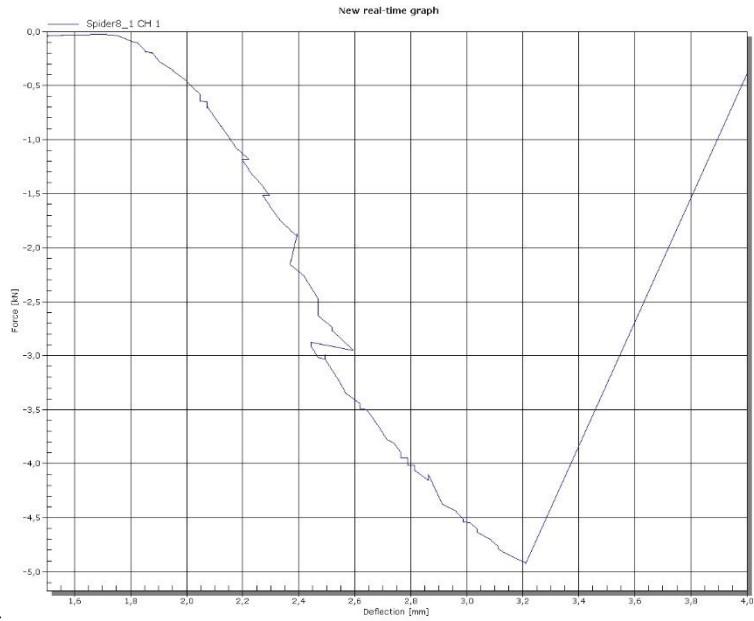
Graphs: RIMR134 Resin L=90mm



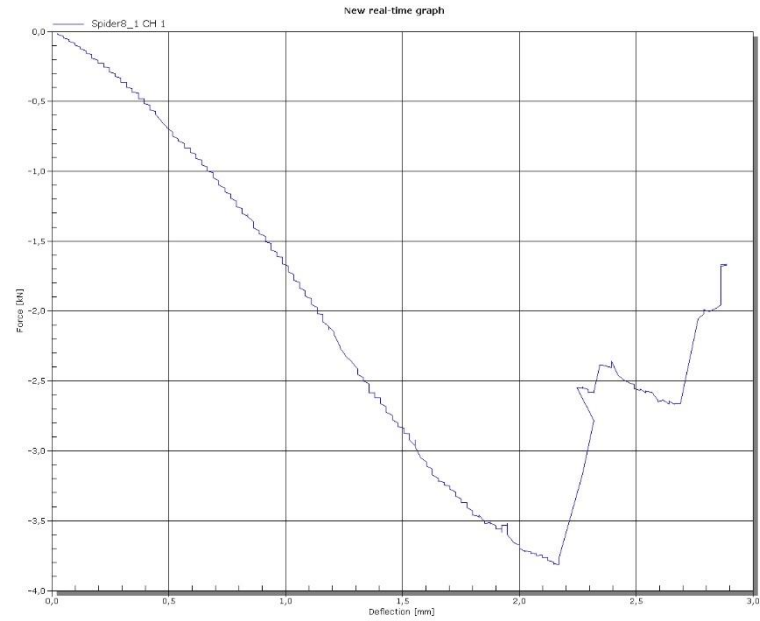
Inf 10 - -



Inf 10 - I

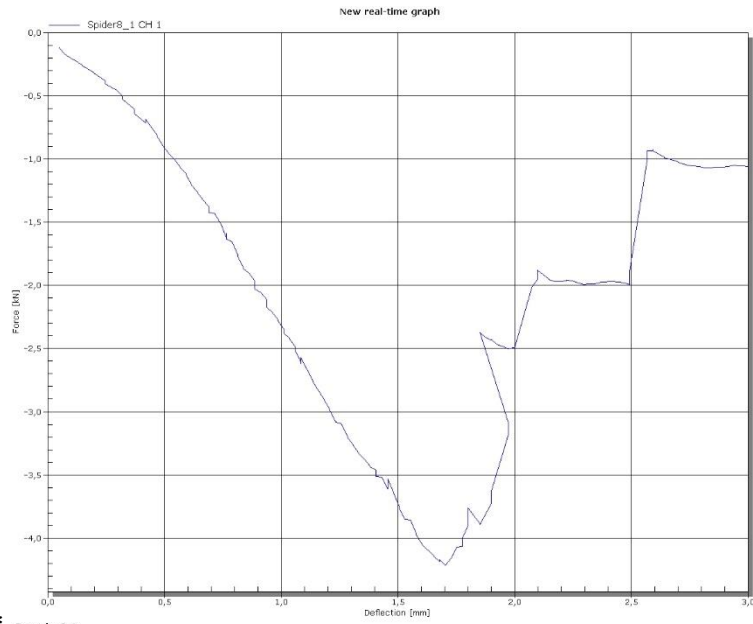


Inf 10 II*

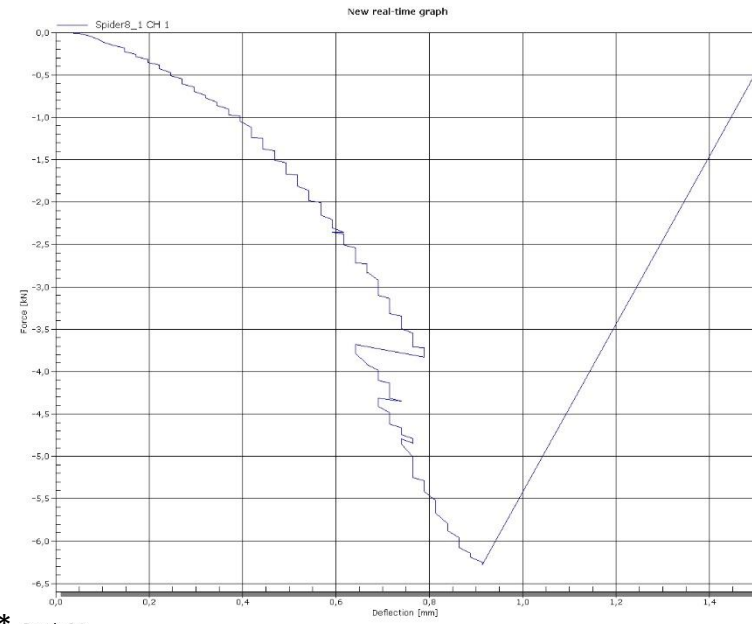


Inf 20 -

Graphs: RIMR134 Resin L=90mm



Inf 20 – ** This window: 2 min



Inf 20 |* This window: 2 min

- *Support slip causing distance jump(s)
- **Excess epoxy adding to weight and strength